Microfluidic Tools for Metabolomics

by

John Paul Urbanski

B.A.Sc. Mechanical Engineering
University of Waterloo, 2003

S.M. Mechanical Engineering
Massachusetts Institute of Technology, 2005

Submitted to the Department of Mechanical Engineering
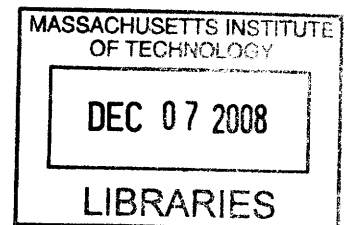in Partial Fulfillment of the Requirements for the Degree of

Doctor of Philosophy

at the

MASSACHUSETTS INSTITUTE OF TECHNOLOGY

September 2008

Author ....

John Paul Urbanski
Department of Mechanical Engineering
August 8, 2008

Certified by ....

Todd Thorsen
Associate Professor of Mechanical Engineering
Thesis Supervisor

Accepted by ....

Professor Lallit Anand
Graduate Officer, Department of Mechanical Engineering

Microfluidic Tools for Metabolomics

By

John Paul Urbanski

Submitted to the Department of Mechanical Engineering
August 8, 2008 in partial fulfillment of the
requirements for the degree of
Doctor of Philosophy

Abstract

A primary challenge in embryology is to understand the factors that govern the development of preimplantation (PI) embryos and how these factors relate to embryo viability in the field of *in vitro* fertilization (IVF). This is particularly important as clinical policy moving towards single embryo transfer (SET) has gained awareness to manage unprecedented numbers of multiple births, such as twins and triplets, resulting from artificial reproductive techniques. Conditions that correlate with developmental potential of candidate embryos are disputed in the field, however, as the requisite data is difficult to obtain.

The metabolic profiles of embryos during *in vitro* culture have been suggested as a key indicator of developmental potential, and approaches have been clinically implemented to select transfer candidates which make the most efficient use of nutrients. Existing microdroplet analysis techniques are accurate and suitable for non-invasive assessment of single embryos. Unfortunately, the process of determining metabolite levels in nanoliters of culture media through fluorometric assays is low-throughput and requires specialized expertise, hindering widespread clinical use of these methods.

The goal of this thesis is to develop microfluidics-based approaches for improving metabolic analysis of PI embryos and mammalian cells. This challenge necessitates two competencies: methods for automating chemical assays and methods for supporting cell cultures, which can be integrated with analysis. Contributions include a standalone platform for determining the metabolite use of single embryos. Profiles may be acquired automatically, which reduces significant technician hours and improves repeatability. Techniques are developed for performing embryo culture in the smallest culture volumes to date in microfabricated environments. Microfluidic approaches have enabled culture that outperforms the current state of art approach based on cell count measurements. An integrated system is introduced, merging analysis and culture competencies to perform metabolic profiling of separate cultures of mammalian cells in parallel. Finally, new paradigms in microfluidic design are presented based on the concept of vertically integrated architectures, suitable for overcoming density limitations of microfluidic assays. A scalable analysis platform for refining embryo selection has been long warranted and would enable pursuit of the difficult questions relating metabolism and embryo viability as the clinical movement towards SET continues.

(This page intentionally left blank)

Acknowledgements

(This page intentionally left blank)

Table of Contents

(This page intentionally left blank)

Chapter One - Introduction

1.1 The Advent of ART

More than 130,000 assisted reproductive technology (ART) cycles are started annually in the U.S, accounting for approximately 1% of total births[1]. The development of ART (referring to any process by which oocytes, zygotes or embryos are manipulated to achieve pregnancy) allows fertilization of the female egg cells with male sperm to be carried out in a laboratory setting. In a process known as *in vitro* fertilization (IVF), pre-collected eggs are fertilized in a lab with sperm, monitored over several days to assure proper preimplantation development, then transferred to the target female's uterus through the cervix where it will expectantly implant in the uterine lining and further develop into a fetus. IVF accounts for 99% of ART treatments in the U.S., and is often used to achieve pregnancy if a prospective mother's fallopian tubes are damaged or missing[1]. The success of this procedure (measured by the number of live births per ART attempt) is traditionally low, around ~30%[2,3], which can be attributed in part to imperfect *in vitro* culture conditions [4]. This procedure can cost families several thousands of dollars for each attempted cycle, so to ensure a birth many patients and/or clinics traditionally opt to transfer multiple embryos to increase the probability of success. For 2005 in the U.S., the mean number of embryos transferred ranged between 2.4 to 3.3, for women between the ages of 35 and 43[1,5].

The impact of multiple births in the United States due to ART began to attract concern towards the late 1980's, when it was necessary for the American Society of Reproductive medicine to introduce guidelines for limiting multiple embryo transfer. Following the increases in implantation rates, nearly half of the resulting pregnancies were twins, even when only two embryos are transferred[5,6]. Of total births annually in the U.S., approximately 15% of twins, 50% of triplets and 30% of quadruplets (or higher order births) are the result of ART assisted

pregnancies[5]. As a result, *in vitro* embryo selection has been accepted as an effective direction towards eliminating multiple births and thereby avoiding the serious problems associated with such pregnancies[7] including pre-maturity, low birth weight, disability, and death. For twin births, the relative increase in preterm delivery, cerebral palsy and infant death are respectively five, four and six times more likely. For higher order births, potentials incidence of early births occur nearly ten times more often, with cerebral palsy and infant death nearly 20 times more likely overall[1].

Interestingly, due a chance collision of science and demographics, the state of Massachusetts has ranked first in the U.S. in multiple births for 2003-2006[8, 9]. It is hypothesized that due to overall higher levels of education, potential mothers are more likely to postpone motherhood in pursuit of professional advancement following school. While the probability of having twins increases slightly with a mother's age, the majority of these births may be related to ART, and multiple embryo transfer[8]. Accessibility of health insurance, and subsidies for assisted reproduction by the state, make assisted pregnancies via IVF or other means a viable option. Further, the general high level of education ensures families are not deterred from seeking reimbursement from often confounding insurance systems. In Massachusetts, approximately 4.7% of pregnancies result in multiple births (4.5% are twins), compared to a national average of 3.4% (3.2% twins)[9]. Affluent neighborhoods surrounding Boston produce the highest percentage of multiple births (5.6%). The states of New Jersey and Connecticut, with similar demographics of wealthy professionals, are a close second and third in the rankings of multiple births. Unfortunately, multiple births do not scale well economically and result in a disproportionate toll on social systems. Since twins and triplets are born prematurely on average (born by ~35 and ~33 weeks, respectively), additional observation is necessary in hospital wards. Multiple births accounted for 35% of patient days in neonatal units in Boston in 2006[8]. Overall long terms costs to parents and social systems can be even more substantial due to the risks involved in multiple births including neurological and physical disabilities. These risks again stress the importance of pursuing the practice of single embryo transfer for IVF.

1.2 Embryo Metabolism and Selection

It is possible to have multiple fertilized eggs in an IVF cycle (typically 5-20, depending on the age of the donor) from which to select the most promising candidate(s) for implantation. Medications are often used in conjunction with egg collection from a donor or from the intended parent to stimulate ovaries into producing multiple oocytes, which increases probability of successful retrieval and laboratory fertilization[‡]. The only certain method of preventing multiple gestations is through single embryo transfer (SET)[10], which is a practice gaining much attention in recent years[5] (for example, SET has already been standard policy since 2003 in Sweden). It is thor>Urbanski</Author><Year>2006</Year><RecNum>1</RecNum><record><rec-ref-type name="Journal Article">17</ref-type><contributoDIN EN.CITE

Development of innovative selection metrics is very effective in both reducing multiple pregnancies, and reducing the total numbers of embryos to be transferred. Traditionally, cleavage rates of embryos in culture and qualitative morphology have been used exclusively for selection. In recent years, however, it has been suggested that metabolism may be a superior indicator of viability amongst morphologically identically embryos[13, 14].

There are several methods to measure the metabolism of cells. Many conventional techniques typically involve damaging the cell in question, or necessitate the use of radio-labeled substrates to target specific metabolic pathways[15]. Non-invasive assays therefore have the advantage of not disturbing cell integrity or function, which is of foremost importance when studying preimplantation embryos from a candidate pool. Non-invasive approaches, however, do have limitations in the depth of data that can be obtained. Rather than targeting numerous specific metabolic pathways, non-invasive assays provide a "black box" approach to infer glycolytic activity of cells. To estimate the glycolytic activity in a cell, it is possible to assay samples of used culture media to quantify both glucose consumed as well as lactate produced. Although such an approach can give an indirect measure of glycolysis, it cannot exclude the possibility that the lactate produced could have come from another source within the cell, likely from any

---

[‡] The oocyte is the cell from which the unfertilized egg, or ovum, develops following a series of meiotic divisions. When fertilized with a male's sperm, this cell is referred to as the zygote, which develops into the multi-cellular embryo at cleavage. For nomenclature, refer to Figure 1.1.

pyruvate generated from the metabolism of specific amino acids or from pyruvate taken up from the surrounding medium, or from the use of endogenous glycogen[15]. Notwithstanding such limitations, the ability to infer single cell metabolism using non-invasive procedures is a powerful technique.

A direct approach to analyzing biological compounds in nano and picoliter volumes was pioneered using specifically constructed glass micropipettes[16], and later modified by embryologists during the investigation of the nucleotide content in single mouse oocytes and embryos[17, 18]. Micropipettes can be used to manually dispense volumes of sample and fluorescent based reagent into droplets on microscope slides under mineral oil. After the fluids mix by diffusion and the reaction proceeds to completion, the resulting fluorescence intensity is directly proportional to the metabolite concentration in the media. Using this general approach of combining metabolite specific enzyme cocktails with culture media, a variety of metabolites concentrations such as glucose and lactate can be inferred[18]. Complete details of the existing assays and materials are reviewed in Chapter 2.

While very sensitive and capable of providing insights to the developmental process, there are numerous drawbacks to this micropipette technique which has hindered widespread clinical adoption. Performing the necessary fluorometric calibration and assays on many samples of used embryo media takes a several technician-hours for each metabolite. The glass micropipettes are custom made, and their volumes must be painstakingly calibrated prior to assays. Manual manipulation of samples with glass micropipettes limits the opportunity for automation, and precludes the possibility of integrating these assays in line with embryo culture.

Clinics that have developed innovative measurement techniques and implemented selection metrics based on the quantifiable metabolic activity of candidate embryos have in turn delivered significantly higher pregnancy rates[3, 13]. Nevertheless, the correlation between metabolism of preimplantation embryos and viability remains an open debate in the field due to the scarcity of quantitative chemical data. A high-throughput tool would be an invaluable asset to understand the metabolic factors that play the most important roles during the dynamic embryo culture period.

1.3 Suitability of Microfluidics

As the metabolite analysis process essentially involves repetitive steps of metering nanoliter volumes, mixing an enzyme cocktail and performing fluorometric measurements, the process is particularly suited for high-throughput automation in a microfluidic construct.

In recent years, microfluidics has demonstrated novel methods of studying and culturing cells. Microfluidics is a continually growing field of biotechnology, where fluid samples in the nanoliter to microliter range, may be manipulated in microfabricated channels in a manner analogous to the control of electrical signals in a microprocessor to automate complex biological and chemical laboratory procedures. Fluid flow at these small length scales is laminar, which presents both advantages (precise fluid control, reduced sample volumes, ability to perform biochemical processes in parallel, sample isolation) and certain tradeoffs (difficulties in fluid transport, mixing and surface chemistry)[19] when adapting this technology to miniaturize and automate biological protocols. Simplifying the laborious process of cell culture has been of particular interest in microfluidics, and recent research has delivered promising results and improvements to this field[20-22]. Within well-defined volumes comparable to the sample of interest, media, nutrients or toxins may be precisely targeted to individual cells via diffusion or advection, enabled by integrated valves and pumps. Microfluidic environments enable precise and repeatable control of temperature, pH, culture volumes and fluid concentrations[20, 23, 24].

Existing metabolic profiling techniques are particularly cumbersome and laborious and have gone unchanged for more than 20 years since their inception. For widespread adaptation in the receptive ART community, it is desirable to standardize and automate the selection procedure into a platform capable of carrying out the embryo culture and measurement procedures on individual embryos. The growing field of microfluidics is well poised to fit this role, and offers the potential to further improve the selection procedure in IVF.

1.4 Scope of Thesis

To address the need of controlled culture environments and improve embryo health and subsequent positive implantation rates, this thesis explores the development unique platforms of software programmable microfluidic devices for both culturing embryos as well as quantifying metabolite levels in the culture media. Such contributions, which will be of significant utility to the embryologist and the field of assisted reproduction, represent a diverse set of challenges in across biology, computer science and mechanical engineering.

This thesis is divided into four sections, each structured to elucidate contributions to the engineering field. First, a microfluidic platform is introduced to enable automation of the current micropipette metabolite assay. Next the methodology and systems for embryo culture in microfluidic environments are developed. With the goal of tying together the assay and culture techniques to a single platform, a microfluidic platform is invented in the third section which is capable of real time metabolic profiling of several cell cultures in parallel. Finally, new microfluidic design paradigms are conceived and implemented to extend device feature densities and capabilities for cell based assays.

1.4.1 Non-invasive metabolic assessment of single cells

Non-invasive techniques have been pioneered by embryologists to assess the metabolic activity of preimplantation embryos during IVF culture[13, 16]. While it is agreed upon that glycolytic rates are correlated with developmental success, metabolic analyses for candidate selection for implantation have not been widely adopted in the majority of clinics, as existing manual measurement techniques are simply too cumbersome and low-throughput.

To address standalone metabolite analysis, Chapter Two introduces a high-throughput microfluidic platform configured to automate the previously described enzyme based metabolic assays. The complete analysis system consists of the microfluidic device and supporting hardware, a fluorescence microscope equipped with a motorized shutter, a CCD camera which may be externally triggered, as well as the software to coordinate and run analysis routines. The sensitivity and repeatability of this platform is capable of measuring the metabolic activity of single embryos by analyzing sub-microliter samples of their spent media.

The microfluidic device consists of a flow channel network for loading and mixing inputs, as well as a control channel layer for orchestrating the movement of fluid in the flow layer. These devices are fabricated from the silicone elastomer polydimethylsiloxane (PDMS) using the well established multilayer soft-lithography fabrication process[25]. Input reservoirs to the chip contain all of the enzyme cocktails, calibration standards and a rinse buffer. Media samples for analysis are loaded into the remaining ports. Rather than coordinating measurements in nanoliter droplets, reactions and measurements are now completed on chip, in much less than a minute each. These non-invasive microfluidic approaches offer potential benefits of sample throughput, measurement repeatability and compatibility with existing cultures. As all measurements are automated through software, it is straightforward to record data and create custom mixing routines.

For the device to be of utility to clinical users, it is desirable to bring the microfluidic software and instrumentation to a state where a non-microfluidic specialist is capable of loading and analyzing samples without concern for the microfluidic details. To ensure the most accurate assays with this approach, thorough calibration studies were undertaken. Operational features of the microfluidic approach have been characterized, including minimum mixing times of enzyme and sample, the volume of media required for every assay, and robust operating pressures. Macro scale issues such as the device service life have also been examined. One of the key challenges was to provide a robust solution to the problems of culture sample transfer and loading. Additional considerations are also considered in the transition to a microfluidic construct, such as modification the enzyme cocktails to improve mixing times and minimum detectable fluorescent signal, which make the platform more attractive to IVF practitioners.

As a proof of utility of the microfluidic platform, spent culture media of individual preimplantation mouse embryos were metabolically profiled in a non-invasive manner. Less than 500 nl of collected media was required to infer the consumption of nutrients and production of waste products for a single embryo. Assays could be completed automatically over several hours using software routines, rather than requiring attended hours by a clinical technician

working with glass micropipettes to manipulate nanoliter droplets. Routines for image acquisition and data analysis also simplify the inconvenience of manual data logging.

The architectures and methods develop herein should also extend to analysis of other types of cells beyond IVF, as well as generate interest in automating related analytical assays. This is an important development as it may be used in conjunction with standard embryo culture techniques, and may also be integrated with microfluidic culture in the future. Before that next step is possible, however, the methods required for supporting embryo culture in microfluidic environments must be improved. These challenges are the goal of Chapter Three.

1.4.2 Microfluidic Based Embryo Culture

Extending the reach of this work in developing a means to non-invasively measure the amount of metabolites in culture media, methods are developed to enable embryo culture directly in microfabricated devices. Tools which both enable a repeatable and systematic means of single embryo culture, as well as the ability to later integrate microfluidic components to measure metabolic activity of individual embryos, should be of significant interest to an embryologist. With robust protocols for microfluidic culture, it will be possible to implement culture channels in a modular manner upstream of the architectures required for microfluidic metabolite analysis.

In conventional embryo culture, embryos may be cultured in microdroplets of media, in small groups of embryos in 1-20 µl of media in a Petri dish. To prevent evaporation, oil is simply overlaid on the droplets. While straightforward, this technique does not enable automatic methods for metabolite analysis to be integrated to the culture process. If it becomes possible to culture preimplantation embryos on chip with integrated valves and pumps, then it will be possible to develop complete culture systems with chemical measurement capability. To date, no research group has attempted to culture embryos in isolated, defined volumes on chip.

The field of embryo culture for IVF applications is of particular challenge for microfluidics. In contrast to many cells routinely cultured for research purposes, oocyte cells are particularly valuable and their safe retrieval from culture systems is a primary concern. The length scales of channels in microfluidic devices are generally in the 10 - 100 µm range. As the secondary

oocyte is the largest cell in the human body (~100 μm in diameter, which can increase to ~150 μm by the blastocyst stage), embryo samples can push the limits of volumes within a microfluidic channel. For reference, the murine samples used in the present research have typical oocyte and blastocyst diameters of ~70 μm and ~100 μm, respectively. Microfluidic systems must therefore be carefully designed to enable reliable sample loading and retrieval when working within the constraints poised by conventional microfabrication techniques[23, 25]. In addition to tight control over culture volumes, integrated microfluidics provide additional protection for the valuable embryo from the surrounding lab environment and thermal fluctuations. Potential avenues of this work enable studying the effects of single embryo culture in sub-microliter volumes, which will be precisely created by microfabricating channels of appropriate dimensions.

The surface area to fluid volume ratio also increases within miniaturization, which necessitates the consideration of surface interaction, either due to the absorption of small molecules and proteins from the culture media[20, 23], or due to the diffusion of toxins from the device walls into the culture chamber. Engineering appropriate systems and processes are key challenges in consideration of potential implications of the interaction between the fluid environments on sample development.

It has been hypothesized that numerous variables associated with laboratory culture systems (including accumulation of metabolites, such as lactate and ammonia and depletions of necessary nutrients, namely glucose and pyruvate) are related to the low yields of viable embryos *in vitro*. *In vivo*, the female reproductive tract is constantly active, resulting in movement of the embryo down towards the uterus as illustrated in Figure 1.1. This movement also washes the embryos through constantly changing physiological conditions through the oviduct to the uterus, maintaining a gradient for the supply of necessary nutrients and oxygen, and the removal of waste products[26]. As the *in vivo* environment is dynamic, it has thus been hypothesized that the use of an active system may be beneficial for *in vitro* culture.
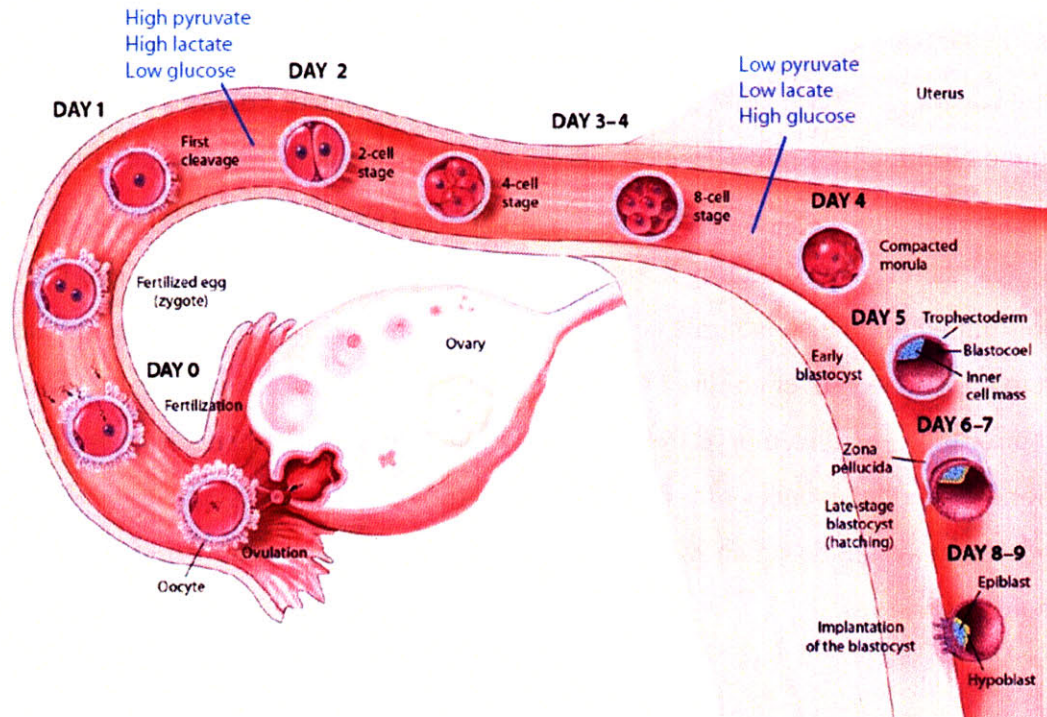
Figure 1.1: Developmental stages (and nomenclature) of an embryo in vivo (image courtesy of David K. Gardner and by Vitrolife AB, Sweden). For IVF, fertilization and the first three days of culture are performed in lab settings. More commonly over recent years, the culture is now continued until day five (blastocyst stage) in vitro prior to implantation, due to the advance of improved culture methods, which results in significantly higher pregnancy rates. The cleavage rates (for example, the transition from two-cell to four-cell through day two) are well characterized, and used as developmental markers in lab culture. Different embryo culture media is often used after the eight cell stage to imitate the dynamic environment of the female reproductive tract.

An embryo's metabolic requirements differ with developmental stage[27]. The pre-compacted embryo (prior to day 4) has a low metabolic activity and has a very limited capacity to utilize glucose. During the first few days an embryo generates energy from low levels of oxidation of pyruvate, lactate and amino acids. Approximately 95% of the zygote's energy is metabolized through the citric acid cycle (commonly known as the TCA cycle), while glycolysis of glucose accounts for only ~4%[4]. Proliferation and compaction are also stimulated by the presence of non-essential amino acids and EDTA[28]. In contrast, the embryo post-compaction (days 4 and 5) has a higher metabolic activity. It uses glucose as the preferred nutrient and requires a wider array of amino acids for cell proliferation and differentiation, as well as specific vitamins to maintain oxidation[28]. By this time, aerobic glycolysis and the TCA cycle now account for about 45% each of the energy metabolized, with the remaining due to the pentose phosphate pathway[4].

In response to the known metabolic preferences of the preimplantation embryo, different media formulations may be substituted across days of culture. The advent of sequential IVF media in the past two decades has been very effective in supporting the development of viable human embryos and blastocysts in clinical settings[27, 29, 30]. Standard microdroplet culture techniques, however, are limited to providing homogeneous concentrations of metabolites to embryos. Research to advance culture approaches would benefit from systems which are capable to more closely replicating and sustaining physiological chemical gradients.

As culture volumes are reduced into the sub-microliter per embryo range, secreted autocrine (or from neighboring samples, paracrine) growth factors are more concentrated and are believed to enhance development during the preimplantation period[31]. Standardization of such procedures and culture conditions is particularly important when comparing results from multiple cell samples, and also allows researchers in separate laboratories to replicate procedures using their own microfluidic platform. The advantage of using a microfabricated culture environment is to mimic the biological environment through agitation or recirculation of media, which may in turn be modeled from a mechanical and chemical standpoint. Techniques have been developed to improve the culturing via software control and feedback driven culture protocols[32, 33]. Related approaches in dynamic (continuous flow) perfusion culture are also reviewed in the context of studying and isolating the interactions between different types of cells.

Two of the primary challenges in enabling microfluidic embryo culture to be addressed in Chapter 3 are the issues of device preparation to prevent toxicity, and the development of methods to accommodate loading and retrieval of large embryos. Unlike engineered somatic cell lines used in routine biological research, gametes and embryos are particularly sensitive to their surrounding environment[23, 34], and are susceptible to poisoning by residual chemicals used to fabricate devices[25]. The second main challenge addressed is in developing a new type of channel and valve system capable of accommodating such large samples. Conventional multilayer soft-lithography devices use two layers of channels to form pneumatic valves integrated into the PDMS chip. Such valves have traditionally been restricted to flow channels in the 10-50 μm height range, and as such, are incompatible for accommodating embryos which are 100 μm or greater in diameter. Microfluidic devices with deep valves for sealing culture chambers

containing embryos will enable integration with microfluidic metabolite analysis, as well as address outstanding questions to improve static culture. Culture within specific volumes of media is necessary for our proposed method of embryo profiling by observing the uptake and production of metabolic factors over time. In this work, the largest multilayer soft-lithography valves to date are developed using a novel mold fabrication process, capable of sealing channels greater than 150 μm in height. These valves are compatible with standard control techniques and allow the safe passage of embryos into culture chambers.

Until now, no microfluidic research groups have tackled closed-volume issues in microfluidic embryo culture. While embryos have been cultured in open microchannel systems (not containing valves) by other research groups, effective media volumes have been an order of magnitude or two larger, and the devices are incompatible with our proposed methods of metabolic screening. This research is the first to culture embryos in truly confined chambers on chip, and irrefutably, in the smallest microfabricated volumes.

Microfluidic embryo culture will be applicable to pursue several open questions in the field of embryology. For example, it would be of particular value to determine if there exists an optimal volume for static culture, and whether that volume is limited by metabolite depletion. Also, since the *in vivo* environment is dynamic, it could be assessed whether gentle agitation or recirculation of media using integrated pumps improves overall culture. Regiments for replenishing spent media could be automated and reduce the need to manipulate samples manually.

1.4.3 Providing inline cell culture and metabolic profiling

Chapter Four describes the amalgamation of the engineering contributions introduced in Chapters Two (detection) and Three (culture), by the development of a microfluidic platform for integrated culture and metabolic analysis. Beyond simply incorporating these two functions on a single device, a unique scalable architecture is presented which can perform non-invasive metabolic assays on parallel nanoliter cultures of mammalian cells simultaneously. This platform is a major step towards an integrated culture system which may manage and metabolically assess several individual embryos in an automated manner.

Key features of the of the microfluidic networks developed in Chapter Two are adapted to automate metabolic assays on samples of spent culture media. It is necessary to locate this functionality directly downstream from on chip culture chambers. To improve the functionality of this platform and identify suitable operating conditions, this new device is run through a series of calibration studies. These studies cover device operations such as sample metering, rotary mixing for metabolic assays, as well as mixing for circulation of culture media over samples.

Rather than use embryos on this first generation system, mammalian cells lines are used as model systems. Individual culture chambers are capable of hosting approximately 100 cells each were designed into the chip. While these cells are more stable than murine embryos, it was still necessary to use the lessons learned in Chapter Three to enable robust cell culture on chip. Parametric cleaning and surface treatment studies were completed to determine the necessary protocols which would allow adherent cells lines to thrive in these microfluidic chambers. Results of these parametric studies would also be of interest to researchers sustaining subcultures of cells and tissues in microfluidic environments.

This high-throughput platform with both culture and chemical detection functionality has several implications in the fields of biological research. An integrated system can be used to implement feedback driven culture, and upstream treatment of samples can be modified based on the current metabolic measurements of samples. Robust systems for studying the metabolism of cells would also be of interest to medical researchers. Cancerous cells exhibit unique metabolic profiles in contrast to their normal state, which provides opportunities for identification and treatment. It may be possible to use metabolic inhibitors to target cancer cells by shutting down their main sources of energy, while healthy cells can adapt to alternative metabolic sources[35]. Enabling a systematic approach for quantifying the effectiveness of various cancer inhibitors on tissue and cell lines (or even combinations of inhibitors for simultaneously addressing different metabolic pathways) would be very powerful. Further, by using software driven routines it will be possible to pursue to the optimization of culture conditions of various cell lines based on their metabolic profiles.

1.4.4 Extending the capabilities of microfluidic architectures

In Chapter Five, a new design paradigm known as vertically integrated microfluidics is introduced and implemented to extend device feature densities for on chip assays. Vertically integrated microfluidic architectures will also open new avenues of research in fields of biotechnology including cell culture and protein crystallization, where sample density on chip is of paramount importance.

The majority of microfluidic devices in modern research consist of either one, or two layers of channels. Devices containing integrated MSL valves used throughout the thesis up to this point are in the later group, where the first channel layer containing fluidic samples of interest is regulated using a complimentary valve layer[25]. The size of channels and valves is a function of the samples to be studied. For example, mammalian cells with diameters of ~ 10 μm, necessitates that channels are probably 20 μm or larger. As such, the number of parallel assays completed in microfluidic constructs cannot necessarily be increased by miniaturization alone.

One way to alleviate this bottleneck is to increase the number of functional layers within a microfluidic device. The most complex microfluidic architectures to date have demonstrated 1000 fluidic storage chambers with a single flow layer device, necessitating a stamp sized footprint (~ 25 mm x 25 mm). Assuming a constant feature size, to increase the total number of features by ten-fold, would require a footprint of approximately 80 mm x 80 mm. Twenty-fold more chambers would require a device footprint with a staggering 110 mm x 110 mm base. Large areas significantly increase the likelihood for assembly defects, and the large field of view complicates sample inspection. In this chapter, it is reasoned and demonstrated that a preferable way to increase the number of features on a microfluidic devices is to add layers, akin to performing biological research in a skyscraper as opposed to a bungalow.

Methods to independently address layers of microfluidic chambers are developed, which are key to this technology. Vertical multiplexors allow a user to address one functional flow layer at a time, while reducing the total control overhead. In this manner, experiments between layers remain independent, while on chip resources such as reagents and control valves are provided by common inputs.

Optical techniques are reviewed, and the necessary conditions for monitoring samples in overlapping layers independently are discussed. Unique manufacturing techniques are developed to allow the fabrication of such complex systems. Limitations of existing thermal assembly techniques have prohibited the previous development of such systems. If thermal techniques had to be used, the assembly time scales linearly with the number of layers. As such, a ten layer device would take at least ten times as long to manufacture. The last thing microfluidic researchers desire is more time spent fabricating devices. A hybrid thermal-plasma approach is devised, where the forgiving nature of thermal bonding is combined with the parallel processing nature of plasma bonding. Complete details of these processes are provided in Chapter Five.

With the conceptual nature of this work in place, applications of this powerful technique are demonstrated. In the first set of applications, large scale fluidic storage arrays are implemented. For a proof of principle, it is shown that vertical large scale integration (VLSI) can be used to implement networks with 2^{14} (= 16384) independently addressable storage chambers located across eight flow layers, while necessitating a device footprint of only 25 mm x 25 mm. The number of features can be increased by simply adding more layers.

Relating the implications to biological research, vertically integrated devices are then implemented for cell based toxicity assays. Different architectures are developed for row & column based toxicity assays[36], as well as methods for addressing sub cultures on chip independent from one another. The techniques and design principles pioneered herein will be of interest to biologist and engineers working to automate demanding high-throughput applications such as protein crystallization and drug discovery. The manufacturing techniques may also provide inspiration to alleviate other aspects of microfluidic assembly carried out in the microfluidic community.

1.5 Research Outlook

It is of particular interest to use feedback driven agitation schemes in microfluidic systems, which could be based on the metabolic activity of the present concentration of nutrients and waste products, in relation to the metabolic activity. By studying embryo nutrition on chip, it should possible to formulate more suitable culture conditions and develop non-invasive tests of embryonic health prior to transfer[37]. Microfluidics may present one of the most promising viable options to readily adjust the culture conditions dynamically.

Non-invasive measurement techniques have become an integral method of embryo profiling for SET, but the laborious and time consuming nature of existing tools restricts the amount of data that can be gathered from the cells during the culture process. Current techniques for assaying metabolites are sufficiently cumbersome that they are not useful clinically. Automatic, real time metabolite monitoring may enable the ability to dynamically modify and optimize culture conditions *in vitro*. High-throughput tools such as those introduced in this work will also help to address the difficult questions relating metabolism and developmental potential of embryos.

Microfluidics offers the opportunity to adapt precise fluid metering and measurement techniques to approach the limit of continuous and automatic monitoring of single embryo culture conditions. This work to automate such procedures through novel methods should increase effectiveness and practicality of non-invasive embryo selection to a broader audience in assisted reproductive medicine. By combining single embryo culture and real time analysis functionality into a single automated platform, parameters affecting embryo viability may be studied and understood with unprecedented accuracy. As these tools work to improve the probability of healthy pregnancy using SET and reduce the expected number of ART cycles per pregnancy, they may reduce financial burden and disappointment of patients undergoing these procedures.

Chapter Two - Non-invasive Microfluidic Metabolic Profiling of Single Cells

2.1 Introduction

Metabolomics represents an important approach to studying functional biological systems, and provides valuable complementary information to that obtained from gene and protein expression studies. The development of new tools and techniques for the analysis of cellular metabolites (specifically various nutrients and waste molecules generated by living cells) has found important application in exploring directed evolution, drug toxicity and cancer[38, 39]. Metabolomic studies of single cells are advantageous because the complexities associated with cellular heterogeneity can be avoided. For studies of organisms composed of a single or small number of cells, such as embryos during early development, single cell sensitivity is an absolute necessity.

There is also a strong impetus from the clinical field of assisted reproduction to develop non-invasive methods for evaluating the health and developmental potential of embryos. The current prevailing method for selecting embryos in clinical *in vitro* fertilization (IVF) programs is based on physical characteristics identified through light microscopy. It is well recognized within the clinical community that morphology is not only subjective but a relatively poor indicator of developmental potential[40]. As a result, more than one embryo is often transferred to the uterus in an IVF cycle, frequently leading to multifetal pregnancies which increase risks to the pregnancy, the mother and the child[41]. In an effort to move toward single embryo transfer, a variety of non-invasive approaches to assess embryonic developmental potential are being developed[42].

One of the most intensely investigated biologic processes in early embryonic development is metabolism. Studies over the last four decades have revealed that the early embryo undergoes dramatic changes in its metabolism, switching from a low to a high basal metabolic rate[43]. Commensurate with this increase in metabolic activity is a switch in utilization of nutrients, switching from a pyruvate to a glucose based metabolism (following Figure 1.1)[43]. These metabolic changes are similar to those seen when a variety of cell types undergo cancerous transformation[44]. Furthermore, it has been demonstrated that situations in which embryonic development is abnormal are associated with alterations in metabolism. Studies of murine embryos have shown that those blastocysts with an elevated glycolytic rate have impaired developmental potential[4]. Energy metabolism may also serve as a biomarker for the developmental potential of human embryos, but no appropriate prospective trials have been performed to date[45]. Much of the reason for the limited data on embryonic metabolism resides in the challenges of measuring metabolites in the small volumes of media that are used for culturing individual embryos.

The most common means of non-invasively assessing metabolism of embryos has been to evaluate what embryos consume and produce through analysis of culture media. Several studies have used fluorometric enzymatic assays to evaluate utilization of the energetic substrates, specifically glucose, pyruvate and lactate. For these assays, the metabolite of interest is a substrate for an enzymatic reaction that either consumes or produces NAD(P)H, which fluoresce when in the reduced form. A number of important metabolites, including glucose, pyruvate, lactate, citrate, and several amino acids can be readily assayed using NAD(P)H enzymatic assays[16]. For example, pyruvate is assayed by measuring the consumption of NADH in the lactate dehydrogenase-catalyzed reaction. Reactions are detailed further in section 2.2, and Appendix A. Due to the very small samples, often in the sub-microliter range, these assays are performed using constriction pipettes that can be calibrated to the low nanoliter range[46, 47]. The drawbacks of this technology are that the method is incredibly labor intensive and pipette construction is complex. Other recently developed approaches with promise for non-invasively evaluating embryonic metabolism include the evaluation of oxygen consumption using a variety of specialized oxygen probes, amino acid turnover using high-performance liquid chromatography (HPLC), and metabolic profiling using various forms of spectroscopy[48-51]. All

of these studies seem to support the hypothesis that embryos with differing developmental potential can be segregated by metabolic activity, yet much work remains to be done to determine what specific markers should be evaluated and how they should be detected.

An array of microfabricated approaches have been previously developed with the shared goal of studying cellular metabolism, many of which are technically more complex and may not be suitable for routine clinical use. Electrochemical microphysiometers have been used for monitoring changes glucose and lactate concentrations in cell cultures using both continuous[52] and discrete[53] fluid flow approaches that necessitate larger sample volumes and are prone to difficult calibration. Scanning electrochemical microscopy (SECM) has been demonstrated as a non-invasive means for studying the metabolism of single cells, though probe fouling, instrumentation as well as calibration can also be challenging. Through SECM, oxygen consumption of single bovine embryos has been measured with relation to embryo viability[54], and custom probes for glucose and lactate have recently been used to generate two dimensional concentration maps surrounding individual cancer cells[55]. Picoliter chambers with integrated electrodes have been used for the quantification of glucose and lactate changes of stimulated single heart cells[56, 57]. In addition, devices have also been fabricated for monitoring changes in glucose and lactate from cells attached to beads with NAD-linked enzyme assays[58]. These specialized methods exemplify the challenges involved in developing flexible systems that are compatible and can be integrated with embryo culture.

These specialized methods exemplify the challenges involved in developing flexible systems that are compatible and can be integrated with embryo culture. Continued advancement in this field also conveys the desire and excitement of studying metabolism at a single cell level with a robust system. With the goal of improving the ability to analyze media for substrates of energy metabolism, an automated microfluidic platform for performing NAD(P)H-dependent enzymatic assays has been developed. Development of such a system represents a multitude of mechanical engineering challenges and the contributions described herein would be of particular interest to researchers in the fields of both engineering design and metabolomics.

2.2 Assay Background and Existing Clinical Protocols

There are several methods to measure the metabolism of cells. Many conventional techniques typically involve damaging the cell in question, or necessitate the use of radio-labeled substrates. Non-invasive assays therefore have the advantage of not disturbing cell integrity or function, which is particularly important when studying preimplantation embryos from a candidate pool. Non-invasive approaches however, do have limitations in the depth of data that can be obtained. For example the use of radio-labeled substrates can assist in determining the relative activity of a specific metabolic pathway, such as the use of [5-^{3}H] glucose to measure the activity of specific pathways[15].

Rather than targeting numerous specific metabolic pathways, non-invasive assays provide a "black box" approach to infer glycolytic activity of cells. To estimate the glycolytic activity in a cell, it is possible to quantify in the surrounding media, both glucose consumed as well as lactate produced (glycolytic activity can be calculated on the basis that 1 mol glucose produces 2 mol lactate, and is often expressed as a percentage[4]). Although such an approach can give an indirect measure of glycolysis, it cannot exclude the possibility that the lactate produced could have come from another source within the cell, likely from any pyruvate generated from the metabolism of specific amino acids or from pyruvate taken up from the surrounding medium, or from the use of endogenous glycogen[15]. Blastocysts with elevated glycolytic activity during the preimplantation period (with a lactate production beyond that which can be accounted for by glucose consumption) presumably waste energy reserves[4], and are suggested to be less viable for IVF transfer. It is proposed that these blastocysts are less likely to implant in (the relatively oxygen deprived) lumen of the uterus due to premature exhaustion of their necessary glycogen stores[4]. Notwithstanding the limitations to identify all sources of energy expenditures, the ability to infer single cell metabolism using non-invasive procedures remains a powerful technique.

2.2.1 Microdroplet Assays

A direct approach to analyzing biological compounds in nano and picoliter volumes was pioneered using specifically constructed glass micropipettes[16]. Micropipettes were used to manually dispense volumes of sample and fluorescent based reagent into droplets on microscope

slides under mineral oil. An example of a custom fabricated glass micropipette is illustrated in Figure 2.1.
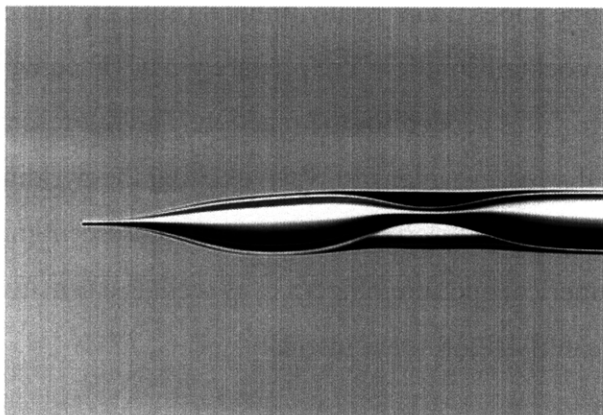
Figure 2.1: A doubly constricted glass micropipette calibrated to dispense 1 nl samples (Image courtesy of Mark T. Johnson and Fertility Labs of Colorado).

After the fluids mixed by diffusion and the reaction had gone to completion, the fluorescence intensity of the droplets was measured directly under oil to quantify the product of the assay. This simple micropipette assay was modified by embryologists during the investigation of the nucleotide content in single mouse oocytes and embryos[17, 18]. Rather than using a fluorescent reagent, the procedure was a miniaturized version of existing methods of enzymatic analysis in which the nucleotides NADH and NADPH are generated or utilized in enzyme based reactions, as described by Lowry[46]. These pyridine nucleotides are excited around 340 nm, and when the reduced forms are excited with UV, they emit fluorescence at 450 nm and above (These nucleotides fluoresce when excited where the oxidized forms, NAD+ and NADP+ do not). Using this general approach of combining custom made enzyme cocktails with culture media, a variety of metabolites and enzymes can be studied[18].Fluorometric assays for metabolites and enzymes are based on the generation or utilization of the reduced pyridine nucleotides, NADH and NADPH in coupled enzymatic reactions (See Appendix A).

The intensity of the measured product is related to nominal concentrations using calibration standards for the metabolite of interest. Thus it is necessary to create calibration curves for every metabolite prior to every assay (glucose, lactate, and pyruvate) over the range of interest. When the details of the conventional measurement technique are briefly reviewed, the applicability to automation through microfluidics becomes apparent.

Fluorometric analysis of metabolites in culture media have been conventionally performed in 1-20 nl droplets on microscope slides under heavy mineral oil to prevent evaporation. For each assay, metabolite specific cocktail solutions are prepared in advance which contain a buffer and all of the co-factors and enzymes needed for the reaction. The fluorescence of each droplet is measured by quantifying fluorescent intensity when exciting the pyridine nucleotides in the cocktail by a UV light source. This is done using an epi-fluorescent microscope equipped with a DAPI filter set, a high numerical aperture objective, as well as a sensitive CCD camera or photomultiplier tube to quantify fluorescent intensity.

To start the assays, 1-5 nl of media sample is added to the cocktail drop to initiate a reaction (the volumes may differ based on the particular assay, but as a rule of thumb, 1 part of media sample is mixed with 10 parts of enzyme cocktail). The drops on the slide are then left until the reaction has gone to completion. As mixing occurs by diffusion only in these microdroplets, mixing can take anywhere from several minutes to an hour. All droplet reactions are prepared in a serial manner using a micropipette (sometimes attached to a micromanipulator) under a microscope. The difference in fluorescence between the reagent cocktail drop before and after addition of the sample should be linear within the concentrations to be assessed. It is necessary to measure a range of calibration standards with known amounts of glucose, lactate and pyruvate for each experiment to determine fluorescence range of the substrate. Acceptable linear regression values for intensity vs. concentration curves are $R^2 > 0.99$.

To perform metabolic assays on cells or embryos, clean drops of medium are prepared under oil in a dish. Depending on the sample, droplets may be in the 50 - 1000 nl range (larger volumes are typically used for human samples). Individual embryos are transferred from their original group culture into these temporary incubation drops using small glass pipettes to minimize cross contamination from previous media. Linear rates of uptake or production may be determined for each cell by taking subsequent samples from the incubation pool at regular 30 - 60 minute intervals. Control droplets which do not contain embryos are also often sampled in parallel to account for any breakdown of media that may have occurred during this period. If the collected aliquots of media are not to be analyzed immediately, they may be frozen, and measured at a

later period. This is particularly helpful in the current research, as samples prepared in IVF clinics may be analyzed offsite.

There are numerous drawbacks to the existing techniques. Performing the calibration and assays often takes a period of several hours as measurements for each metabolite are performed in triplicate in a clinical setting. The glass micropipettes are custom made, and their volumes must be painstakingly calibrated using radio labeled techniques prior to use.

Shapes of the microdroplets are prone to change experiment to experiment, and the free surfaces of droplets are dependent on the wetting properties of the glass, cocktail and oil. The curvature of microdroplets also leads to variation in fluorescence imaging. It would be ideal to work with identical volumes for every measurement, and to not have to mix nanoliter droplets manually in order to obtain important metabolic information. As the metabolite analysis process essentially involves repetitive steps of metering nanoliter volumes, mixing an enzyme cocktail and performing a measurement, the process is particularly suited for high-throughput automation in a microfluidic construct. As a benchmark to microfluidic based measurements, these conventional microfluorometric assays were also performed in calibration studies for this chapter using doubly constricted micropipettes[47].

2.2.2 Enzymatic Assay Preparation

Metabolite specific enzyme cocktails were prepared following Leese and Barton[18] and Gardner and Leese[59]. Complete recipes for the metabolic cocktails used, as well as additional assay detailed are presented in Appendix A. The assay mechanisms for the metabolites of interest are presented below based on Gardner and Leese. In the case of pyruvate, measurements are based on the reduction in NADH. For lactate and glucose, fluorescence is due to the generation of the pyridine nucleotides NADH and NADPH, respectively.

Pyruvate Assay:
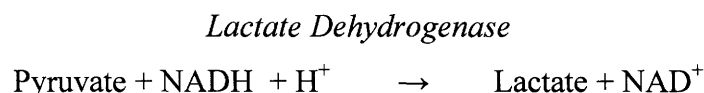
$$\textit{Lactate Dehydrogenase}$$
$$Pyruvate + NADH + H^+ \quad \rightarrow \quad Lactate + NAD^+$$
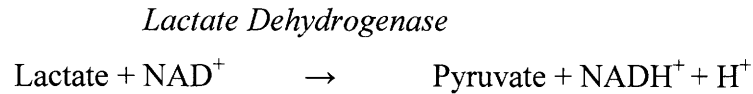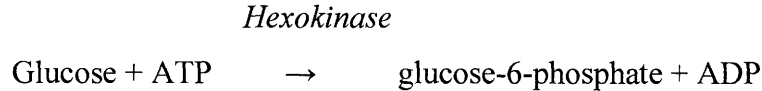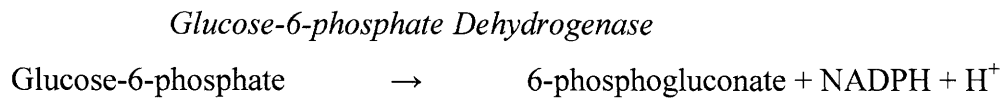
Lactate Assay:

Lactate Dehydrogenase

$$\text{Lactate} + \text{NAD}^+ \quad \rightarrow \quad \text{Pyruvate} + \text{NADH}^+ + \text{H}^+$$

Glucose Assay:

Step 1:

Hexokinase

$$\text{Glucose} + \text{ATP} \quad \rightarrow \quad \text{glucose-6-phosphate} + \text{ADP}$$

Step 2:

Glucose-6-phosphate Dehydrogenase

$$\text{Glucose-6-phosphate} \quad \rightarrow \quad \text{6-phosphogluconate} + \text{NADPH} + \text{H}^+$$

Standards for glucose, lactate and pyruvate were prepared by adding known amounts of the particular metabolite to either water or media formulations. Single use glucose and pyruvate aliquots were stored at -80°C, and lactate cocktails were prepared fresh immediately prior to experiments.

2.3 Experimental

2.3.1 Device Fabrication

Microfluidic detectors in the present study were prepared by the process of multilayer soft lithography using PDMS[25] (Sylgard 184, Dow Corning). Devices were fabricated using the bottom-actuated valve configuration suitable to closing deep aspect ratio channels[60]. A three layer photoresist process was used to fabricate the flow mold on a silicon wafer. Briefly, a 20 µm thick layer of SU8 10 (Microchem) was first used to pattern input sieves near the device interconnects, which prevented debris from entering the channel network. Next, a 50 µm thick layer of positive tone AZ 50 XT (Clariant) was aligned and patterned. After development, the AZ was reflowed by placing the wafer on a hotplate at 120°C to create channels with round cross sections followed by a hard bake overnight at 130°C. Finally, a layer of 50 µm thick SU8 50 was aligned to the existing AZ, and used to add new channels segments with rectangular cross sections in the mixing chamber for fluorometric imaging. Sufficiently hard baking the base AZ

layer made the resist impermeable to most developers and allowed subsequent processing with SU8. The control wafer for the detector chip was created using two layers of 25 μm thick SU8 10. The second layer of SU8 was patterned over the base layer where valves were located. This made it unnecessary to neck down the width of the control channels where the lines crossed flow channels and enabled faster valve performance. Molds were treated with silane to facilitate PDMS casting. The flow and control layers of the device were cast and thermally bonded at 80°C using 5:1 and 20:1 PDMS, respectively. After curing of the two layer device for approximately 36 hours, input ports were punched with biopsy tools and chips were cleaned using ethanol and nitrogen. Individual detector chips were bonded to pre-cleaned 1 mm thick glass slides using a 30 second air plasma treatment on target surfaces at low RF power (Expanded Plasma Cleaner, Harrick Plasma, Ithaca, NY).

2.3.2 Embryo Culture and Sample Preparation

Female F1 hybrid (C57Bl/6 X CBA) mice at 5 weeks' age were superovulated with 5 I.U. pregnant mare's serum followed 48 hours later with 5 I.U. of human chorionic gonadotropin (Sigma) and then immediately mated with F1 hybrid males. Zygotes were collected from the oviducts 21 hours after mating and cultured individually in 1 μl microdroplets of embryo culture media blanketed by paraffin oil in a Petri Dish. Every 24 hours, the embryos were transferred to microdrops of fresh media and the dishes containing the spent media were frozen at -80°C until assays were performed. In this non-invasive approach, sampling is not performed from droplets containing embryos; rather pools of spent media are used for assays. Embryos were cultured in modified G1 medium for the first two days and modified G2 medium for the second two days[61]. To facilitate metabolic analysis, the glucose and pyruvate concentrations were adjusted to 0.3 mM and lactate was omitted from the media. Media were supplemented with 5 mg/ml human serum albumin prior to culture. All cultures were performed in an incubator at 37°C with 5% O_2 and 6% CO_2. Developmental progress of each embryo was assessed daily by examining the morphology. Half of each spent media drop (500 nl) was transferred to a replicate plate and then both sets of plates were frozen at -80°C until used for metabolic analysis.

Variations of this media sampling approach are also possible, always with the intention of protecting samples. For example, if embryos were being cultured in larger volumes (~10-20 μl),

it is possible to transfer samples to smaller temporary media droplets for predetermined amounts of time before being returned to their original droplet. Again, this would be performed to assess changes is metabolite levels per embryo per unit of time within these temporary droplets. By using smaller volumes, changes in substrate concentrations are more dramatic and easy to detect.

2.3.3 Hardware and Automation

Parallel microfluidic workstations were developed both at M.I.T. and Fertility Laboratories of Colorado. Open source JAVA based software platforms at both locations were used to orchestrate all device operations, image acquisition and data analysis[62].

Microsolenoids were used to control the integrated multilayer soft-lithography valves, and were controlled by JAVA software as previously described[62, 63]. Typical operating pressures were 15 psig for the control valves, and 3 psig on sample and reagent inputs. Fluids were interfaced to the device using Tygon tubing (500 μm ID, Cole-Parmer) and sterilized stainless steel pins (New England Small Tube Corp).

The device was mounted on an Olympus IX-71 epifluorescent microscope equipped with a long working distance 20X objective (NA = 0.45), a neutral density filter (ND 0.25), a Sutter Smart Shutter and a Prior motorized stage. Fluorescent reaction products were imaged through a DAPI (340 nm/420 nm, EX/EM) filter set. The objective was focused on a microchannel with a rectangular cross section within the mixing section of the chip for image acquisition.

A cooled CCD camera (Apogee Alta U2000) was externally triggered using JAVA and custom scripts through MicroCCD (Diffraction Limited). 16-bit grayscale images were captured for every sample measurement using an exposure time of 0.5 seconds at 2 x 2 binning and a CCD temperature of 0°C. The shutter was synchronized with image acquisition to prevent photobleaching of reaction products prior to measurements. ImageJ (NIH) routines were integrated into the JAVA control software to analyze acquired images in real time. Area averaged background intensity on the chip was subtracted from fluorescence intensity in the microchannel for each measurement.

Calibration standards with known amounts of glucose, lactate and pyruvate diluted in G1 or G2 culture media were used to generate calibration curves to relate measured fluorescent intensity to metabolite concentration. It was possible to use standards containing known amounts of all three metabolites in the same stock, which reduced the number of required fluid inputs to the device. Metabolite specificity of enzyme cocktails was ensured through calibration studies. Calibration curves were highly linear in the range of 0-1 mM for the metabolites glucose, lactate and pyruvate, consistent with the values expected physiologically in embryo culture media. Detection limits were estimated to be below 10 μM for the three metabolites of interest using the current imaging settings, although it is straightforward to use a variety of methods such as longer camera exposures or deeper detection channels to provide more signal, if it becomes necessary to extend fluorometric limits in future work. Linear regression values on calibration curves typically exceeded $R^2 = 0.999$ (in conventional microdroplet assays, $R^2 > 0.99$ on five point calibration curves are considered sufficient). In additional calibration trials, linearity was obtained in the 1-5 μM range, is indicative of a very high signal to noise ratio when imaging in microfabricated channels. Standards were interspersed alongside media samples on chip during analysis routines for fluorometric calibration. Slope and intercept values for fluorometric calibration of each metabolite were updated continuously over the course of routines to account for any changes in background light levels, or degradation of enzyme.

2.4 Detector Design and Performance

The microfluidic detector device consists of a flow channel network for loading and mixing inputs, as well as a control channel layer for orchestrating the movement of samples and reagents. Input reservoirs to the chip contain all of the enzyme cocktails, rinse buffer, and ports for loading multiple media samples for analysis. A schematic of the microfluidic detector is shown in Figure 2.2.
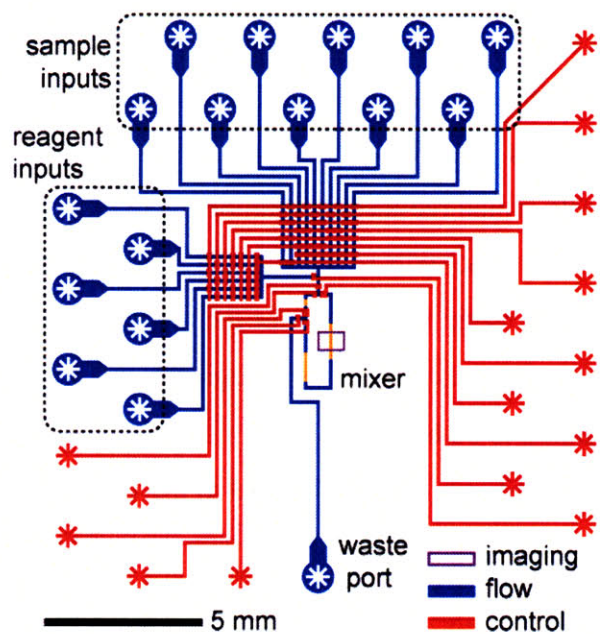
Figure 2.2: Schematic of the microfluidic metabolite detector fabricated using multilayer soft lithography. Red and blue features denote control and flow layers of PDMS, respectively. Six fluid inputs are reserved for supply of enzyme cocktails and wash buffers, while ten inputs are used for loading media samples and calibration standards. To perform assays, samples of culture media are metered into the central mixing ring and combined with a metabolite specific cocktail. A fluorometric measurement is recorded after complete mixing (camera field of view denoted in purple). Finally, the mixer contents are washed prior to the next assay.

Initial studies were performed with calibration standards to establish the fluorometric sensitivity of the microfluidic detector, which relies on the detection of UV-excited pyridine nucleotides, NADH and NADPH, in enzyme coupled reactions. Inlet and outlet channels on the rotary mixer were arranged to prepare ~1:10 compositions of media samples to enzyme cocktails, and samples were mixed using a rotary peristaltic scheme[64]. To facilitate uniform fluorescence signals, detection channels of rectangular cross section were included in line with the rounded channels containing valves.

Figure 2.3 demonstrates the high degree of linearity obtained when sampling dilute NADH standards in 50 μm tall channels. The results of these fluorometric assays with dilute standards, ensures that the optical depth of the channels is sufficient. The field of view imaged covers a channel volume of approximately 2.2 nl. While taller channels were previously tested, 50 μm tall channels provided an acceptable balance between sample volume consumed and reliable

fluorescent signal-to-noise ratio. Rather than performing measurements in inconvenient oil covered nanoliter droplets, reactions are now completed serially in a fixed channel network.
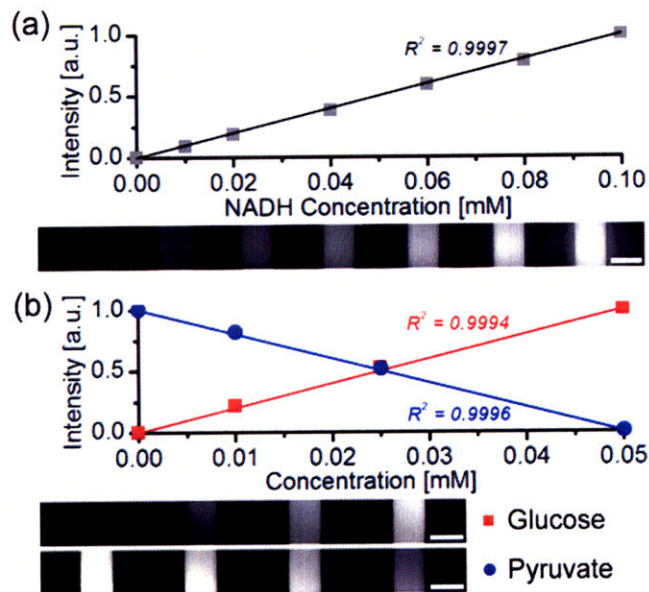
Figure 2.3: Example calibration curves and corresponding microchannel images. (a) Assessment of device sensitivity with dilute NADH. (b) Typical metabolite calibration curves and typical microchannel images demonstrates linearity of the microfluidic detector. Scale bars indicate 100 μm.

The amount of embryo media per sample available for assays is extremely limited, driving the need to consume minimal sample per assay to enable replicate measurements. In light of these considerations, a peristaltic pumping scheme regulated the amount of media consumed when transporting media samples from the input wells into the mixing ring[65]. Sample flowrates were calibrated at a variety of pumping duty cycles (over 10 minute averages) to determine the minimum achievable loading time. Input flowrates were approximately ~0.5 μl/s without active regulation, which reinforces the necessity of this metering approach. While the flow of samples was regulated, regular pressure driven flow was used on reagents and wash buffers to minimize loading time. The on-chip metering sequence and measured flowrates are illustrated in Figure 2.4 (For the interested reader, movies of the metering and mixing operation are available at http://pubs.acs.org).
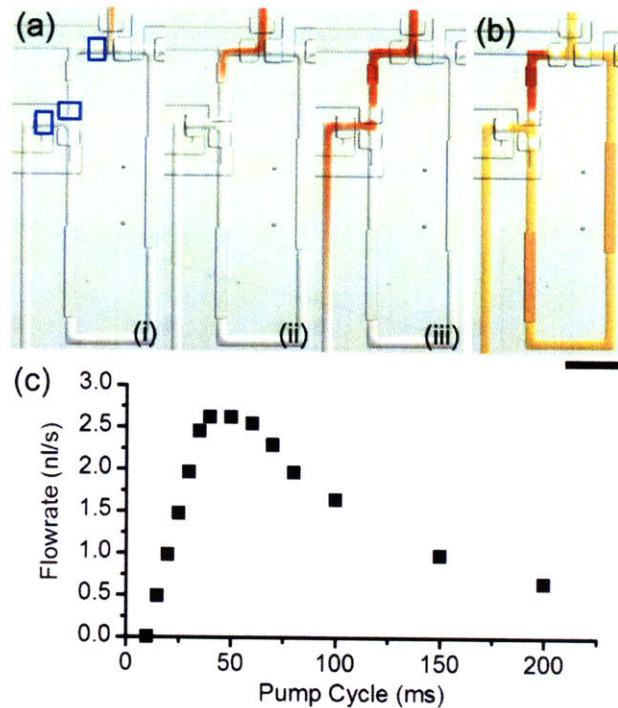
Figure 2.4: Peristaltic metering is used to regulate the amount of valuable sample consumed per assay. (a) Three valves, outlined in blue, are actuated in sequence to meter samples into the mixing ring. The path of a sample through the upper left of the mixer is illustrated with red food dye in frames (i) - (iii). (b) Enzyme cocktail (presented with yellow food dye) is loaded through the opposite path of the ring prior to the mixing operation. Scale bar indicates 500 μm. (c) The flowrate of samples into the mixing ring was calibrated to determine the optimal loading rates and required sample volume. Each data point represents a 10 minute average at an input pressure of 3 psig.

Every measurement requires metering a volume of media sample, and subsequently actively mixing it with an enzyme cocktail. To increase the throughput of the detector chip, optimization studies were also completed for both metering and mixing operations. The results of the throughput studies are presented in Figure 2.5. Using glucose standards as mock inputs, the linearity of calibration curves was assessed as a function of the amount of sample consumed. It was found that curves were dependent only on the total volume of sample metered, and not on the rate of metering. While the sample segment of the mixing circuit accommodates only 4 nl, it was found necessary to meter more than this volume from the input channels to ensure the greatest level of linearity due to Taylor dispersion during transport and potential cross contamination in shared input channels. Figure 2.5 (a) illustrates that at least 15 nl of media per assay should be used to ensure complete filling of the 4 nl chamber. To compensate for any device to device variances, 20 nl was metered for each assay which takes approximately eight

seconds based on the flowrate calibration. The minimum volumes required for sampling are in excellent agreement with the volume of the channel between the sample multiplexor and the mixing ring, also illustrated in Figure 2.5. The can serve as a simple design guideline for estimating minimum sample volumes when scaling up to more complex devices in the future (such as those developed in Chapter 4).

A similar optimization study was performed to determine the minimum required mixing time. The rate limiting process of the mixing operation was both a function of mechanical mixing and the rate of the enzyme reaction after fluids have been fully mixed. Maximum linearity was obtained in approximately 20 seconds of mixing for the three duty cycles tested. By contrast, conventional microdroplet assays are completed by diffusive mixing alone, which imposes a delay of at least several minutes per sample prior to imaging[13]. In addition to the metering and mixing operations, injection of cocktail and image acquisition each required approximately one second each. The mixing ring was also flushed with water between successive measurements, which resulted in a total operating time of just over 30 seconds per assay. Complete runs consisting of ten replicate measurements of ten samples (including calibration standards) with three metabolites could be completed unattended in less than three hours. For more complex experiments, the architecture may be scaled to accommodate additional enzymes and sample input lines.
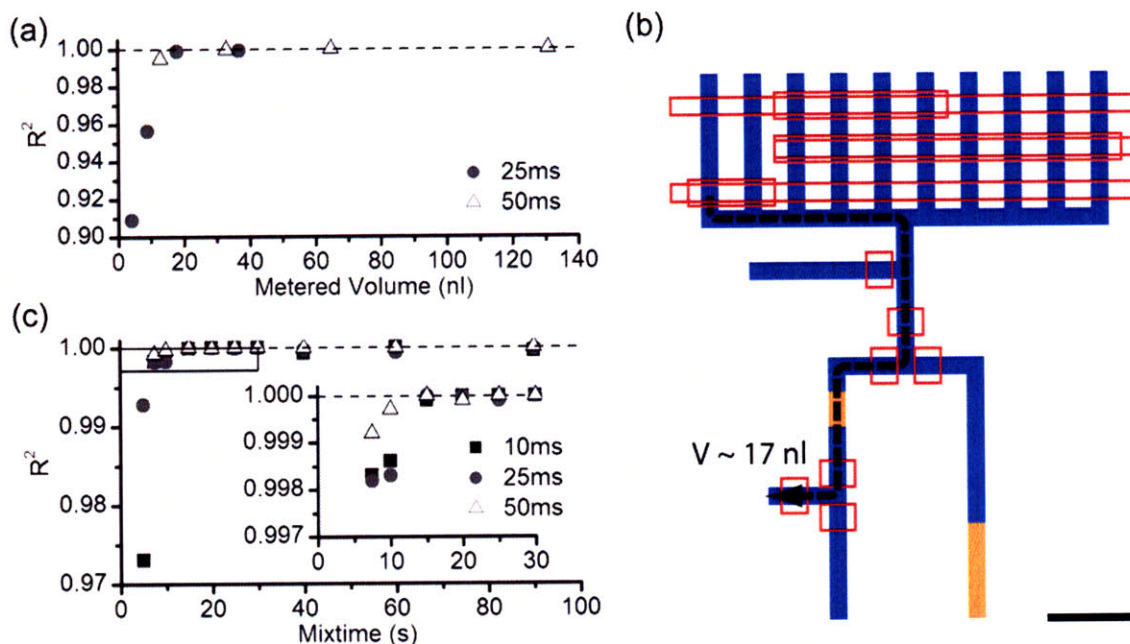
Figure 2.5: Optimization of microfluidic metering and mixing operations. (a) Four point glucose calibration curves were prepared under a variety of conditions. The linear R^2 regression of calibration curves is presented as a function of sample volume assayed. Linearity is independent for sample volumes greater than 15 nl, and metering rates follow from Figure 2.4. (b) The minimum metered volume for samples corresponds closely with the nominal path volume between the sample multiplexor and the mixing ring. (c) Linear regressions as a function of rotary mixing time with enzyme cocktail prior to fluorometric imaging. Based on these calibrations, 20 nl of sample is metered for every assay, and actively mixed for 20 seconds with cocktail.

2.4.1 Detection Accuracy and Repeatability

It was observed that the fluorescence measurements of repeated samples would decline over several hours after chip setup. The pyruvate assay was most susceptible, presumably due to photobleaching or oxidation of the NADH present in the cocktail. Microfluidic routines, therefore, were written to ensure frequent calibration of all three metabolites, and values for slope and intercept of linear curves were updated continuously. Culture sample measurements were referenced using interspersed standards loaded onto chip, such to minimize inaccuracy due to diminished signal. A replicate run was discarded if the calibration curve did not exceed $R^2 =$ 0.99. The high-throughput performance of the system allowed many (typically ten or more) replicate measurements to be performed for each sample and metabolite to ensure consistency. The ability to calibrate continuously and perform unattended replicate measurements on samples

represents distinct advantages of the microfluidic approach in contrast to the manual droplet technique.

Parallel analysis of mock samples was completed with standards containing known concentrations of glucose, lactate and pyruvate to assess accuracy and repeatability of fluorometric measurements. The data presented in Figure 2.6 shows very good agreement between nominal and measured values, with accuracy on ten replicate measurements typically within 5%, and standard deviations of approximately 20 µM across these three metabolites.
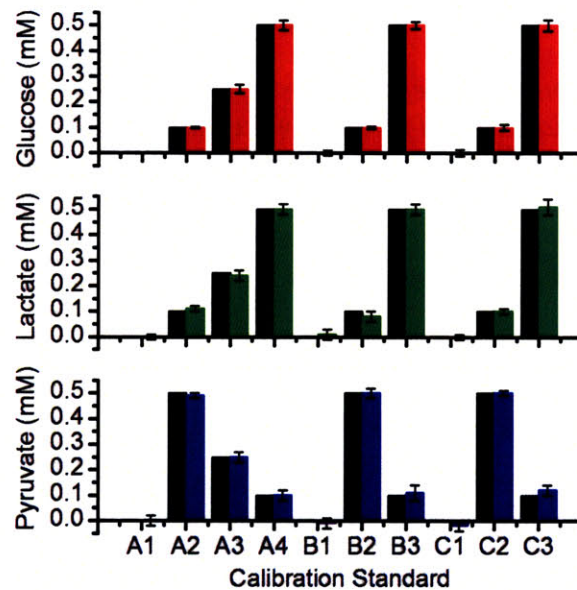
Figure 2.6: Calibration curves to demonstrate repeatability of ten samples measured in parallel, with sample types A, B and C, based in water, G1 media and G2 media, respectively. Black columns indicate expected concentrations for each metabolite. Error bars represent the standard deviation on ten replicate measurements.

In addition, calibration measurements were carried out using the same device for several consecutive days to evaluate service life of the device. No significant variation in accuracy or repeatability was observed over several days of operations, provided the device was cleaned and dried after use as demonstrated in Figure 2.7. This further reduces setup time for a metabolic profiling of cells in a lab setting, since control lines do not have to be reconnected to a fresh device for every experiment. Detectors were typically replaced every couple of days depending on whether any debris was accidentally introduced to the device.
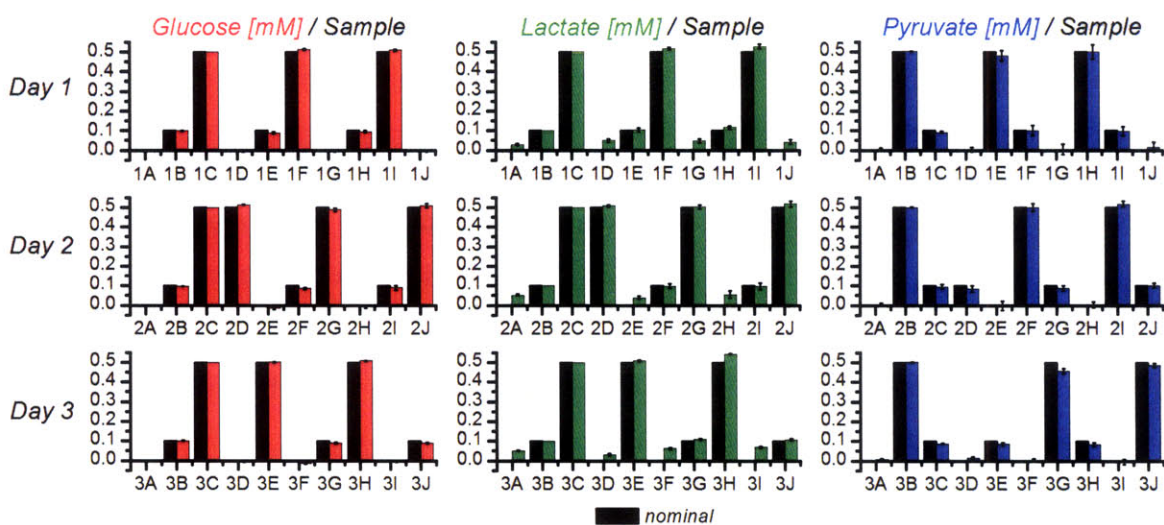
Figure 2.7: Device repeatability and service life study. Media-based standards containing known amounts of glucose, lactate and pyruvate were analyzed on separate days using the same device, which was cleaned after each run using water and ethanol before being dried with nitrogen. Sieve channels on the fluid input ports also significantly reduced debris from entering and clogging channels. Device to device repeatability was also confirmed when standardizing sample loading protocols and operating pressures.

Microfluidic experiments were also performed relative to manual microdroplet assays to enable direct comparisons between approaches (with thanks to Becky Hamilton of Fertility Labs of Colorado). The glass pipettes were rinsed in acetone between each sample to prevent cross-contamination. Figure 2.8 presents the results of glucose assays completed on ten water and media based samples using both a micropipette and the detector. As evident by the comparison to expected values, both methods produced accurate measurements. With reagents and the enzyme cocktail already prepared, however, microdroplet measurements require approximately three hours of continuously manned time to perform a calibration curve and measure ten samples in triplicate. By contrast, the microfluidic device generated measurements at a rate of ~30 seconds per point, unattended. In routine clinical settings involving multiple metabolites and multiple samples, these differences in labor compound quickly. Automated image acquisition and analysis also avoids the inconveniences in manual data logging.
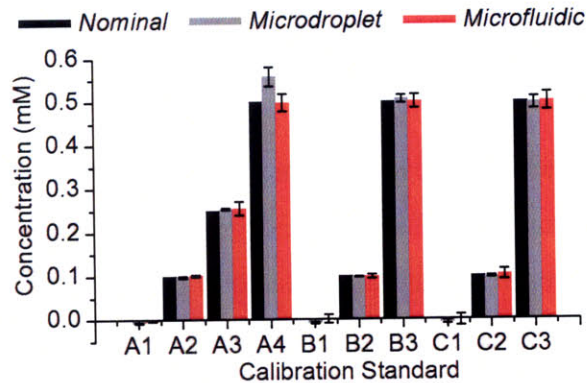
Figure 2.8: There is good agreement in accuracy between the conventional microdroplet and present microfluidic analysis for a number of calibration standards with known amounts of glucose. Samples A1 - A4 are water based standards, while standards B and C are based on types G1 and G2 sequential embryo media, respectively. Error bars represent one standard deviation on three measurements for the microdroplet technique and ten measurements for the microfluidic device.

2.4.2 Management of Sub-Microliter Samples

In any lab setting, metering and handling of sub-microliter samples is not a trivial matter. This is particularly true in the present research where it would be desirable to perform chemical measurements in replicate for each of three markers (glucose, lactate and pyruvate), from a total media sample of only several hundred nanoliters. As such, losing any media sample prior to analysis is a critical concern. With these issues in mind, two different strategies have been devised for loading media to a microfluidic chip. In the first approach, it is possible can adapt the use of the custom glass micropipettes used in embryo culture for carefully loading samples < 0.5 μl directly to channels in the chip rather than using microbore tubing. On chip pumps may be used for drawing samples from this larger volume to perform metabolite measurements. The advantage of this approach is that no modification of the media is required and this technique may be preferred if the culture is being performed next to the microfluidic workstation. Unfortunately, the glass pipettes are very fragile and are custom made. Loading would have to be performed under a microscope for each sample, which slows down the entire assay process. In case of operator or software error during the metering process, the very small sample may accidentally be blown through the channels before all required analysis are completed (flowrates in channels during sample loading can approach several hundred nl/s). Devices employing this

loading technique were designed and fabricated, but the tedious nature of sample loading negated many of the advantages of a high-throughput tool.

In a second proposed approach, it is possible to pre-dilute culture samples to the microliter range to alleviate difficulties in manual fluid transfer. For example, if media samples and calibration standards are diluted with a buffer solution by a factor of ten, it will now be possible to transfer working volumes of ~5 µl or greater. Initial sensitivity experiments demonstrated that the signal-to-noise ratio when performing measurements in microchannels is still adequate when standards have been diluted by ten times. Physiological concentrations of glucose expected are in the 0.1-0.5 mM range[14]. If samples are pre-diluted by a factor of ten, we expect to have metabolite levels between 0.01-0.05 mM. In the fluorometric assays, we further dilute this sample with 10 parts of enzyme cocktail, which indicates we require reliable signal in the 1-5 µM range. Based on these assumptions, fluorescence calibrations of NAD(P)H in the µM range were performed to assess this approach. Highly linear curves ($R^2 > 0.999$ over five points) suggest the feasibility of this dilution technique and indicate that performing such assays in well-defined microchannels is significantly more sensitive than the microdroplet format. While the drawback of this methodology is that samples must be pre-diluted, it alleviates difficulties in transferring and loading sub-microliter samples and allows standard microfluidic tubing and ports to be used.

It was particularly important to avoid transferring any of the mineral oil (used to blanket and prevent evaporation of the culture samples) into the detector. Narrow gel loading round pipette tips (~0.5 mm OD) were found to be ideal for transferring fluid from the oil covered samples directly into segments of Tygon tubing that would be connected to the microfluidic device. This technique was found to be suitable for preventing the introduction of mineral oil into the microfluidic circuit. The loading sequence for pre-diluted samples is presented in Figure 2.9.
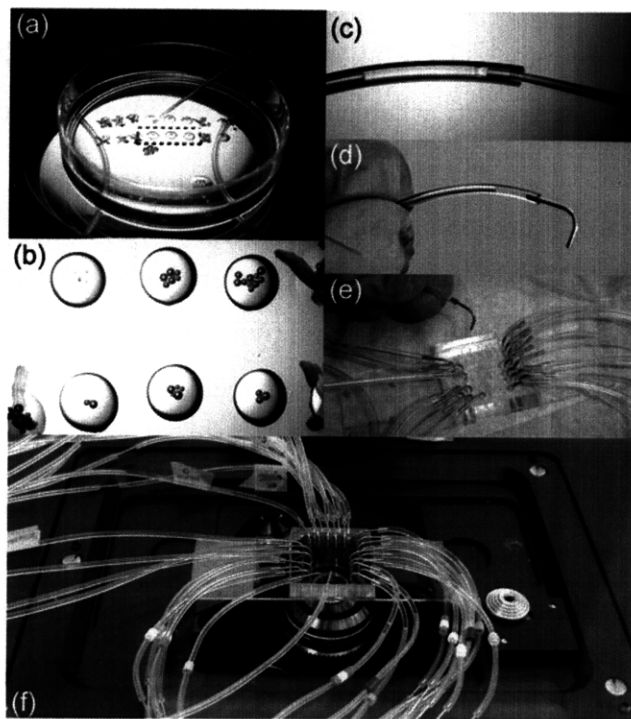
Figure 2.9: Sample loading sequence. (a, b) Pre-collected embryo media samples are stored in a Petri dish (35 mm) under oil to prevent evaporation. (c) A gel loading pipette tip is recommended for transfer of individual media samples (typically 1-5 µl working volume) directly into a length of 500 µm ID Tygon tubing. (d) The end of the tubing may be cut to prevent the carryover of any oil prior to adding a sterilized pin. (e) All samples and reagent lines are connected to a detector chip which already is connected to control manifold, then (f) mounted on an inverted microscope for the experiment.

2.5 Metabolic Analysis of single murine embryos

As a proof of principle of our microfluidic detector, we performed metabolic profiling of ten morphologically similar murine embryos in a parallel manner. It was particularly important to avoid transferring any of the mineral oil (used to blanket and prevent evaporation of the culture samples) into the detector. Difficulties in loading sub-microliter media samples from Petri dishes to the chip were circumvented by employing the sample dilution scheme introduced in the previous section to increase the working volume of fluid. All 500 nl sample droplets were diluted to 5 µl with DI water, and allowed to mix by diffusion. The use of gel loading pipette tips allowed transfer of these aqueous samples from under the oil to the tubing without carryover of oil. Total time required to load 10 samples into the device was approximately 10 minutes. Calibration standards and reference media samples which did not contain embryos were also

treated in a similar manner to ensure consistency in the loading and measurement process. Prior detection trials at a variety of metabolite dilutions beyond the expected physiological range were completed to ensure reliable sensitivity when employing this loading scheme.

Individual aliquots of spent culture media that had contained single embryos for 24 hours, as well as reference media that did not contain embryos, were both analyzed to ascertain the difference in concentrations of glucose, lactate and pyruvate. In all cases, measurements were non-invasive since assays were performed only spent media aliquots which had contained a single embryo for a limited amount of time. Embryos are transferred to fresh media droplets daily prior to media collection, which maintains sample integrity and viability. Media samples from day four were selected for analysis as the embryos are particularly active during this preimplantation period. Each measurement was performed ten times, with calibrations completed automatically for each replicate in approximately three hours.

The heterogeneity in nutrient utilization amongst similar day four embryos is apparent as presented in Figure 2.10. Overall, the measured values are in good agreement with reported literature values[13]. Expected metabolism of glucose, lactate and pyruvate are in the range of -5, +5 and -1 pmol/embryo/hr for murine embryos[4, 13, 18] (+ and - denote production and consumption, respectively). Experimental measured values (± s.d.) of nutrient utilization for this embryo population are -4.82 ± 1.40, +5.70 ± 2.13 and -0.92 ± 0.76 respectively.
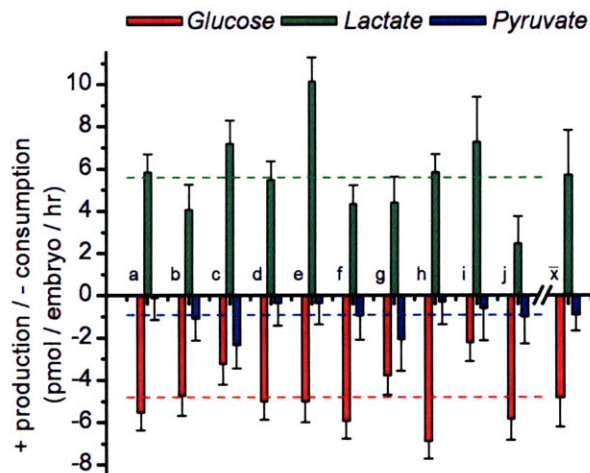
Figure 2.10: Metabolic profiles obtained from ten murine embryos, labeled a through j. Results are from day 4 of culture, and are presented relative to original G2 media (analyzed in parallel with culture samples) to ascertain the changes in metabolite levels due to embryo activity. Individual embryos were cultured in 1μl of medium G2 for 48h prior to analysis. Heterogeneity in metabolism becomes apparent amongst morphologically similar embryos. Error bars indicate one standard deviation. The mean values for this population are represented by x, with dashed lines for visualization.

These data serve to support the utility of a microfluidic detector in a research or clinical setting. Since this assay approach is non-invasive, the integrity of delicate cells is never compromised. It is not unreasonable to consider evaluating hundreds of samples with only a few devices. This would be well within the range required for a large experimental or clinical study. It is also possible to include additional enzymatic assays. A large number of molecules can be detected using three or fewer enzymatic reactions. Other substrates of particular interest that could be measured include asparagine, glutamine and alanine, several of the amino acids that have been shown to identify human or murine embryos with better developmental potential[48, 49]. With a few modifications, we anticipate that the throughput of the device could be even further enhanced. The number of input ports could be doubled or quadrupled with the addition of just two or four additional control lines added to the multiplexor, respectively[66]. It would also be possible to design a device with several mixing circuits so that the measurements could be performed in parallel. Such a device would either need to be designed so that the detector bins are within the same field of vision, or a motorized stage would be used to image several distinct locations on the device.

A further step toward automation will occur when this analytic device is placed in line with a culture system as this would eliminate manual handling of spent culture media. Furthermore, it should greatly reduce the volume required for these assays. Several groups have made considerable progress in culturing embryos in microfluidic devices[67, 68]. One concern that will need to be addressed with using NAD(P)H-based assays is that a high energy excitation illumination is required (wavelengths in the ultraviolet spectrum). It will be necessary to shield embryos from exposure to the ultraviolet light, potentially using carbon black doped PDMS[69] or separating microfluidic components[70]. Alternatively, enzymatic assays that produce products that fluoresce at lower energy excitation could be used[71].

While embryologists may adapt to microfluidic approaches in the future as advancements in cell screening[36, 72] and embryo culture continually evolve[23, 26, 68, 73], the majority of embryo culture will take place in microdroplet formats for the coming years, particularly in regulated clinical settings. For these reasons a standalone, non-invasive microfluidic metabolite detector is an important development as it may be used in conjunction with standard embryo culture techniques. Our microfluidic approach alleviates the issues involved with electrochemical instrumentation and enables high-throughput fluorometric measurements with single embryo sensitivity.

The two principal barriers to widespread adoption of this system are the availability of devices and the need for a fluorescent microscope with imaging capabilities. With the widespread dissemination of lithographic equipment and the growing interest in soft lithography, it is likely that facilities to produce these devices will become more prevalent. Software is currently being developed that will expedite and improve microfluidic device design[74]. Once the molds for a particular device are made, the costs of producing casts are quite nominal. Many IVF centers have high quality microscopes with imaging systems for micromanipulation of gametes and embryos. In the future, it is quite likely that the device will have integrated illumination and detection capabilities. The remainder of the equipment to run the devices is anticipated to cost less than $3000, making this technology very competitive in terms of up-front costs as compared to spectroscopic or chromatographic equipment required for other analytic approaches.

2.6 Conclusions and Contributions

The objective of this multifaceted work was to develop an automated system for non-invasively evaluating metabolism of single embryos. While several techniques have been developed for culturing embryos in microchannel environments, none have addressed the challenge of using these devices to assess embryonic metabolism. By combining the sensitivity and automation enabled by microfluidics with previously characterized enzyme-linked assays, a practical tool has been developed that should have applications to many types of cell culture. The utility of this platform was demonstrated by measuring metabolite profiles of individual murine embryos. With variations of the approaches introduced in this research, a large scale clinical trial to pursue the relationship between metabolism and developmental potential should be within reach.

As all microfluidic measurements are automated through software, it is straightforward to record data and create custom assay routines. Optimization of these assays and enzyme cocktails should improve throughput further making such measurements more attractive to other embryologists. With measurement accuracy on par with existing micropipette methods, the microfluidic approach provides repeatability, scalability, and most importantly, the ability to perform assays unattended. Since it is non-invasive, the microfluidic detector is also compatible with any format of cell culture, the mechanics of which can be integrated downstream of other culture devices for closed-loop analysis.

High-throughput tools such as those introduced in this work would be an invaluable asset to understand the specific metabolic factors that play the most important roles during the dynamic embryo culture period, and offer a tractable means to elucidate the relationship with developmental potential. While the three of the most common metabolites have been demonstrated in the present study, non-invasive fluorometric techniques can be expanded to include additional metabolites of interest.

Looking forward, it would be desirable to standardize and automate the assay procedure to an integrated culture platform capable of carrying out the metabolic measurements on individual embryos and other cells in parallel for the entire culture period. A better understanding of embryonic metabolism is likely to improve the probability of a healthy pregnancy following

single embryo transfer, ultimately leading to reduced numbers of IVF cycles per pregnancy and reduced incidence of multifetal pregnancies. These advances would lessen the financial burden and improve the experience of patients undergoing assisted reproduction.

The methods introduced in this chapter should also extend to analysis of other types of cells beyond IVF, as well as generate interest in automating related analytical assays. This independent detector device is an important development as it may be used in conjunction with standard embryo culture techniques, and may also be integrated with microfluidic culture in the future. Before that next step is possible, however, the methods required for supporting embryo culture in microfluidic constructs must be improved. These challenges are the goal of Chapter Three.

Chapter Three - Microfluidic Embryo Culture

3.1 Introduction

The desire to culture various cell lines and tissues in microfabricated environments has been one of the driving forces to improve the design of microfluidic devices over the past decade. In turn, devices which become more robust through iterative design and experimentation offer the opportunity to gain insights to biological samples with unprecedented control of chemistry, environment and repeatability.

Relative to conventional Petri dishes, unforeseen difficulties can arise when culturing delicate tissues in micron scale chambers, reflective of the interplay of very high surface area to volume (SAV) ratios surrounding samples, which increases dramatically with miniaturization[22]. This high SAV ratio can be exploited for studying new surface treatments and rapidly culturing bacteria and cells on complex surfaces. Conversely, increased interaction with surrounding, artificial environments can be fatal to sensitive samples if care is not taken to prevent chemical contamination, evaporation, or depletion of nutrients. These are key considerations in moving forward to improve the embryo culture process in such at way that can be incorporated with microfluidic analysis systems.

3.1.1 Culture Background and Considerations

As overviewed in the previous chapter, the predominant current method of culturing embryos in clinical settings is by using microdroplets. Following conception, zygotes are carefully placed in pre-equilibrated pools of media in a Petri dish that have been blanketed in a light mineral oil to prevent evaporation. Embryos may be cultured individually, or in small groups provided there is sufficient media volume to prevent starvation. The media volumes are generally in the 10-20 μl

range, with evidence that smaller volumes and larger group numbers are beneficial for culture[75]. The culture takes place in incubators which are maintained at 37°C and are supplied with tri-gas (typically 5-7% O_2, 5-6% CO_2 and remainder N_2) to mimic the fallopian environment. Development and optimization of sequential media for embryos, to further replicate temporal changes in nutrient levels *in vivo*, is in itself an involved research area[27, 29, 30, 76]. The general strategy is to use a high glucose media for the first two days over culture, followed by an exchange with a lower glucose media for the following days to reflect the needs of the developing embryo[27] (following Figure 1.1). Actual compositions of the media are quite complex and in many cases are protected by commercial vendors[28].

Additional protocols have been empirically developed to improve the culture process of environmentally sensitive embryos. In fertility labs that have implemented stringent quality control programs, all raw materials such as Petri dishes and pipettes are contact tested on a shipment by shipment basis with samples at the clinic before they may be used for human embryo culture[76]. For example, a surprising one-quarter to one-third of sterilized Petri dishes are found to be incapable of supporting embryos based on the quality guidelines in place at the Fertility Laboratories of Colorado, in which case the entire batch must be discarded (MTJ, personal communication). The number of times in which an incubator door is opened during embryo culture is also carefully monitored, since subtle atmospheric lead to cumulative damage and hinders sample development. As such, to prevent adverse effects to others' samples many small, separate chambers are preferred over only a few large incubators. The list of incremental improvements in culture continues on and on, and while these may seem tedious or trivial, these convey the attention necessary to enable consistent culture of zygotes to the blastocyst stage. Overall, these improvements have played a major role in improving pregnancy rates of IVF over the past two decades.

3.1.2 Motivation and Goals

Building on the ability to perform microfluorometric metabolic measurements on pre-collected aliquots of spent embryo media, the next logical step would be to remove the need to manually transfer samples to a microfluidic detector. If it were possible to both culture and profile embryos on a single platform in an automated manner, the clinical implications in IVF by

reduction of labor and increase in quantitative data for implantation decisions would be profound.

With that in mind, the process of culturing embryos using microfluidics is a challenge that has been approached by a limited number of research groups. Even in conventional culture, embryos are particularly sensitive to their surrounding environment and subtle changes in temperature or oxygen levels can be detrimental to development. With proper engineering and process design, microfluidics offers the potential to shield embryos from these adverse environmental changes and automate steps in the culture process, such as the changeover of media.

In this chapter, we develop the microfluidic expertise necessary to culture embryos, directly from zygotes all way to day five, to the blastocyst stage. Unique engineering challenges are addressed, including the methods of loading and retrieval, and the difficulties in surface contamination. In contrast to previous work in the field, where embryos have been cultured in millimeter scale channels with continuous perfusion of media, successful culture protocols are demonstrated for the first time in truly confined sub-microliter media volumes by the integration of large scale microfluidic valves. Development and implementation of these culture protocols will enable the scalability to study multiple embryos in parallel and the ability to collect precise amounts of culture media for downstream metabolic profiling on a single device.

It has been hypothesized that numerous variables associated with laboratory culture systems (including accumulation of metabolites, such as lactate and ammonia and depletions of necessary nutrients, namely glucose and pyruvate) are related to the low yields of viable embryos *in vitro*. *In vivo*, the female reproductive tract is constantly active, resulting in movement of the embryo down towards the uterus. This movement also washes the embryos through constantly changing physiological conditions through the oviduct to the uterus, maintaining a gradient for the supply of necessary nutrients and oxygen, and the removal of waste products[26]. As the *in vivo* environment is dynamic, it has thus been hypothesized that the use of an active system may be beneficial for *in vitro* culture. Microfluidic techniques have already been demonstrated to improve bacteria and cell culture via similar recirculation and pumping protocols[32, 33].

An preimplantation embryo's metabolic requirements evolve during the five day developmental stage[27]. In response to these known preferences, different formulations of media are desirable for different days of culture. Standard microdroplet culture techniques, however, are limited to providing homogeneous concentrations of metabolites to embryos. With microdroplet culture, it is presently necessary to pick up embryos manually and place them into new droplets of fresh media in response to metabolic preferences. Continued efforts to improve culture conditions would benefit from devices which are capable of reproducing physiological chemical gradients.

In the past, no microfluidic groups have tackled closed-volume issues in microfluidic embryo culture. This research will be the first to culture embryos in truly confined media volumes on chip. Culture within specific volumes of media is necessary for our proposed method of embryo profiling by observing the uptake and production of metabolic factors over time. It is believed that in the future, microfluidics may the preferred approach for embryo culture suitable to spatially and temporally replicate *in vivo* conditions, while enabling the capability providing real time feedback on developmental progress and viability.

3.2 Related Research

3.2.1 Embryos in Microfabricated Environments

Several groups have taken initial steps to demonstrate embryo culture in microfabricated systems with varying degrees of success, all on the premise that these systems will become superior for replicating the *in vivo* environment. In most cases, the microfabricated systems resemble more of an open cavity, as opposed to a closed channel. As such, these approaches whether or not they are capable of supporting embryo culture, may not be suitable for integration with the method of fluorometric metabolite analysis introduced in the previous chapter. When culture volumes are reduced into the sub-microliter per embryo range, secreted growth factors are more concentrated and are believed to enhance development during the preimplantation period[31, 75]. Standardization of such procedures and culture conditions is particularly important when comparing results from multiple cell samples, and also allows researchers in separate laboratories to replicate procedures using their own microfluidic platform.

Potential advantages of perfusion or recirculation of media for embryo culture have been discussed, but only a limited number of detailed experiments have been completed with culture conditions that are difficult to compare. In a study by Lim *et al*, it was observed that an increased fraction of bovine embryos successfully developed to the blastocyst stage when perfusion was used only in the first day of culture[77]. Overall, development rates using the dynamic environment were significantly lower than that observed in static systems, and in many cases mouse embryos were arrested by the four cell stage.

The Beebe research group has pioneered much of the early work in static microfluidic embryo culture. They have characterized embryo compatibility with many materials commonly used in microfabrication including silicon, borosilicate glass, chromium, gold, as well as PDMS[78]. While claiming that Sylgard 184 PDMS was not found to inhibit embryo development, they acknowledge difficulties with surface interactions and suggest that for widespread adoption of microfluidic culture systems will benefit from development of alternative biocompatible materials[79]. They have developed several devices to microchannel embryo culture, including devices fabricated with combinations of silicon/borosilicate, or PDMS/borosilicate. In the later case (with borosilicate glass channels mounted on top of a PDMS bottom) they observed that nearly 80% of embryos developed to the blastocyst stage, compared with only 50-60% of control samples in 30 µl droplets. The devices were reasonably large for "microfabricated" systems, with channels containing 0.5 ml of static media (including the input wells). Beebe states that the "effective" volume of these systems is actually of the order of microliters per embryo, by diffusion and high surface area to volume arguments[80]. Unfortunately, these claims neglect the fact that culture periods for embryos are on the order of days and even when limited by diffusion, nutrients or toxins can be transported from distant channels. The group has also admitted that some of their observed benefits (consistently faster cleavage and higher blastocyst rates) of static microchannel culture could be magnified by sub-optimal aspects of their microdroplet culture techniques[81]. In any case, this thorough groundwork in microchannel culture supports the potential benefits of transitioning from microdroplet methods.

Interesting perfusion culture results were obtained by Hickman *et al*, in using a large glass channel to continually flow media over a group of preimplantation mouse embryos[26]. In the

absence of flow, cleavage rates between the microfluidic embryos and control samples using traditional culture methods were similar. As flow was introduced, developmental rates accelerated initially (from two to four cell stages), but were ultimately hindered by the use of flow rates in the range of 1 to 5 μl / hr in a channel with dimensions of 1000 μm by 250 μm. Unfortunately, the exact conditions of this setup were not well described , since the experimental protocols described would imply average perfusion velocities of only ~1 μm/s (non-embryo continuous cell culture studies have been successful at local velocities which are one to two orders of magnitude higher[82, 83]). The authors offer additional explanations for developmental problems with their perfusion system including poor control over pH, and the likelihood that potentially useful compounds from the embryo group were also washed away with waste. Secreted growth factors are also removed which are believed to help regulate metabolism. Similar studies have pointed towards the possibility of using pulsatile flow to mitigate these shortcomings and more closely resemble dynamics of *in vivo* conditions. Preliminary developmental results with this approach have been promising[67], as indicated by the increased percentage of embryos which successfully developed through to blastocyst stage in comparison to a static control culture. Although, to avoid the difficulties in sample loading and isolation in such work, open channels with millimeter scale dimensions were used[67] (which could be argued as poor usage of the term "microfluidics").

These studies provide a starting basis for additional work to be performed in dynamic culture, but flaws exist in these early microfluidic approaches. First, the same media was utilized throughout the culture period, while it is widely recognized in the clinical community that sequential media is recommended[27] (by mimicking the composition and concentration in nutrients present in the oviduct during the first three days of embryo development, and in the uterine for the following two[84]). Second, it was not investigated whether continuous or periodic fluid flow should be applied to the microenvironment, as the nutrient demands of a developing embryo evolve over a culture period of up to five days. Also, only embryo morphology was used as a measure of effectiveness for the microfluidic culture systems. Reiterating, morphology alone is not sufficient to understand the implications on the health of cells and does not correlate with latter developmental competence[4]. To strengthen the conclusions of these studies, the quality of blastocyst development should be supported with inner cell mass and trophoblast cell

count data (discussed in section 3.4). Ideally, measurements of metabolic activity should also be integrated to more accurately quantify the implications of dynamic culture. The devices used in the aforementioned studies also lacked the flexibility to alter flow fields and do not enable the option to recirculate media over embryos. In the present work, microfluidic approaches have been conceived and implemented, to address some of these shortcomings and enable improved culture flexibility.

3.2.2 Modeling Implications of Perfusion Based Culture

In reflection of dynamic culture systems, it is interesting to relate the dominant fluid flow in the channel system to the potential nutrient uptake by a sample. In the aforementioned continuous perfusion systems, the cell proliferation has not been related back to increased nutrient diffusion resulting from advection. As a sample case, the potential uptake of glucose by an embryo in media is modeled with the goal of providing some insights to the effects of advection with the developmental period. To start, the diffusivity of glucose molecules in solution may be estimated using Einstein's relation:

$$D = \frac{kT}{6\pi\mu a}$$

Here, k is Boltzmann's constant (1.38E–23 J/K), T is the temperature of the solution (37°C = 310 K), μ is the viscosity of the medium (~0.001 Pa s for water) and a is the effective radius of the molecule (~0.43 nm for a glucose molecule). By this, D is approximately 5.3E-10 m^2/s for glucose in culture media. Now, consider the Sherwood and Peclet numbers for our system consisting of an absorbing sphere in the presence of a flowing media. The Peclet number relates the relative contribution of advection and diffusion in fluid flow:

$$Pe = \frac{UR}{D}$$

Here, U is the fluid velocity, R is the sample radius (assume an embryo diameter of ~100 μm) and D is the previously calculated nutrient diffusivity. For the sake of this simple comparison, we are interested to learning the potential increase in glucose uptake for the embryo when the rate of adsorption is not diffusion limited. Thus we make the assumption that the concentration

of glucose is zero at the surface of the embryo (a perfect absorber) - that is, this embryo will absorb all glucose molecules which reach the surface by diffusion or advection. The Sherwood number is used to calculate the enhancement in adsorption at a surface due to the effect of advection. For a perfectly absorbing sphere, the Sherwood number is expressed as:

$$Sh = \frac{1}{2}\left(1 + (1 + 2Pe)^{\frac{1}{3}}\right)$$

In the case of zero flow (Pe = 0), the Sherwood number is 1 and molecular flux is occurs by diffusion only. This is the case of static microdroplet culture. For positive values of Pe, the Sherwood number increases significantly for large radius samples such as embryos. In a flowing nutrient stream, small (< 10 μm) absorbing cells do not benefit appreciably from fluid flow with velocities (due to low Peclet and Sherwood numbers at small length scales). Samples with larger diameters (~ 100 μm), however, can experience appreciable enhancement in nutrient adsorption in the presence of flow due to their length scale.

For example, modeling of an ideal absorbing sphere of 100 μm diameter in the presence of a moderate 10 μm/s flowing stream of dilute glucose corresponds to a Sherwood number of ~1.3 (that is, the total mass flux of molecules across the surface is 30% greater than that due to diffusion alone). By the same scaling, mass flux across a 100 μm absorbing sphere doubles if the average velocity approaches 100 μm/s, while 10 μm spheres would only experience a moderate ~20% increase due to advection.

Though idealized, these scaling arguments suggest that embryos in continuous flow systems[26, 77] may have been provided a level of nutrients which is greater than what would be experienced physiologically, ultimately distressing development. Unfortunately, it is difficult to quantify to what effect the removal of secreted growth factors had on embryonic development in these studies. Additional effects, including responses due to fluid shear stress on embryos and unreported environmental fluctuations, certainly play a coupled role in metabolic regulation. As such, future experiments in a controlled environment should be performed to accurately quantify and understand the uptake of nutrients by samples resulting from dynamic culture.

3.3 Open Microfluidic Chambers

With the first goal of moving towards static microfluidic culture in microliter volumes, an "open channel" approach was designed and implemented. All early attempts to culture embryos were performed using such PDMS channels, consisting of only one inlet and one outlet. While primitive, these experiments and feedback driven design cycles were critical to identify and resolve the most troublesome issues involved with microchannel culture.

Initial work involved finding methods to allow consistent loading and retrieval, as well as circumventing the difficulties with manufacturing channels sufficiently large to accommodate our embryos. It became apparent that the first major design change would involve the microfluidic interconnect ports. Conventional 500 µm diameter ports, created by punching PDMS with a sharp biopsy tool, would not be acceptable for retrieving embryos from channels. While working under a stereo dissecting microscope, it was nearly impossible to visualize an embryo, or to fit a glass pipette to the bottom of a port to pick or place an individual embryo. Several larger biopsy tools were tested, and 4 mm tools were found to be adequate. With these large ports, it would be possible to deposit an embryo at the bottom of a well near the entrance of a culture chamber using a mouth pipette. From there, a syringe pump (or small volume pipette) connected at the exit port would precisely be able to draw the embryo into the chamber. In a reverse manner, for collection an embryo could be gentle pushed back towards the input port, and picked up.

Initial straight channels used for loading experiments, fabricated in PDMS using ~100 µm tall molds were found to be too constrictive for culture. Thus it was necessary to transition to a two step photoresist process to achieve this channel height on molds using SU8 100 photoresist on silicon wafers. Further, since embryos are non-adherent, it is also possible that embryos may move around within their chamber due to pressure variations or capillarity from the interconnect ports during loading. To prevent embryos from leaving their intended culture channel and leaving via the exit well, constriction channels were placed near the far end of the channel simplifying the oocyte gratings proposed by Suh[23]. The 50 µm wide constrictions were

fabricated using a 50 μm tall layer of SU8. The main culture chamber had 150 μm channel heights.

The mold for the device was fabricated using a two step photolithography process. The base layer of SU8 was patterned using a transparency photomask and cross linked. Another layer of SU8 photoresist was then coated, and the second set of features on a complimentary photomask was exposed using an alignment tool[85]. All features were developed in one step, leaving a mold was distinct channel heights. An example of an open chamber device is presented in Figure 3.1, with a nominal chamber volume of 1 μl.
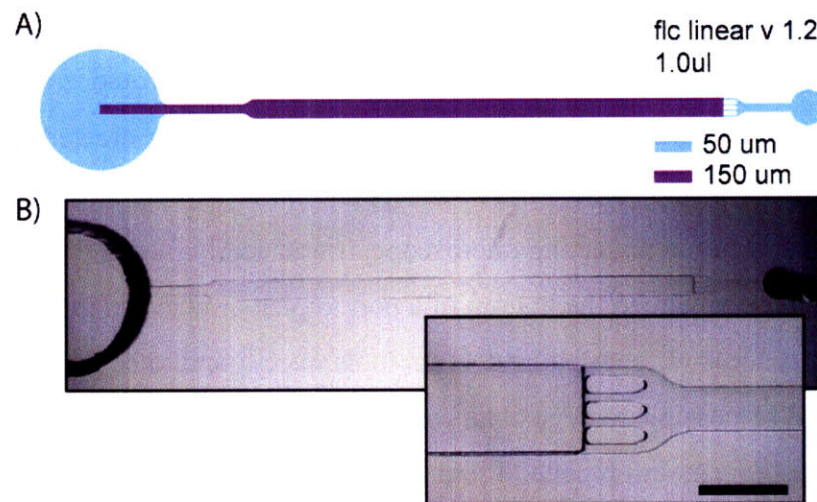
Figure 3.1: An open chamber device used to develop microfluidic embryo culture protocols. Several varieties of such devices were tested to investigate and resolve the major issues in sample handling, loading and retrieval. In addition, open channel devices were essential to debug issue with device fabrication and toxicity. A) Schematic of a culture device with a nominal 1 μl channel volume. The blue and purple regions indicate channel heights in distinct regions. B) Image of a physical PDMS device, with a 4 mm diameter port on the left for loading of embryos. The inset clarifies a sieve used to prevent embryos from accidentally flowing out the exit of the device during loading. Scale bar is 500 μm.

The device was cast using Sylgard 184 PDMS. Rather than bonding single layer devices directly onto glass slides, it was decided that a PDMS bottomed device would more closely resemble the assembly process used for the devices in Chapter Two. Further, by surrounding an embryo sample with PDMS on all four surfaces, it would simplify the questions in determining whether potential contamination is due to the PDMS device, or from the sealing surface. To achieve

enclosed devices, a thick layer of PDMS containing channel features was first cast and punched to create interconnect ports. It was then was bonded to a thin layer of PDMS (~100 μm) which had been coated on a blank silicon wafer, using either thermal techniques or a plasma treatment. The sealed devices could then be removed from the blank wafers, cleaned, then sealed to pre-cleaned glass slides. Several generations of these devices with varying SAV ratios were implemented over a 12 month period, with iterative improvements to the chambers design and methods of fabrication based on the experience of culture trials.

3.3.1 Fabrication and Cleaning Protocols

Through numerous initial rounds of culture with murine embryos, mixed results were obtained in the open chamber devices. Appropriate loading techniques were practiced using large 100 μm fluorescent beads, although first generation devices had large gratings that allowed smaller embryos to slip through on occasion during loading. Most troubling during these early design stages, embryos often would arrest within hours of being placed within channels filled with media.

Numerous causes of this failure were suspected, owing to either mechanical or chemical stress. The design of the channels had been already improved with wider inlet channels to prevent collision of the embryos with PDMS walls or gratings, so this was dismissed as the primary cause. More likely, interaction of the device surfaces was either introducing toxic byproducts from the fabrication process into the media, or causing the depletion of essential nutrients from the chamber. PDMS is gas permeable and semi porous, which makes it suitable for gas transfer during culture. However, the porous nature makes PDMS susceptible to adsorption of small molecules[86]. The key causations and solutions for microfluidic device preparation that were established in parametric culture studies are discussed below.

Silane and dummy casting:
While PDMS is generally considered non-toxic, silane-based release agents are often employed in the process of replica casting of PDMS microfluidic devices using photoresist based molds[25]. Release agents, such as chloro-trimethyl-silane or perfluoro-octyltrichloro-silane, may be

evaporated onto silicon molds to assist removal of cured PDMS and extend the service life of often-fragile photoresist features.

Unlike somatic cell lines used in routine biological research, gametes and embryos are particularly sensitive to their surrounding environment[23, 34]. In particular, engineered mammalian cell lines are often robust against chemical contamination during culture. Although silane agents have not interfered with the growth of cells on chip in past studies[36], it proved to be fatal in all of the initial culture trials. To achieve successful culture, it was found necessary to remove silane from the device fabrication process. It is believed that excess silane was being absorbed by the bulk PDMS through the walls similar to other small molecules[86], and this silane in turn may leach into the culture media. This poisoning would be exacerbated by long periods (several days) of diffusion through static media culture, as opposed to dynamic culture, which would remove toxins by advection.

From experience, high-aspect ratio photoresist features are prone to delaminating from the molds during peeling if no release agents are utilized. The tradeoffs for using molds that have not been silanized are a reduced service life, and an increase in the minimum feature size. Fortunately, due to the large diameters of embryos, the minimum features were typically 50 μm or larger.

Further to the removal of release agents from the molding process, a "dummy" cast was performed on newly fabricated SU8 molds. The first set of PDMS, that was cast over the channel molds and blank wafers that would be used for sealing the bottom of the channels, was tossed. This was found to improve the culture performance of subsequent cast chips, possibly by removing residual photoresist products on the mold surfaces from the clean room.

PDMS Ratios:
The devices used in the present study consisted of two PDMS layers; the thick layer (~4-5 mm) which contained the culture channels, and a thin layer (~100 μm) which sealed the bottom of the channels. In standard MSL, these layers may be bonded thermally by varying the amount of PDMS curing agent between the two layers[25]. PDMS is nominally cured by mixing 10:1 / PDMS based: curing agent. Standard MSL is performed by using 5:1 PDMS for the thick layer,

and 20:1 for the thin layer, which can be used for thermal bonding of partially cured layers using the concentration differential at mating PDMS surfaces. However, this method introduced the suspicion that excess curing agent or base may interfere with culture. To remove this variable, all PDMS was cast using the "stoichiometric" 10:1 ratio.

In the absence of a curing agent differential to perform interlayer bonding, the devices were instead assembled using a plasma treatment. Thick layers were fully cured, interconnects were punched and following a brief cleaning with ethanol and nitrogen, devices were plasma bonded to blank cured sheets of PDMS. A 30 second air plasma treatment at low RF power (Harrick Plasma, Expanded Plasma Cleaner) was found suitable for bonding PDMS surfaces. Devices were removed from the thin layer molds, cleaned again, and then bonded to 1 mm thick glass slides ready for culture.

Oven and PDMS curing time:

A shared laboratory grade gravity oven maintained at 90°C had previously been used for casting of all microfluidic devices. However, this common resource used by many group members and collaborators over the years to cast microfluidics and a variety of other unknown chemical substances could have been subject to contamination. Devices cast on silicon molds were observed to catch a yellow-colored tint if left uncovered in the oven. Residual odors were also noticeable, likely from plastic Petri dishes which had been forgotten and melted in the oven. To remove the variable of chemical contamination during PDMS curing, a clean new oven was acquired which was reserved solely for casting devices for embryo culture. A separate oven also prevented environmental contamination with other microfluidic molds which have been treated with silane.

Studies were also performed to determine the minimum required curing time of PDMS culture devices. Although 10:1 PDMS can cure to a solid rubber within 20 minutes of curing, mechanical properties can continue to change even after hours or days of extended curing as residual traces of uncross-linked monomer are cured. It was found that a minimum curing time for devices was 48 h prior to culture, and that longer curing times were not detrimental.

Pre-Equilibration:

After the extended bake time was complete, channels were filled with ethanol and soaked for 24 hours, followed by a rinse with water. This concept was a simplified version of multi-step solvent extraction protocols that have been used to purify PDMS for temperamental biological samples[87]. To reduce osmolarity shifts during culture[88], devices are then primed by soaking channels in G1 embryo culture media for an additional 24 hours at room temperature before culture. This was performed to saturate the walls with any small molecules which may be drawn out of media in later cultures[86], as well as hydrate the thick layer of PDMS to prevent evaporation. The chips were finally refreshed with clean G1 media and allowed to equilibrate for pH and temperature in an incubator for at least 4 h immediately before loading embryos for culture.

Final Protocol:

In summary, the recommended protocol for device preparation requires:

- Dummy casting of all new silane free molds with PDMS.
- Devices cast using 10:1 PDMS for both thick and thin layers, plasma bonded together.
- Devices bonded to glass slides with a total bake time of at least 48 h at 90°C.
- Solvent extraction for 24 h with ethanol followed by an equilibration for 24 h with media.
- Pre-equilibration with fresh media in an incubator for at least 4 h before loading embryos.

While it may be possible to reduce the suggested lengths of treatment, these were found to give satisfactory results without necessitating excessive handing of devices. By using the techniques, it became possible to culture zygotes through five days all the way to expanded blastocyst and even hatching stages. Figure 3.2 illustrates the first experimental hatch observed in a 1 µl microfluidic channel, alongside control embryos performed in a 10 µl microdroplet.
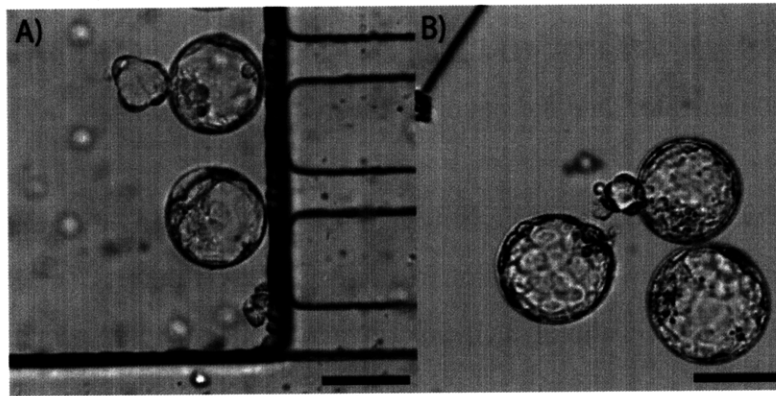
Figure 3.2: A comparison of microfluidic and microdroplet culture. A) Two expanded blastocysts cultured in a 1 µl microchannel. The top blastocyst has hatched, which is often a sufficient, but not necessary, condition for an embryo to be considered a strong candidate for implantation. Sieves towards the exit channel are visible on the right. B) The complimentary controls for this experiment cultured in a 10 µl microdroplet. Scale bar indicates 100 µm.

3.4 Culture Results

With fabrication and preparation protocols set, microfluidic culture chambers were tested in direct comparison to microdroplet controls in three rounds of experiments. To quantify the performance differences between these formats, cell counts were performed on collected day five blastocysts at the end of each culture cycle. The cell counts represent a total of the ICM (inner cell mass, or embryoblasts) and TE (trophoblast) differentiated cell lines, of the blastocyst. The trophoblasts which are located on the shell of the blastocysts later become the placenta in fetal development, while the ICM eventually develops into the actual adult organism. For murine embryos a total cell count from the mid 70's to low 80's (with an ICM count above 20) is considered good (MTJ, personal communication). Fluorescent dyes may be used for identification of these separate cell lines to simplify the process of manual counting.

In these culture experiments, performed over several weeks, fresh murine embryos were collected following the methodology from Section 2.3.2. Briefly, female F1 hybrid mice were superovulated with 5 I.U. pregnant mare's serum followed 48 hours later with 5 I.U. of human chorionic gonadotropin and then immediately mated with F1 hybrid males. Zygotes were collected from the oviducts 21 hours after mating. Embryos were washed using GMOPS buffer (Invitrogen AB) then transferred into pre-equilibrated G1 media in either a microchannel or microdroplet (volumes from 1 to 10 µl) under paraffin oil in a Petri dish. Microfluidic devices

were housed in covered Petri dishes under a few millimeters of water before being placed into incubators at 37°C, 5% O_2, 6% CO_2. The additional water was necessary to combat humidity control issues in the incubator, and did not enter the microchannels.

These experiments were performed at Fertility Labs of Colorado (Englewood, CO) with much appreciation to Mark T. Johnson, David Potter and David K. Gardner. Complete cell count data collected by D.P. at the conclusion of each experiment is presented in Appendix B.

3.4.1 Culture Set One

The first set of culture trials used a total of 21 embryos, with small groups of embryos being cultured in four individual microfluidic devices and the remainder cultured as control samples in microdroplets. The results of the five day long experiment are summarized in Figure 3.3. Complete details of the experimental conditions are presented in Appendix B. On some devices, sequential G2 media was flowed into the microchannels after the embryo had reached the eight cell stage (around day three of culture). Similarly, in the control experiments, some embryos were transferred to new microdroplets of G2 to implement the sequential media.
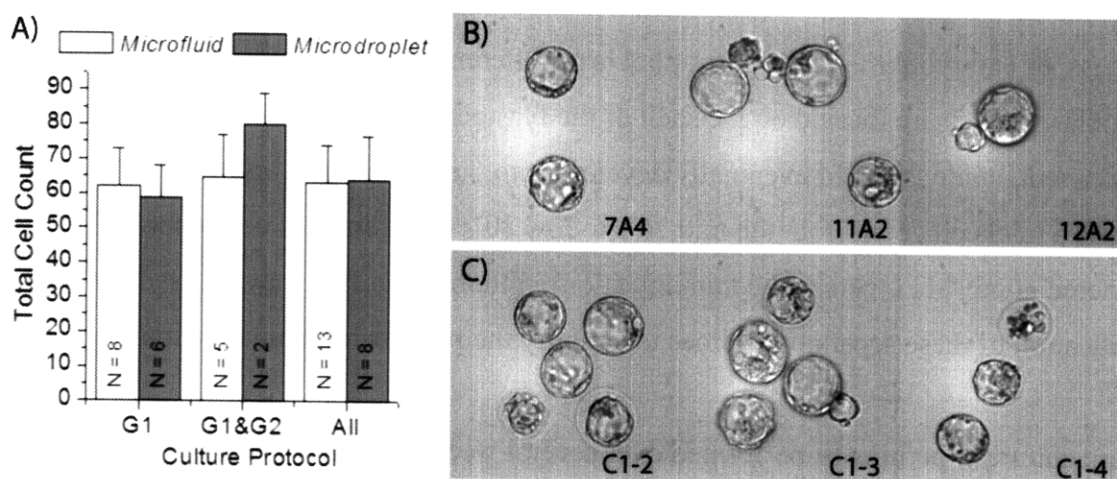
Figure 3.3: Results of Culture Set One. A) Cell counts on chip were consistent with microdroplet controls, although cell counts rarely exceeded 70. B) Embryo images from three different devices at day five appear morphologically similar to those cultured in C) microdroplets.

This culture experiment was regarded as highly successful benchmark. Numerous expanded blastocysts were developed in the microchannels, including several hatches (in three of six separate devices). On average, embryos cultured using microchannels performed on par with the

microdroplet controls, although total cell counts were rarely over 70. The difference in cell counts due to sequential media protocols is not markedly different in this set of devices. As this was the first set of experiments necessitating a media changeover while samples remained inside of microchannels, it is possible that the flushing may have been too abrupt, or introduced excessive fluid velocities to the samples. With practice and refinements to this process, further improvements to cell counts in the microfluidic chambers were expected.

3.4.2 Culture Set Two

Before proceeding to additional experiments with sequential media, additional experiments to assess the device preparation process were performed. In this experiment, two devices were prepped using an ethanol extraction, and two devices were extracted with ethanol for 24 h followed by an overnight equilibration in media. It is evident that the ethanol extraction of microfluidic devices promotes improved embryo culture, as summarized in Figure 3.4.
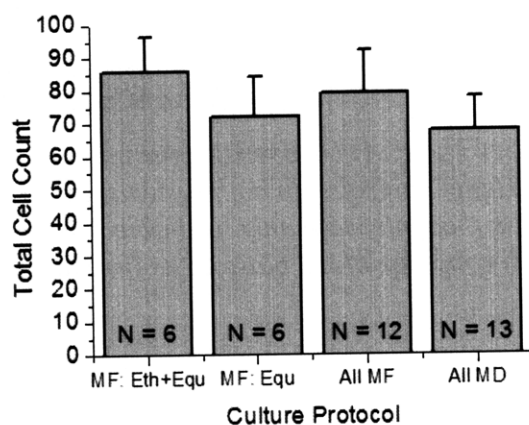
Figure 3.4: Results of Culture Set Two. The six embryos which were culture in devices which were both extracted with ethanol and pre-equilibrated with media outperformed those in devices which were not ethanol extracted. All four microfluidic devices outperformed the microdroplet controls.

These data support the necessity of thoroughly cleaning the PDMS channels prior to use. There may be alternative extraction protocols worth exploring to either reduce the 24 h treatment time, or improve the microchannel biocompatibility even more. Fortunately, solvent extraction with readily available ethanol is simple to carry out and highly effective with a minimal amount of labor.

3.4.3 Culture Set Three

A third set of culture experiments was completed using 12 embryos in four separate devices. Sequential media was applied to two of the devices, which the other two used only G1 media for the entire culture period. Consistent with the previous trials, the microfluidic channels yielded higher cell counts on average, compared with the microdroplet controls. The results of this culture trial and sample images are presented in Figure 3.5.
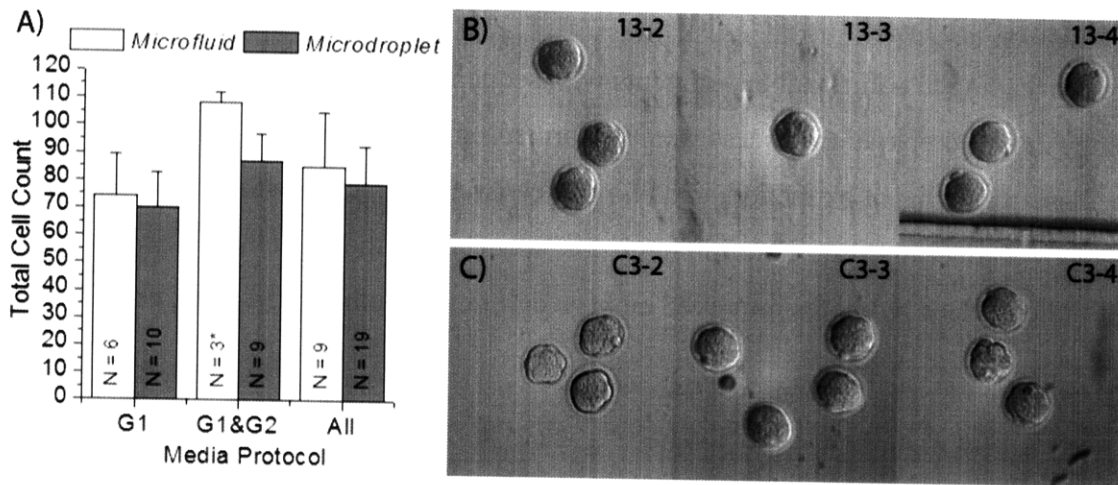
*Figure 3.5: Results of Culture Set Three. A) On average, the microfluidic devices produced cells counts greater than the microdroplet controls. In both systems, the use of sequential media provided superior culture results (*counts were only available on three of the six microfluidic embryos in this case). B) The morphology of the blastocysts in channel on day five compares well with the controls in C).*

Unfortunately in this round, cell count data was lost from an additional three blastocysts which also hatched in a microchannel (this data set is marked with an asterisk, and noted in Appendix B). In contrast to the first formal set of experiments, it is evident that the microfluidic results have improved relative to the microdroplet controls. This can be attributed in part to the operator learning curve, as with practice, transfer of embryos into microchannels becomes easier and reduces additional handling time.

In previous microfluidic culture trials in the literature, concerns were acknowledged about the sub-optimal quality of microdroplet control samples. Specifically, controls in past studies used large 30 µl microdroplets of non-sequential media[68, 80], although it is generally accepted in the clinical community that microdroplet culture is improved with higher embryo density culture in

smaller volumes (on the order of 0.5 - 2 µl)[75]. Thus, the improvements in microchannel culture relative to "standard practices" may have been overstated. In these studies, murine embryos in the microdroplet controls were performed using clinical expertise, with protocols and reagents consistent with the state of the art (it is also noted that the Fertility Lab of Colorado has been recognized for producing the highest IVF pregnancy rates in the U.S.). Thus, improved cell counts relative to controls in the present studies are considered noteworthy. At the same time, only a limited number of embryos were available in these studies, and larger scale trials must be pursued to demonstrate statistical significance.

The open channel culture device has yielded many new insights to the embryo culture process, and to some of the logistical issues which may be faced by embryologists using microfluidics in the future. The microfluidic environment offers environmental protection to the embryo by dampening changes in temperature or gas exchange. It was demonstrated that in well defined microfluidic geometries, it is possible to perform embryo culture with total cell counts that compare with, if not outperform, standard microdroplet culture on average. With further refinements to the fabrication and loading process, microfluidic culture should consistently outperform microdroplet culture, and a clinical study would be warranted to pursue this opportunity.

3.4.4 Transition to Closed Chambers

With the protocols and designs in place for embryo cultures in microfluidic devices, the challenges of sample transport on media collection were to be addressed. With the intent of developing culture methods compatible with metabolic profiling, it would be advantageous if it were possible to separate embryos into closed chambers on chip to retain all metabolites in spent media. In the open chambers, nutrient diffusion from the inlet and outlet ports may interfere with the metabolite levels in the vicinity of the embryo, and subsequent metabolite analysis on spent media samples would provide inaccurate measurements of actual nutrient utilization and waste production. To enable a device which can load and store embryos into closed microchannels, it was necessary to engineer a new class of microfluidic valves compatible with both embryo culture, as well as existing microfabrication techniques.

It has been hypothesized that numerous variables associated with laboratory culture systems (including accumulation of metabolites, such as lactate and ammonia and depletions of necessary nutrients, namely glucose and pyruvate) are related to the low yields of viable embryos *in vitro*. *In vivo*, the female reproductive tract is constantly active, resulting in movement of the embryo down towards the uterus. This movement also washes the embryos through constantly changing fluids in the uterus, possibly maintaining a gradient for the supply of necessary nutrients and oxygen, and the removal of waste products[26]. As the *in vivo* environment is dynamic, it is suggested that the use of an active system may be beneficial for *in vitro* culture. A concept for a recirculation culture system is presented in Figure 3.6.
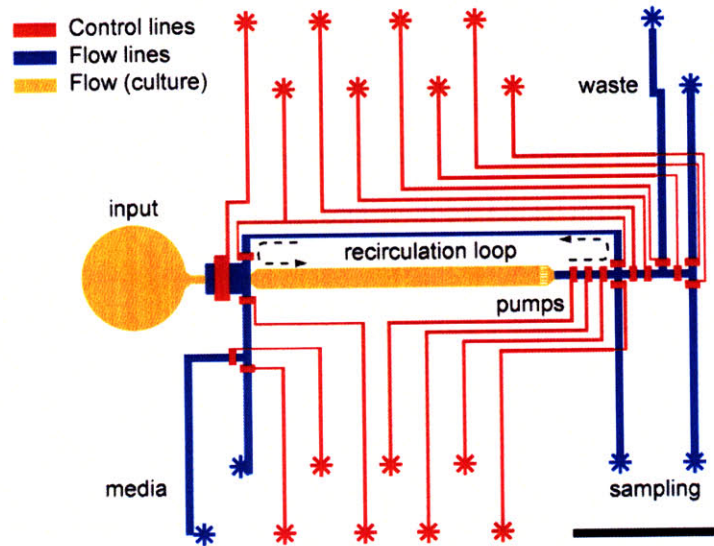
Figure 3.6: Schematic of an open loop culture device modified to include a recirculation pump. Flow lines would enable the collection of spent media for later metabolic analysis, as well as allow new media to be refreshed automatically. Three valves actuated as a peristaltic pump are used to recirculate media over an embryo which remains in the culture channel. The scale bar indicates 5 mm. The left-most valve near the inlet must be capable of passing an embryo, as well as fully seal a microchannel 150 μm in height. These specifications were beyond the capabilities of MSL valves.

Several devices were designed to enable greater control of the fluidic environment and capability for automatic media sampling. The culture channel dimensions were based on those successfully used in the open channel system, fabricated using SU8 based molds. Additional flow channels, compatible with integrated valves, were fabricated using positive photoresist. Unfortunately,

when loading embryos from the input well to the culture chamber it is necessary that an embryo (diameter ~100 μm) must traverse past at least one multilayer soft-lithography valve, typically limited to ~50 μm in height by availability of positive photoresist. There are a multitude of microfluidic valves which have been presented in the literature, but none of which could be easily integrated with the computer controlled microfluidic devices and open channel culture protocols developed thus far. It was therefore necessary to revisit the microfluidic design options available, and examine solutions to the embryo valve problem.

3.5 Development of Microfluidic Megavalves

In order to enable culture in closed chambers, it was necessary to develop of a new class of integrated valves suitable for safely loading and retrieving embryos from microfluidic devices. The most simple closed culture device would consist of an embryo culture channel (similar to those already demonstrated), with valves implemented on the inlet and outlet. The motivation of closed culture defined by valves was to isolate a sample from the surrounding environment, from other embryos located on the same device, or to enable fluid manipulation such as automatic collection of media samples for chemical analysis. Culture within a defined volume allows retention of critical growth factors and all metabolic byproducts that could otherwise diffuse away from culture chamber.

3.5.1 Assessment of Valve Alternatives

While multilayer soft-lithography valves are straightforward to integrate and control, they are typically limited to channels which are 10 to 50 μm tall. Besides the preferred MSL technique, a wide variety of alternative approaches have been developed in the microfluidics field specifically for the purpose of flow control in larger channels[89]. Alternative valve designs with potential for embryo culture may be classified by the method of actuation. These groups include pH responsive[90], thermal[91, 92], mechanical[93-96], magnetic[97, 98], pneumatic[99-102] or hydraulic[103].

There is likely no limit to the size of channels which can be sealed using pH responsive microgels[90], and there are potentially interesting applications in embryo culture in which flow of fresh media is triggered in response to decreases in media pH in a culture chamber. Practically

speaking, however, such materials cannot be computer controlled in the same manner as MSL valves, and there is concern regarding biocompatibility with embryos in microchannels.

Phase change valves, using plugs of wax which can be repeatedly melted and solidified in situ, have been used to seal arbitrarily shaped channels[91, 92]. These valves have the advantages of having a default "closed" state, but require the fabrication of heaters in the device to melt wax and permit fluid flow. There is also a concern of heat shocking of embryos by local heating of microchannels.

Very large mechanical valves have been developed in a variety of forms. Torque valves with ball screws have been cast directly into PDMS channels, but must be sealed using a screwdriver on top of the device[95]. PDMS "flap" check valves have been demonstrated to regulate flow in channels up to 500 μm wide, but require a positive back pressure to ensure a complete seal[96]. Computer controlled Braille pins have been used to seal microfluidic channels, but devices must be mounted directly on Braille displays which hinders sample observation[94]. The specialized fabrication process which was developed to make large "bell shaped" channel structures compatible for actuation by Braille pins, however, may find useful applications with MSL microfluidics.

Numerous pneumatic valves have been created using flaps of PDMS, sandwiched between two pieces of etched glass or silicon[100, 101]. These diaphragm valves are large enough to accommodate embryos, but the fabrication of these devices is not trivial. Operation of these membrane valves requires use of negative and positive pressures to realize the open and closed states, respectively. While these valves require an involved assembly process, they can be computer controlled and made to be chemically inert[102].

In light of such related alternatives, it is evident that the ideal valve would be a variation of the standard MSL valve to avoid complications involved with new control schemes and device materials. The limiting factor in creating MSL valves with larger dimensions is in the molds used for casting PDMS channels with rounded cross sections. To address this design challenge, a new class of large scale MSL valves (dubbed "Megavalves") was engineered.

3.5.2 The Megavalve Concepts and Development

Multilayer soft-lithography valves require a rounded flow channel profile for closure[25, 60], but the positive resists used to create rounded channels are generally only 10-75 μm thick[103]. To accommodate large samples in microfluidic channels, it is herein demonstrated that it is possible to combine several photoresist steps to create a "megavalve", with flow mold heights of 100 μm or even greater with readily available resists. These megavalves can be readily integrated with devices also utilizing standard sized valves. Large scale MSL valves are advantageous as they are fabricated using the same process as the open channel system, and the valves are actuated using the same microsolenoids as the microfluidic metabolite detector.

Molds for creating rounded channels are conventionally created by patterning a positive photoresist on a substrate followed by a "reflowing" process to melt the resist beyond its glass transition temperature. During the reflow process, the originally rectangular cross section minimizes free surface energy in the molten state, resulting in a continually semicircular shape. The key challenge is obtaining channels that are 150 μm or taller, which have a continuously smooth cross section. Any sharp transitions or edges in the channel geometry prevent MSL valves from fully sealing, and pressurized fluid will leak through the channel.

Early attempts to fabricate a deep channel with rounded cross section simply consisted of numerous layers of thick positive photoresist. For example, a layer of 50 μm could be spun coat on a silicon wafer, partially baked, and followed by application of a second layer of photoresist. Ideally this would provide a channel with a height of 100 μm. Unlike SU8 resist used to create the 150 μm culture channels, positive resist is nearly opaque. It was difficult to sufficiently expose the resist through deep layers to define channel patterns. Even with extended photoresist development steps, it was difficult to remove all the excess photoresist from the mold surface, and the intended channel resist was also observed to deteriorate by excessive submersion in developing solutions. In some cases, very thick layers of photoresist were developed for more than 30 minutes without removing the excess resist. It was necessary to explore other routes to obtain tall valves, preferably with one application of positive resist which could be properly developed.

Another approach to providing sufficient channel height was to stack positive resist on top of underlying SU8 structures. In this method, readily processed SU8 with rectangular cross sections could provide the foundation, and the positive resist could be patterned over top with the intention of creating a continuously smooth channel cross section. This concept is presented in Figure 3.7.
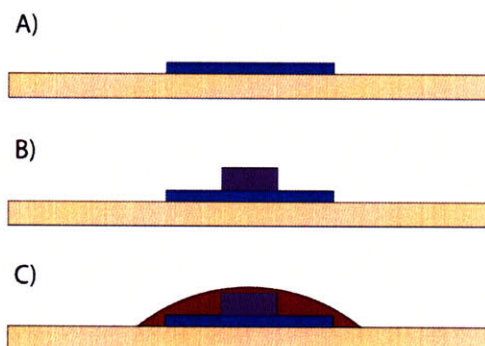
Figure 3.7: A conceptual three layer photoresist process is used to create tall channels with a rounded cross section. A) A base layer of 50 µm SU8 is followed by B) an additional layer of 100 µm SU8. C) Positive photoresist is aligned and patterned over the base structures, then reflowed to yield a rounded cross section. Note that the positive resist must extend beyond the foundation structures all the way to the mold substrate.

In this process, two layers of SU8 are used to achieve a flow channel with a height of ~150 µm similar to the open channel culture chips. In a third photoresist step, a positive resist is coated and patterned in alignment with the base structures. To round the final layer of positive photoresist, the microfluidic mold can be placed onto a hotplate or into an oven after the photolithography and development steps. Epoxy based SU8 photoresist does not reflow after it has been patterned and cross linked, which ensures that the base channels maintain their height and dimensions. The photoresist reflowing step is crucial. When in the molten state, surface tension across the resist surface tends toward smooth continuous profiles to minimize free surface energy, and this profile solidifies when the wafer is cooled back to ambient temperature. The positive photoresist must be gradually heated beyond its glass transition temperature to prevent out gassing residual solvent. If the correct processing parameters are determined that enables such a channel section to be fabricated, then it will be possible to enable MSL valve closure in the largest channel heights reported to date by multilayer soft-lithography. The

proposed assembly process for a complete device consisting of a complementary flow and control layer is presented in Figure 3.8.
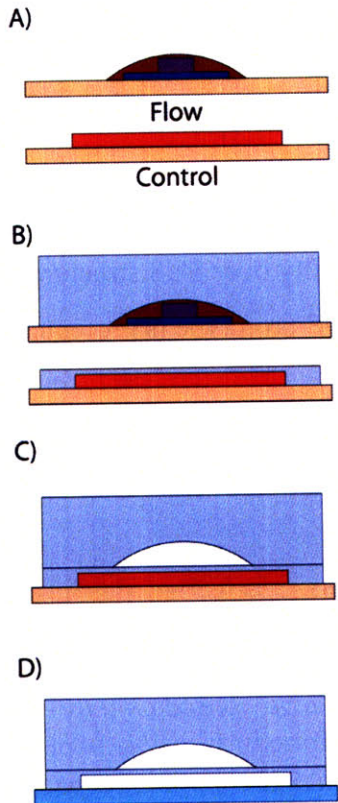
Figure 3.8: Soft-lithography fabrication of a microfluidic device containing megavalves. A) Two molds are required, one for the flow channel and one for the control valves B) The thick layer and thin layers are both cast using 10:1 PDMS, thus are plasma bonded together in step C). D) After the layers have been bonded by plasma, they are removed from the control mold as one, interconnects are punched, and devices can be bonded as usual to glass slides. This fabrication technique is compatible with conventional MSL, and regular valves can be included on the same chip with this process.

A variety of flow and molds were fabricated using the aforementioned process, using the pyramid SU8 approach coated with one layer of AZ 50 XT resist (Clariant, MA). AZ 50 XT was the most suitable resist available for valve fabrication since it is specifically designed for fabricating features with thicknesses of 25 - 70 μm. For reference, the processing of AZ 50 XT involves five steps:

1. Spin coating resist onto the wafer (~1400 rpm for 45 s for a thickness of ~50 μm).

2. A pre-expose bake (either ~30 min in a humid 90°C oven, or ~3 min @ 85°C + 10 min @ 115°C on hotplates).

3. Mask alignment and exposure, at least 1h hour or more following the prebake (~ 6 intermittent exposures, ~1 min each).

4. Development (submersion method with agitation, 400K developer diluted 1:3 in water).

5. Reflow patterned resist (on a hotplate ramped to ~120°C over 3 hours).

These steps were rough guidelines only, and it was found that shorter prebakes or increased exposures could improve pattern fidelity over SU8 structures. Several three layer test molds were designed, and the first successful prototype is presented in Figure 3.9.
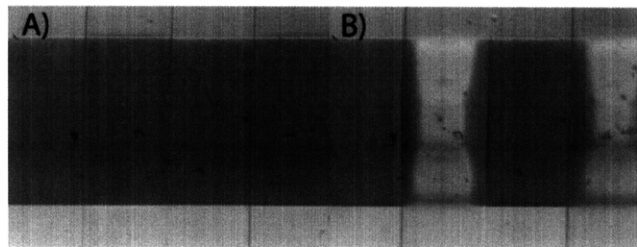
Figure 3.9: The first working "megavalve" based on a three layer photoresist process. The spine of the channel due to a tall photoresist is visible in both A) open and B) closed states. Valve and channel widths are 500 μm and 1000 μm, respectively.

Unfortunately, yield of defect free molds and reliably sealing devices during prototyping was intolerably low. Although the device casting and mold cross sections are intuitively straightforward, the interaction between different photoresists through complete processing cycles was particularly difficult to troubleshoot. Several fabrication issues commonly arose, such as the formation of bubbles in the photoresist during baking, cracking of the positive resist during reflow and, in general, the non-uniformity of channel heights. These defects would yield channel cross sections that were not continually smooth and prevent valve sealing. As observed in Figure 3.9, a sharp "spine" transition near the thickest SU8 layer was the most common failure point of valves. The PDMS membrane could not sufficiently deflect to prevent fluid flow along pronounced spines, as confirmed in microfluidic experiments with 1 μm fluorescent flow tracers which could easily leak past the "closed" valve.

For practical implementation with already challenging embryo culture, it would be important to develop a robust fabrication process and set of design rules such that these megavalve features could be readily integrated into a variety of microfluidic devices by others in the future. A parametric fabrication study was devised to investigate how to fabricate these features consistently.

3.5.3 Fabrication Parametric Study

To debug fabrication issues and identify process parameters for megavalve fabrication, a simple culture device was designed based on the open channel culture concept. Megavalves were implemented on the inlet of the culture chamber, and a regular MSL valve was located on the exit port as illustrated in Figure 3.10.
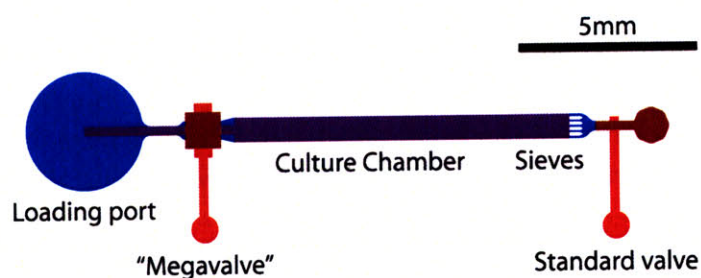
Figure 3.10: A 1 μl culture device with channel heights of 150 μm integrating a megavalve on the inlet port. This simple architecture would be used for optimization of fabrication and development of design rules for integrating megavalves on embryo culture devices.

The effect that the underlying SU8 structure has in the patterning of AZ was not well understood. It was therefore decided to test a variety of SU8 foundations in the parametric study, summarized in Figure 3.11. A pyramid-like layout of underlying SU8 was modified to support AZ resist during the reflow process. The cross section width of AZ in this experiment was 1000 μm. During the reflow process AZ resist may deform and contract slightly on the substrate. It is necessary to avoid any sharp transitions in the cross section of the final channel, either between the AZ and substrate, or between the AZ and SU8 structures, so ensure the MSL valve seats properly.

An interesting "splashing" effect was observed when spin coating thick positive resist over existing SU8. After spin coating, significant waviness of AZ is apparent over the much taller

SU8 features, and due to the viscosity of photoresist, the non-uniformity does not necessarily flatten under gravity. To also investigate the effects of this splashing effect, devices were patterned onto a wafer with various orientations.
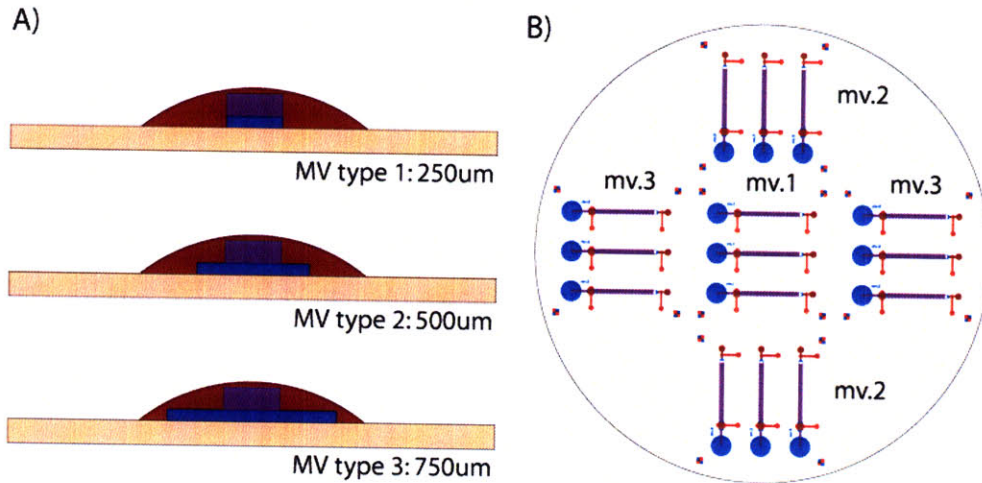
Figure 3.11: Three different megavalve profiles tested. A) The width of the base SU8 in the megavalve structure was varied to determine which design would provide the most consistent channel cross section in fabrication. The total SU8 height in all cases was 150 μm B) Pattern layout on the wafers for the fabrication study. This layout on a 3" wafer would allow the study of variations in channel fabrication that may be dependent to feature orientation in photoresist spin coating. The flow mold consists of a three photomask process (two SU8 layers followed by one AZ), and the control mold was fabricated from a single layer of SU8.

It was determined that the orientation of the tall SU8 features was in fact an important consideration during spin coating of the final AZ photoresist for reflowing. Devices oriented radially outwards from the center of the wafer allowed the resist to coat both sides of the tall SU8 channels equally. Asymmetric features resulted if features were not radially oriented with the direction of material spreading during spin coating, as determined by examination of channel cross sections. This effect was further exaggerated when thinner layers of AZ were tested.

Using flow molds fabricated with various thicknesses of 50XT resist, devices were cast using PDMS and cross sectioned to assess channel quality. To test for valve closure, chips consisting of a flow and control layer were assembled using megavalve types one, two and three. It was found that molds with 50XT thickness greater than 50 μm yielded valves which could be sealed with sufficient control line pressures. Type two designs provided the smoothest channel cross

sections, as sharp transitions were occasionally observed with types one and three. Typical results of the channel mold measurements are presented in Figure 3.12.
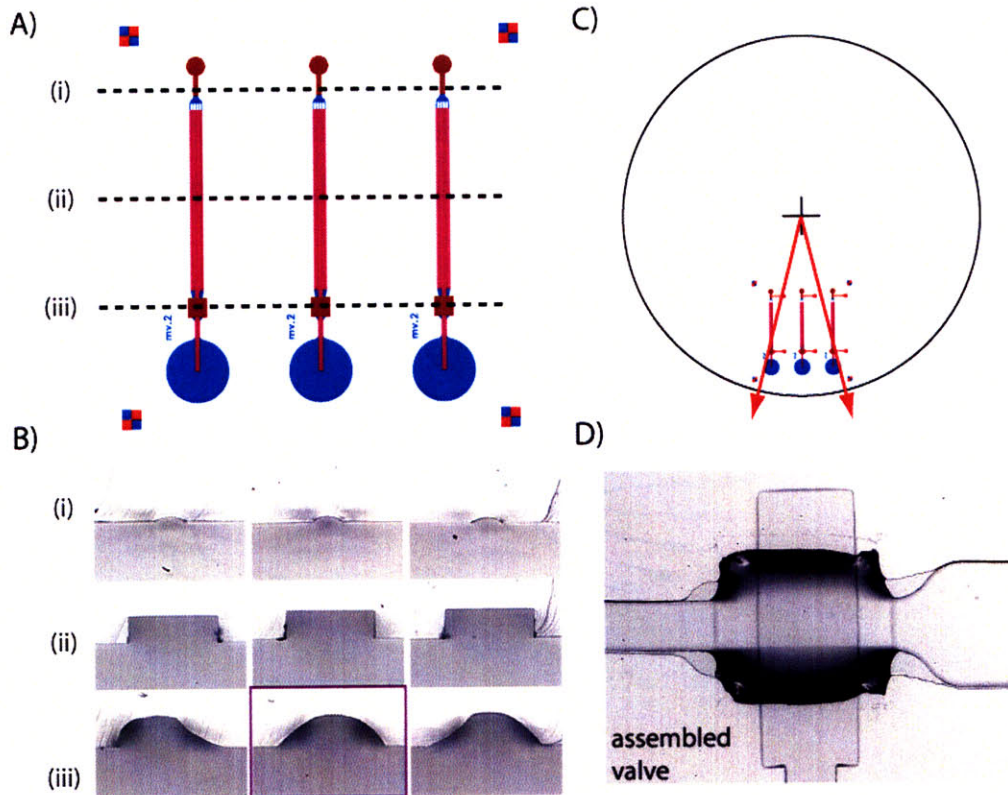
Figure 3.12: Selected results of the megavalve fabrication parametric study A) PDMS Devices were cast using the flow molds and cross sectioned in three sections B) The cross sections of the channels corresponds to the dashed lines in part A). The "splashing" effect during spin coating is apparent in two off-center devices in section (iii). C) Photoresist asymmetry in spin coating may be attributed to the feature locations on the wafer, where material is removed radially D) Devices were fabricated as per Figure 3.8 to test valve performance. This device corresponds to the center sections in B). The valve channel is 500 μm wide.

Type two megavalves were robust, and the reflow process resulted in a channel section that was almost perfectly round. As observed in Figure 3.12, the underlying SU8 is almost invisible below the AZ for the center channel, but transitions are evident on the neighboring channels. This was a result of asymmetric spin coating, since these channels were not radially aligned with the direction of material removal in spin coating. With the centerline device, it was possible to seal the megavalves with applied pressures of 5-6 psig, which is in the standard operating range of MSL control lines.

Based on this parametric study, for large displacement megavalves produced using a single layer of positive photoresist, channel geometries consistent with type two patterns were used. Also, channels encompassing megavalves were to be oriented on the molds in a radial direction if possible, to provide symmetry in the final AZ resist

3.5.4 Implementation of megavalves for culture

Using the protocols and design rules resulting from the parametric study, a new design for parallel embryo culture was ultimately developed. The channel design and fabrication steps are presented in Figure 3.13.
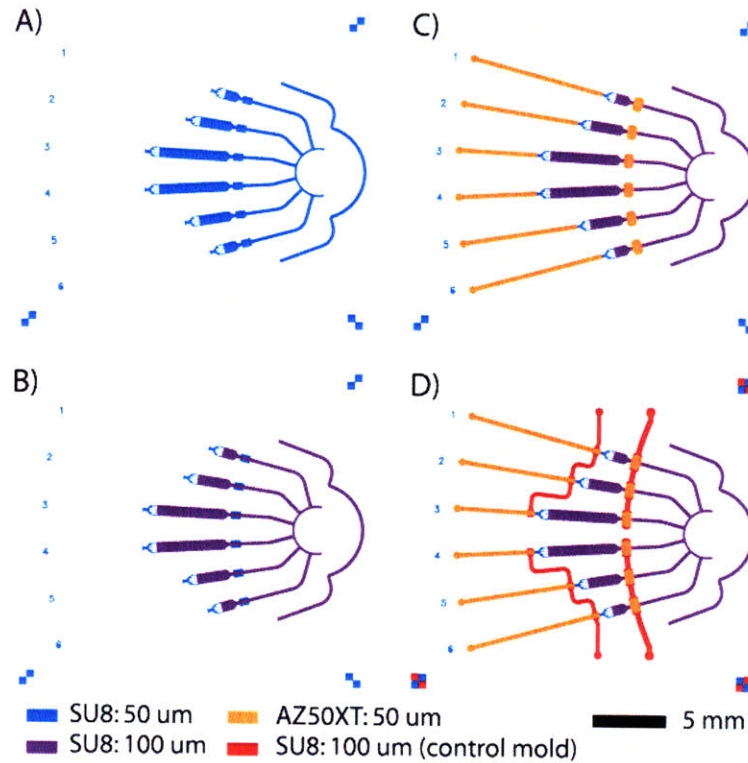
Figure 3.13: Mask layout and fabrication process for closed volume culture devices A) the base layer of SU8 encompassing the sieve channels was patterned to a height of 50 μm followed by B) an additional 100 μm to create the culture channels. C) AZ50XT photoresist was patterned to create the exit channels and megavalves. D) Control valves were patterned on a second mold. The final device contained six embryo culture chambers, which could be sealed using four MSL valves. Concept designed with David Potter of FLC.

The channel spokes were arranged on the silicon molds to ensure radial symmetry. In this way, all megavalves would be nearly symmetric. Further, a larger splash guard of SU8 (on the right hand side of the patterns) was used on later revisions to allow a more uniform positive

photoresist distribution in spin coating. Chambers in the closed volume device were nominally 125 nl, 250 nl and 500 nl, each in duplicate. Channels cast using the "6-legged" concept are illustrated in Figure 3.14. The smooth megavalves profiles, and exit sieves are clearly visible. There is also good consistency between neighboring valves (in contrast to Figure 3.12), due to the radial symmetry of the design.
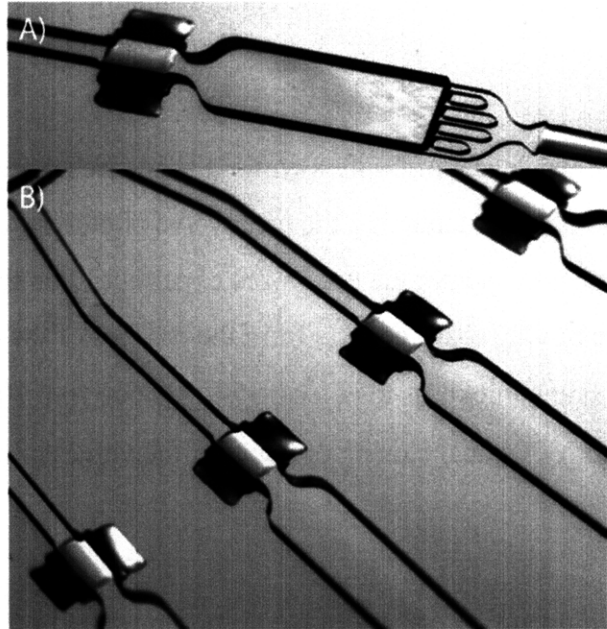
Figure 3.14: Using the fabrication protocols developed in the parametric study, it is now possible to integrate valves with the earlier open channel designs. A) Detail of a single culture chamber consisting of two layers of SU8, with a megavalve on the left and waste channel to the right. The first SU8 layer with sieve patterns is 50 µm, followed by an additional 100 µm in regions for housing embryos. B) Parallel culture channels from a common loading port.

Development of integrated, large displacement valves was a crucial turning point to enable culture in truly closed volumes. With valves on both the inlet and exit, embryos would be cultured in irrefutably the smallest microchannel devices to date.

3.6 Closed volume culture

Combining the design rules for microfluidic megavalves, and the cleaning protocols developed previously, it was now possible to culture embryos in sub-microliter confined devices.

3.6.1 A device for closed volume cultures

Consistent with the open channel systems, all newly fabricated silane free molds were dummy cast with 10:1 PDMS at least once before producing culture chips. PDMS on both flow and control molds was baked for 48 h before assembling the device with a plasma treatment. Devices were ethanol extracted and soaked with culture media, each for 24 h, in preparation for culture. Rather than water, embryo culture media was back filled into the control lines to prevent osmolarity shifts across the PDMS valves into the culture chambers during the course of five day experiments.

Since PDMS devices were being cast off wafers without silane treatments, cured devices had to be peeled very carefully to prevent damaging the megavalve photoresist, and the PDMS valve membrane. Several instances of membrane tears were experienced on the first sets of chips, which was remedied by removing sharp corners from the profiles of the control lines, as well as increasing the valve membrane thickness to at least 35 μm (~600 rpm 10:1 PDMS spun coat over 100 μm thick control molds). Typical closing pressure of the valves of these culture devices ranged from 10 - 15 psig.

A custom control manifold operating off a portable air pump was set up adjacent to the embryo incubator to allow manual control of the device valves. The manifold was connected to individual culture devices with several feet of Tygon tubing, so that control lines could remain pressurized at all times during culture. To assure complete sealing of channels, dyes were tested in the devices as per Figure 3.15.
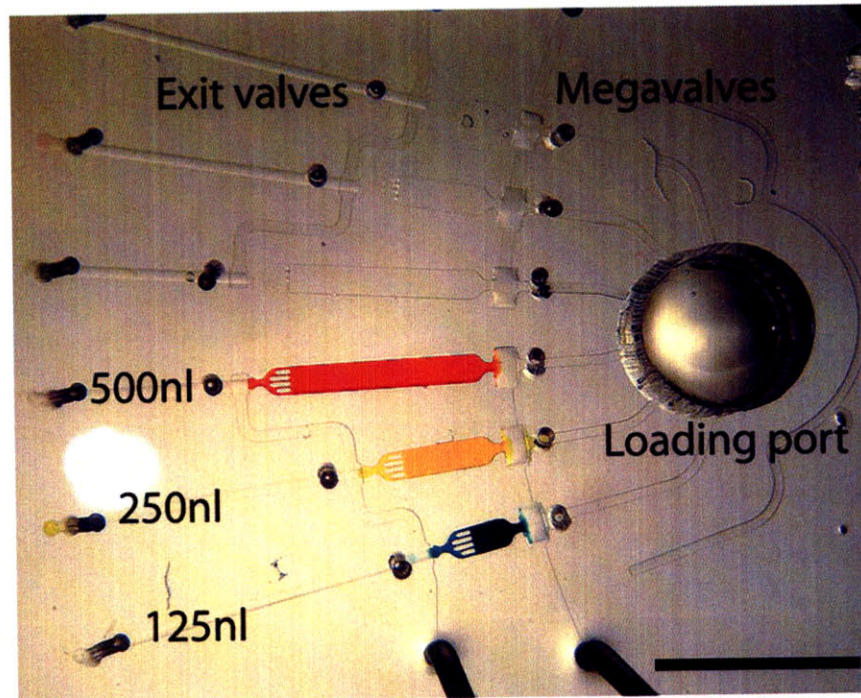
Figure 3.15: Demonstration of chamber isolation using the megavalves. Megavalves are used on the right hand side of the chambers, whereas regular valves on used on the exit port. Holes punched directly on either side of the chambers were used for volume calibration purposes, such that water containing a volume tracer could be isolated within individual chambers when the valves were sealed. The scale bar indicates 5 mm.

3.6.2 Closed culture results

Cultures were completed using the architecture presented in Figure 3.15. In parallel to murine embryos cultured individually in channels of three separate devices, controls were also cultured in various volumes of microdroplets. Microdroplet media volumes less than one microliter were dispensed as accurately as possible with glass constriction pipettes (Figure 2.1). Group cultures were also performed in large 20 µl droplets. As with open channel trials, samples were removed from incubators once daily for optical inspection.

Embryos in two of the three devices produced blastocysts, while some samples were degenerated at the two cell stage in one of the chips. During device preparation, air bubbles were not completely purged from the megavalve channels, which passed through the PDMS membrane into some culture chambers. In the other devices, no air bubbles were observed and culture was

not compromised. Morphological results of the microfluidic and microdroplet trials are presented in Figure 3.16.
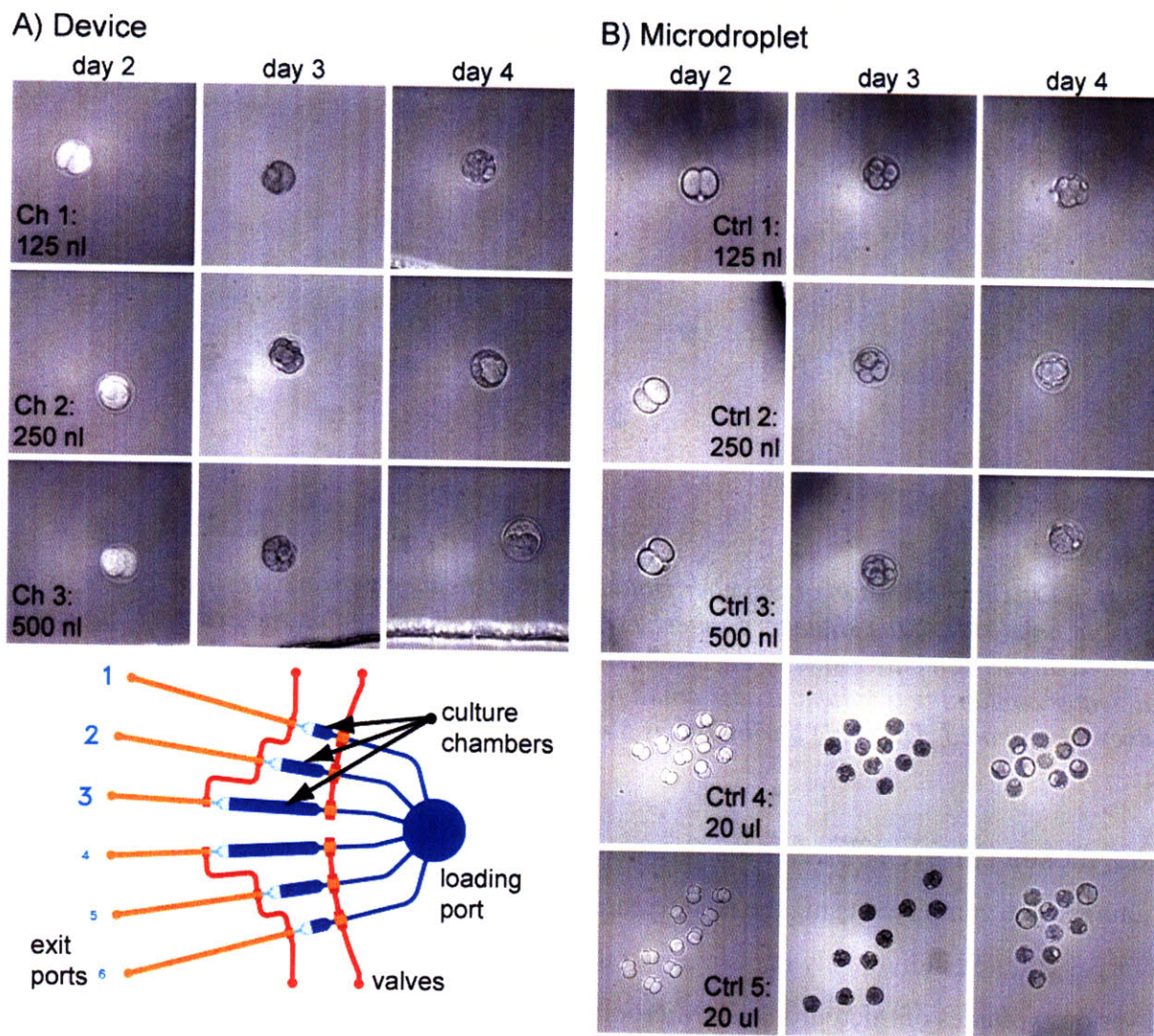
Figure 3.16: Culture results in sub-microliter microfluidic chambers. Embryos were individually cultured in six chambers of microfluidic chips, and controls were cultured in microdroplets of various volumes.

In both the device and droplet cultures, the cleavage rates of the day four embryos are lagging compared to those cultured in larger volumes. The cleavage rates of samples in 250 nl and 500 nl microchannels appeared to lead those performed in microdroplets. Cell counts (ICM and TE) were not performed on these initial trials using closed chambers, although qualitatively, the results are very promising and appear consistent with experiments refined in 1 μl open channels.

Trials are being currently underway with larger embryo populations using the closed chamber architectures to explore the affects of culture in sub-microliter volumes, and to quantify the benefit of microchannel culture. These experiments demonstrated that it is possible to culture embryos through to the blastocyst stage using the smallest microfabricated volumes to date. Integration of large scale MSL valves which accommodate embryos and do not interfere with culture represents a significant milestone in metabolomics for IVF, and opens avenues for integrated profiling.

3.7 Conclusions and Contributions

In this chapter, we developed the expertise necessary to culture embryos in static microfluidic systems, with the goal of enabling integration of downstream metabolic profiling. In contrast to previous static microchannel systems of other groups, using hybrid glass channels with PDMS bottoms, our devices were entirely produced using replica cast PDMS. Our open channel systems allowed us to debug issues with embryo handing, and fabrication toxicity. Through several culture trials, it was demonstrated that blastocyst cell counts obtained from embryos in microchannel systems were on par with, if not better, than samples cultured in conventional microdroplet formats.

Development of integrated, large displacement valves was a crucial turning point to enable culture in truly closed volumes, and to provide unprecedented regulation of flow in culture systems. While a multitude of microfluidic valve techniques have been presented in the literature, none were suitable to accommodating embryos in our microfluidic systems. As such, a new class of "megavalves" were engineered which could be operated in the same methods as standard MSL valves, yet operate on channels greater than 150 μm in height.

Microfluidic embryo culture using tools similar to those introduced in this chapter will be applicable to pursue open questions in the field of embryology. For example, it will be of particular value to determine if there exists an optimal volume for static culture in microfabricated systems, and whether that volume is limited by metabolite depletion. Also, since *in vivo* environment is dynamic, it could be studied whether gentle agitation or

recirculation of media using integrated pumps improves overall culture. Regiments for replenishing spent media could potentially be automated and reduce the need to manipulate samples manually within incubators. With microfluidic channels with integrated valves that have been demonstrated to be compatible in culture, these devices are a major step towards enabling integrated metabolite analysis.

Chapter Four - Integrated Microfluidic Culture with Metabolomics

4.1 Introduction

In the previous chapters we have developed competencies for non-invasive metabolic profiling and embryo culture using microfluidic constructs. Individually these accomplishments should be of utility to clinical embryologists by their own merits. Looking forward, an end-to-end solution for unattended embryo culture and metabolic profiling in real time would combine both of these functionalities to a single device. The objective of this chapter is to develop such a platform, capable of supporting cell culture while performing non-invasive measurements for metabolites of interest.

The tools introduced in this chapter provide a proof of concept for integrating culture and detection capacities in a scalable manner beyond techniques available in the literature. While it was not possible to utilize embryos for the present work due to availability of samples, the architectures and infrastructure designed provide the groundwork for devices with integrated embryo culture and analysis in the future.

A variety of engineering challenges are addressed to enable sustainability of cell cultures on a chip with non-invasive fluorometric measurements. The goal is to develop an approach which is general enough to satisfy the requirements, of not only embryologists, but also of biologists interested in cellular metabolism. Such a platform should accommodate many samples in parallel, offer the freedom to modify upstream culture conditions, and allow various metabolites to be examined without constraints on reagents or protocols. These are distinct advantages of the

approach conceived in this chapter which differentiates it from alternative tools previously reported in the literature.

4.1.1 Potential Applications of Integrated Culture

Several microfabricated devices have been previously demonstrated providing either discrete or continuous monitoring of specific metabolic products in cell culture. However, many of these techniques are invasive and none have demonstrated the flexibility to modify culture conditions in an automated manner based on the outcome of measurements.

Eklund et al developed a macro scale "cytosensor physiometer" with four custom fabricated electrodes capable of detecting changes in extracellular glucose, lactate, oxygen and pH[53]. Electrodes are coated with either glucose oxidase or lactate oxidase that creates hydrogen peroxide in the presence of the respective metabolite. Hydrogen peroxide can be measured amperometrically and the electrical current can be related to concentration. This system has the benefits of non-optical readout, but suffers from difficult calibration (appropriate signals are on the order of nA), lack of compatibility will all media types due to electrochemical compatibility, and the flexibility to measure additional substrates of interest. Leegsma et al also used oxidase based sensors for continuous sensing of glucose and lactate from cell culture contained in a customized enclosed chamber[52]. The sensor was capable of simultaneously detecting glucose and lactate concentrations requiring media flowrates of ~ 1 µl / min, although the system was opaque hindering morphological inspection, it could not be extended to sensing of other metabolites and was subject to noisy calibration. Shiku et al developed scanning electrochemical platinum sensors for oxygen consumption, and used these probes to measure the oxygen consumed by single bovine embryos directly within culture[54]. While the method is "non-invasive" it does require manual holding of an embryo while a 4 µm diameter probe traverses within 5 µm of the surface. The authors did correlate higher oxygen consumption to the developmental potential of bovine embryos, although widespread use of this technique may be hindered by the complex instrumentation and need to manipulate every embryo for measurement. Finally, Ciobanu et al furthered the use of scanning electrochemical glucose oxidase and lactate oxidase probes to be compatible in a wider range of culture media, and demonstrated their instrument could create surface maps of metabolite concentrations

surrounding single mammalian cells at a certain point in time[55]. In many assays, however, such detailed information is overkill and difficult to interpret. Rather, endpoint measurements averaged over longer windows may be more useful to infer the average nutrient utilization of a cell, or group of cells. Many of the aforementioned studies focus on instruments used to detect specific metabolites, which necessitate non-trivial electrochemical calibration. They also lack scalability to analyze additional samples in parallel, and the ability to adapt culture conditions based on feedback of current measurements.

An interesting approach to cell culture would be the integration of feedback driven protocols based on metabolic measurements. For example, if nutrients were depleted, or by-products were produced, beyond predetermined thresholds then media could be replaced. If regulation of metabolic activity was desired, cells could be either physically or chemically perturbed to varying degrees in order to achieve a desired metabolic output. A single microfluidic device may be capable of supporting cell culture, periodically performing metabolic assays, and replacing or even generating new media formulations on demand upstream of culture.

Beyond the overdue embrace of metabolomics in the IVF community, there are many fields of cell biology where metabolic profiling plays a critical role. Directed evolution, drug toxicity and cancer treatment are some of the most pressing research fields where microfluidic tools for metabolomics may be particularly valuable.

A key challenge in cancer therapy is the development of treatments to preferentially kill cancer cells without undo harm to healthy tissues, and metabolism may offer opportunities to new strategies. An area that has received much attention is the potential regulation of metabolic activity of cancer cells through glycolytic inhibitors. Although all causes are not yet understood, it is widely observed that most cancer cells exhibit altered metabolic profiles in comparison to normal adult tissues, and in particular increased levels of glycolysis[35, 39]. Cancer cells depend almost solely on this metabolic pathway to generate ATP as their main energy source, which is known as the Warburg Effect (observed more than 75 years ago by Otto Warburg). The excess of lactate produced by cancerous cells, which may be considered a first order indicator of overactive glycolysis, is known to rapidly decrease the pH of surrounding medium to acidic

levels[55]. The net reaction for glycolysis (the process by which one molecule of glucose is catabolized to two molecules of pyruvate with a net gain of two molecules of ATP) is:

$$\text{Glucose} + 2\ P_i + 2\ \text{ADP} + 2\ \text{NAD}^+ \rightarrow 2\ \text{Pyruvate} + 2\ \text{ATP} + 2\ \text{NADH} + 2\ H^+ + 2\ H_2O$$
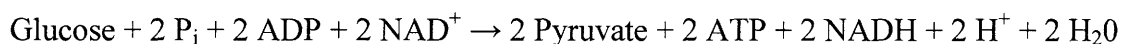
Pyruvate is utilized through the tricarboxylic acid (TCA) cycle and oxidative phosphorylation in mitochondria in healthy cells to generate ATP, but if these cycles are dysfunctional, pyruvate is converted directly to excess lactate by lactate dehydrogenase (LDH). ATP generation by the glycolytic pathway is far less efficient (2 ATP per glucose consumed) than alternative pathways (36 ATP per glucose by oxidative phosphorylation), thus cancer cells consume far more glucose to generate sufficient ATP for metabolism and proliferation[35]. This increase in aerobic glycolysis and dependency on this pathway for ATP generation in malignant transformation suggests the fundamental importance of this mechanism and suggests possibilities to kill cancer cells by therapeutic inhibition of this pathway[35]. Mitochondria of normal cells are able to adapt to alternative sources to generate ATP, such as amino or fatty acids, rather than depend on glucose[35].

An automated approach for studying the effectiveness of various inhibitors on tissue and cell lines (or even combinations of inhibitors for simultaneously addressing different pathways) in a streamlined platform could be very powerful. Most of the microfluidic protocols required for microfluorometric analysis have been studied and understood in previous work. To demonstrate the potential of an integrated analysis approach, a device is devised which is capable of metabolic profiling of mammalian cell cultures in a parallel manner.

4.2 An Integrated Device for Parallel Processing

A platform was developed to enable culture of small populations of mammalian cells lines in separated chambers, each of which is equipped with a downstream mixer for monitoring metabolism non-invasively.

Previous parallel architectures for bacterial culture and processing of nucleic acid from single cells have been previously developed[32, 104, 105]. In recent work, a parallel architecture was developed capable of supporting cell culture in 96 separate chambers for a period of weeks with on demand replenishment of different types of culture media[106]. These devices demonstrate the scalability and automation enabled by microfluidics, as well as the advancements in supporting cell culture on chip. In many of the previous studies, optical inspection of growth quality was performed directly within of culture chambers, while for non-invasive metabolic profiling, it will be necessary to periodically transport samples of media from the cell culture chambers for assays with metabolite cocktail. A layout with modular culture chambers and assay chambers was designed for this purpose.

4.2.1 Utilization of Cell Sieves

In order to seed and grow uniform cell populations on chip, previously characterized microfluidic designs for trapping cells are implemented[36]. These cell sieve designs are easily integrated with standard microchannels. Numerous "C" shaped sieves with open slits of ~ 8 µm are positioned within a culture chamber, and are used to catch mammalian cells with diameters of ~ 10 µm from a flowing solution as illustrated in Figure 4.1. Following the removal of excess cells by a wash with fresh media, adherent cells are allowed to culture within the chamber.
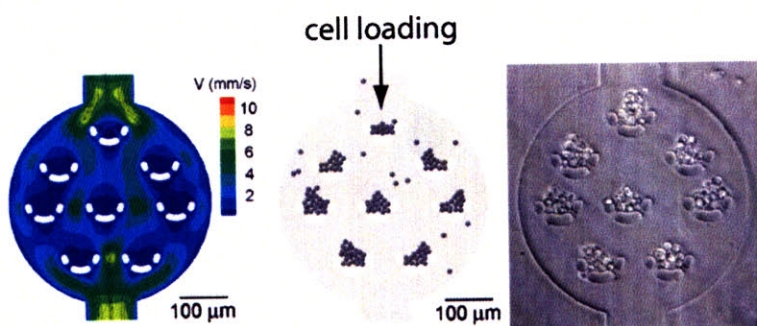
Figure 4.1: A microfluidic cell sieve for delivering highly repeatable populations of cells to culture chambers on chip. These modules are used for containing cell cultures within the implemented device. Figure adapted from M. Kim et al (2008).

Typical diameters for the cells culture chambers are between 400 and 800 µm, with heights in the range of 20 - 25 µm. Approximately 100 cells are seeded per chamber, as governed by the size and number of sieves. The advantage of using microfabricated geometries to trapping cells

is that the number of cells loaded into the sieve tends to an asymptotic value with loading time, which reduces uncertainty in loading due to initial cell density.

4.2.2 Device Architecture and Operation

Using modular cell culture and metabolite detector mixer elements (Chapter Two), a scalable architecture was designed. Assay operations, such as sample metering, loading of metabolite cocktails, and assay mixing can be performed simultaneously across multiple analysis lanes. A schematic of the integrated chip is presented in Figure 4.2
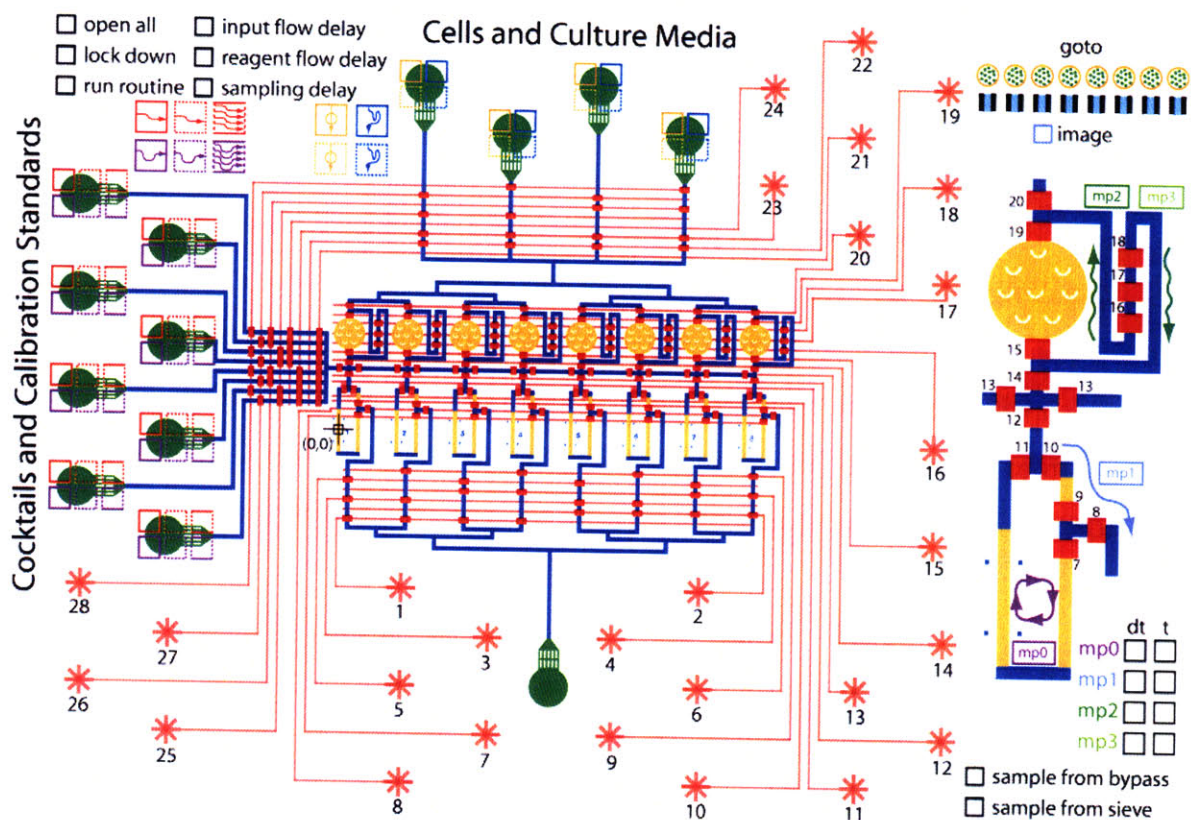
Figure 4.2: A microfluidic architecture with eight culture chambers for parallel processing of metabolic measurements (Figure adapted from software interface, JPU). Reagents including enzymes, washes and standards are located on the left which can be directed to the detection rings. The top four inputs are reserved for cell seeding and for supply of fresh media. Mixing of all eight reactions occurs at the same time using common control lines. A motorized microscope stage enables unattended fluorometric measurements of all reactions.

This architecture contains two independent sets of multiplexors. One set regulates the flow of inputs, and the second is used to select the outlet channels between the mixing rings and the waste port. In this manner, different compositions of media and cells can be directed to each of

the eight individual culture chambers, while analysis can be completed in parallel. Flexibility of this architecture is demonstrated in Figure 4.3, where custom mixtures of media were prepared in six neighboring chambers. While many experiments will only involve a single cell and media type, an advantage of the dual multiplexor approach is that the media can be replenished on unique schedules for each chamber.

Figure 4.3: The integrated architecture contains an additional set of multiplexors on the output channels, to combine the flexibility of independently addressable sample chambers with the high-throughput strategy of parallel sampling. Here, mixtures of food coloring are metered to culture chambers to yield a rainbow pattern. Cell chambers are 800 μm in diameter.

In the context of inhibition assays, it is now possible to deliver different formulations of media to individual cell cultures, yet perform automatic metabolic analysis in parallel. Further, this device was designed to be scalable. As such, only minimal changes to control and flow networks are required to accommodate, 16, 32 or even more chambers for profiling.

4.2.3 Device Functionality

The device was developed with the goal metabolic profiling in a non-invasive manner, similar to the approach that would be implemented for embryo measurements. With this in mind, fluorometric assays on samples of spent media would be performed in reaction chambers

downstream of culture, and the necessary mechanisms for sample collection would have to be designed. It was important that metabolite enzymes never contact the cell cultures.

The integrated assays were separated into three steps. First, samples would be cultured within well defined volumes of media, with known initial concentrations of metabolites. Second, after a predetermined amount of time, used media from the culture chambers would be drawn downstream into dedicated mixer. In the final step of the assay, the sample of media would be mixed with a metabolite cocktail and fluorometric measurements would be recorded in a manner identical to the standalone detector[107]. These mechanisms are illustrated in Figure 4.4.
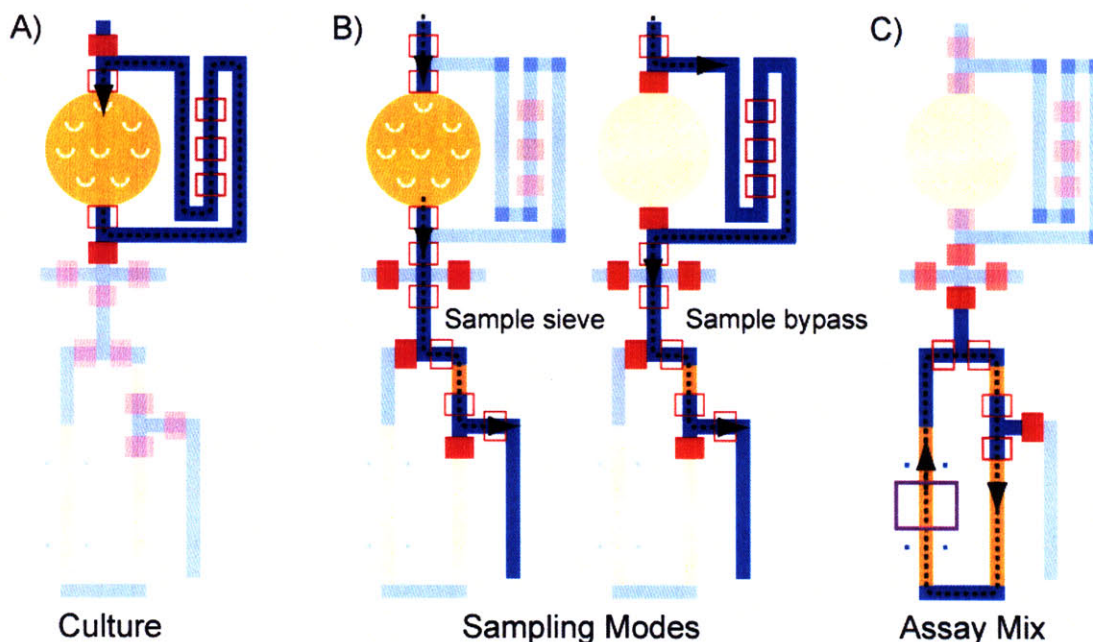
Figure 4.4: Primary operating modes of the integrated metabolic detector. Yellow, blue and red lines represent culture, flow and control channels, respectively. For scale, channels are 100 μm wide. A) In the culture mode, peristaltic pumping may be used to gently circulate media over a population of cells inside of a closed loop. This ensures that metabolites and growth factors are retained and homogeneous throughout the culture media to be sampled. B) The culture loop design enables two different media sampling modes to be used. Samples may be peristaltic pumped from either the culture chamber, or the bypass channel, to the top right of the assay chamber. C) In the assay mode, metabolite cocktail is loaded to the left side closed mixing loop and mixed with the sample. The purple outline indicates the imaging region.

A recirculation loop approach for the culture chamber was chosen to ensure that sampled media has a uniform concentration of metabolites for measurements. The bypass chamber also allows

new reagents to be directed towards culture chambers, while preventing cross contamination of upstream reagents over the cells. Each chamber is expected to contain ~ 100 cells during experiments, with some stochastic variation due to the loading process and exact mold geometry[108], with corresponding changes in metabolite levels expected to be on the order of ~mM per hour (discussed in detail in section 4.4).

With this non-invasive approach, there is a tradeoff in sampling rates for metabolic profiling. If samples are drawn frequently, higher resolution profiles may be determined although the cellular environment may be perturbed more frequently. Longer culture periods between samples would lessen the effects of measurement noise and allow more accurate time averaged metabolism to be reported. It may be necessary to experiment in both these regimes to also determine how the media refresh rates will affect nutrient utilization. With this operating strategy in place, it was necessary to implement the remaining infrastructure necessary for parallel fluorometric imaging.

4.2.4 Device Fabrication and Platform Control

Devices were fabricated using either bottom-up valve configurations with RTV 615 PDMS. Flow molds 25 μm tall were fabricated using a two step photolithography process as per Chapter Two, with rounded channel sections of positive resist (AZ 50 XT, 3100 rpm) compatible with valves, and rectangular channel sections (SU-8 10, 1200 rpm) for cell trapping and fluorometric detection. Control molds were also fabricated with a two step process using layers of 25 μm thick SU-8, also following the design rules from Chapter Two. Chips were cast using standard MSL procedures from the molds treated with fluorinated silane, baked for a minimum of 36 h, and plasma bonded to 1 mm thick glass slides. Prior to use, channels were soaked with ethanol for several hours, and dried using nitrogen.

Computerized valve control and connections of all reagents are as previously described for the single chamber detector. Typical control pressures were ~ 15 psig, and sample inputs were maintained at ~ 4 psig. Rather than water, it is critical that sterile PBS was backfilled into control channels to prevent adverse osmolality shifts of media during culture due to transport through PDMS membranes.

To enable parallel fluorometric imaging of all eight mixing chambers, control of a motorized stage (Prior H117) on the microscope (Olympus IX-71) was integrated with the BioStream JAVA software. A "zero" position was declared over chamber 0 (the mixing chamber on the left hand side of the device). All chambers and mixing rings were identified with nominal (X, Y) coordinates in a driver file, which were referenced by the image acquisition commands. Further, to account for devices which are not perfectly parallel with the glass slides during plasma bonding, coordinate transformations were used to translate nominal (X, Y) locations to actual (X', Y') positions. The coordinate transformations were of the form $X' = X \cos \theta - Y \sin \theta$ and $Y' = X \sin \theta + Y \cos \theta$, where θ is the angle of skew in radians. An example series of corrected images is presented in Figure 4.5.
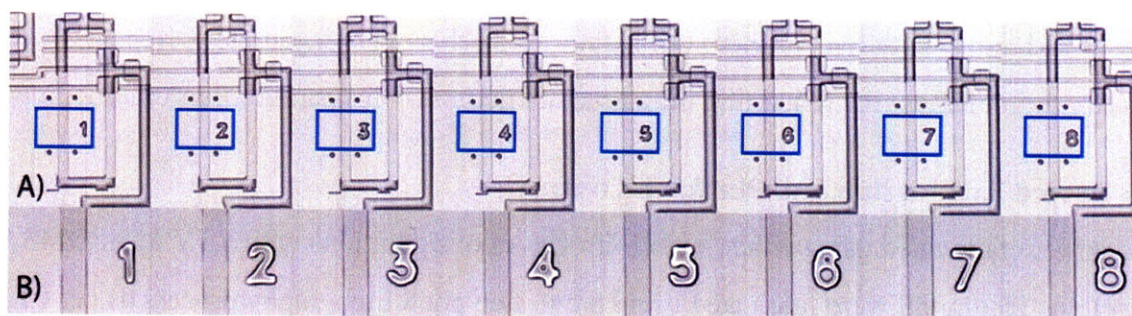
Figure 4.5: Automatic images acquired from parallel lanes of the microfluidic device. A) A subtle ~4° rotation is evident in the device, introduced during the manual plasma bonding of the chip to the glass slide. Since chambers one and eight are ~1 cm apart, this can lead to imaging discrepancies if direct lateral translation is used for imaging (y error = tan (4°) * 0.01 m = 700 μm). B) Coordinate correction of the nominal skew angle allows images to be acquired at identical locations for each detection channel, to improve quality of measurements. Channels are 100 μm wide, imaged at 20X.

With the imaging mechanisms automated, it was straightforward to perform fluorescent analysis sequentially across all chambers in a matter of seconds. The automated scanning routines could also be used to regularly inspect the cell morphology within culture chambers.

4.3 Device Calibration

Based on the experience of developing and troubleshooting the serial metabolic detector device, it was straightforward to identify the key issues that would have to be calibrated on the integrated

platform. With the serial standalone device, sample throughput and repeatability was of primary importance since only one mixing chamber was in operation. In management of parallel analysis channels, not only should results be repeatable on a single channel, but they must be repeatable chamber-to-chamber for the purpose of comparing metabolic results. By these criteria, uniformity between all chambers is more important that absolute speed. For example, it may be possible to draw samples from all chambers for metabolic analysis in under one second, but slower, regulated sampling will ensure similar volumes are used for all eight reactions. As there are eight parallel reactions, the throughput of data is still appreciable even when individual operations are performed at a reduced rate. It was also desirable to ensure consistent treatment across all separate samples being cultured on chip.

Calibration trials were completed on each of the three operational modes outlined in Figure 4.4 to ensure uniformity between chambers, as well as to minimize operating time and sampled volumes. In these trials, inputs of food coloring were used as mock inputs. Example calibration trials and images of sample isolation are presented in Figure 4.6.
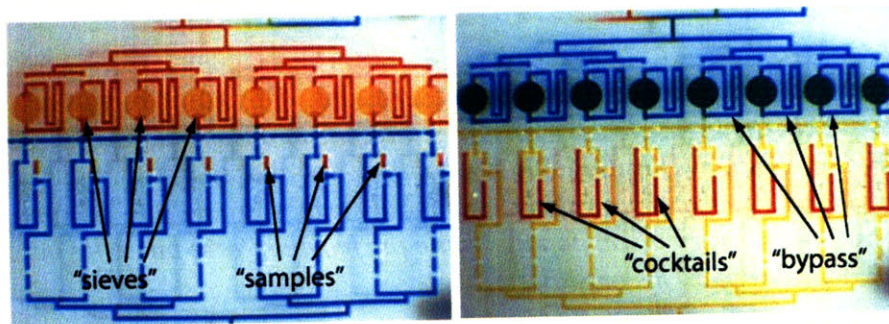
Figure 4.6: Typical images used for loading, sampling and mixing calibration. Key areas of the device are annotated.

In the following sections, important performance parameters are discussed for each of the circulation, sampling and assay operating modes.

4.3.1 Culture Media Circulation

To initiate a metabolite assay experiment, fresh media with known metabolite concentrations would be supplied into both the culture chamber and bypass channels. Cells would be allowed to culture within their chamber, and periodically peristaltic pumps would be used to circulated

media around the chamber to ensure that all nutrients are made available to the cells, and also that the media is homogeneous prior to sampling. A calibration panel is presented in Figure 4.7 for the recirculation pumping trials, where performance of different peristaltic pumping duty cycles was assessed.
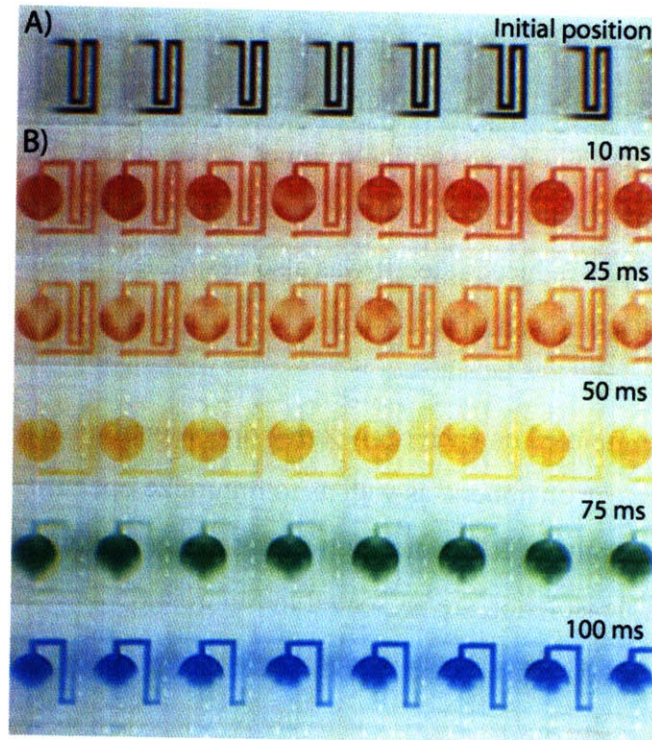
Figure 4.7: Calibration of culture recirculation operations. Peristaltic pumps are used to circulate media within the eight closed loops over the cells to ensure uniform metabolite concentrations for sampling. A) Initially fluid samples were docked in the bypass chamber. B) Fluid was pumped for 10 seconds at various pump duty cycles, from 10 to 100 ms. Some non-uniformity is observed for very fast pumping, while the most uniform pumping across all chambers for duty cycles of 50 ms or slower.

While it was possible to rapidly circulate media around the chamber, differences in valve performance become apparent at high pumping frequencies. Thus more uniform recirculation operations across the device were ensured by using longer duty cycles, which may also prevent adverse effect on culture due to reduced fluid shear stresses.

4.3.2 Sample Metering

Experiments were completed to identify the conditions by which identical volumes of media from the eight culture chambers could be sampled. It was found that while this operation could

be completed very quickly, uniformity would suffer as observed in Figure 4.9. If too much sample is drawn from a single chamber, the bypass chamber or sieve could be exhausted of valuable sample before profiling is completed.
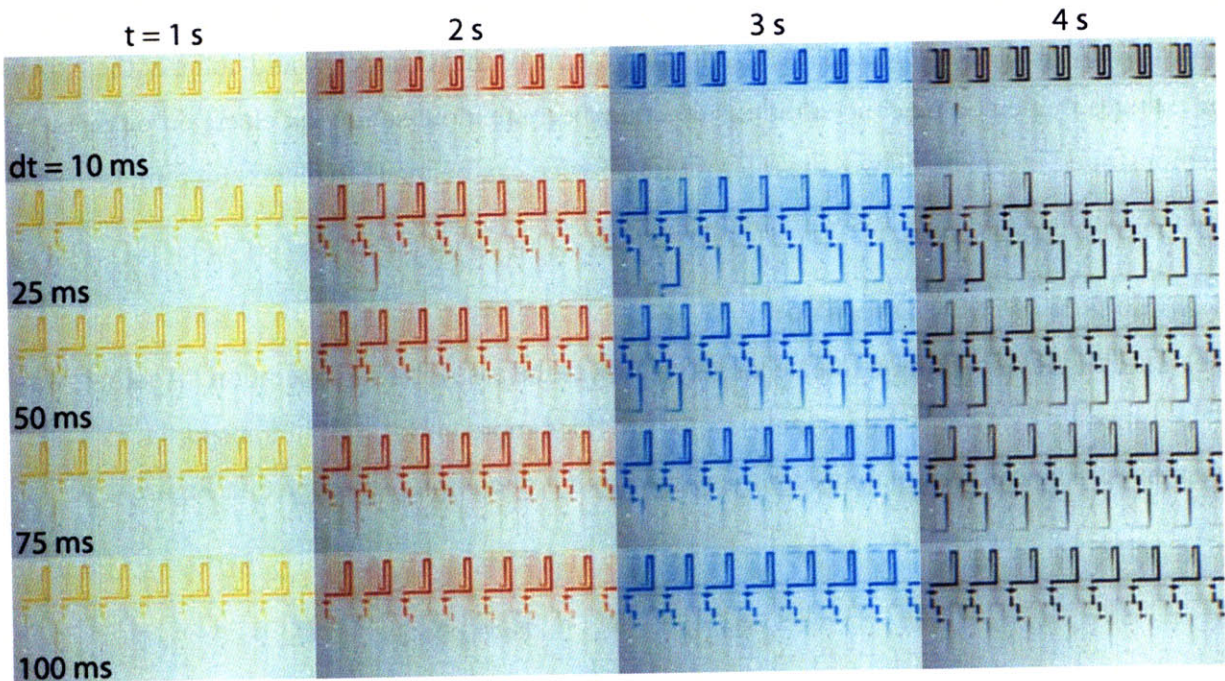
Figure 4.9: Calibration panel of the media sampling operation. Peristaltic pumps in the lower mixing ring are used to draw media from the culture sieve or bypass loop, using various duty cycles (rows) and total metering times (columns). The rate of pumping plays an important role in metering uniformity. For duty cycles 50 ms or less, significantly more media was drawn from some chambers than others (e.g. 25 ms cycles for 3 s). Ideal metering is achieved for duty cycles of 100 ms for total cycle times of three or more seconds.

The channel volume between the culture chambers through the enzyme mixers is nominally 3.3 nl, while the volumes of the sieve and bypass channels are 12.6 nl and 11.2 nl, respectively. Unfortunately with this device configuration and sampling scheme it will not be possible to complete a nominal seven or more ($\sim$ 23.8 nl / 3.3 nl) metabolic measurements. Since the existing culture volumes are replaced with fresh media during sampling, diffusion will dilute the existing media of interest. Taylor dispersion will also work to accelerate the dilution process, since fresh media introduced to the chambers traverses the centerline of the channels approximately twice as fast as the average flowrate of the remaining fluid. The meandering bypass channel was designed with a longer path length specifically for these reasons of diffusion and sample transport.

As a result of this parametric calibration study, it should be possible to draw as many as four or more media samples from the bypass and sieve chambers for replicate metabolic measurements before it is necessary to completely replace the media. If additional replicate measurements are desired, it would be straightforward to scale up the length of the bypass channel to generate larger samples of spent media. Increasing the volume of this channel would come at the expense of changes in metabolite concentrations that may become more subtle to detect, although as demonstrated in Chapter Two, the microfluidic device can be tuned to detect micromolar concentration changes or less without difficulty.

4.3.3 Cocktail Mixing Operation

The third mode of operation to be characterized was the assay mixing operation. Again, it was determined that slower pumping duty cycles provided more uniform fluid transport across all chambers. The calibration panel for the assay mixing operation is presented in Figure 4.8.
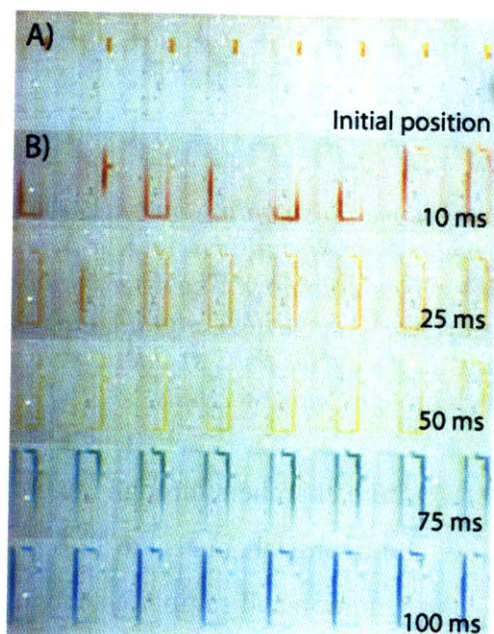
Figure 4.8: Calibration of parallel mixing operations to combine media samples and enzyme cocktails. Peristaltic rotary pumping is used on circular mixing rings, each with a volume of approximately 10 nl (1nl media sample, mixed with 9 nl enzyme). A) In the calibration study, a colored marker was docked in the sample portion of the mixer. B) Uniformity of pumping was assessed at different pumping duty cycles, after a total pump time of ten seconds. Non uniformity of sample mixtures was observed for fast pumping (duty cycles < 50 ms), while pump cycles of 100 ms appear suitable for slightly slower, but highly uniform mixing.

Based on extensions of similar calibration trials , it was decided that pumping should be performed using duty cycles of at least 75 ms, for 30 seconds or more. Fortunately, unlike the recirculation and sampling operations, it is not critical that all assays are performed consistent among one another. It was more important that performance of an individual chamber was consistent from run to run, since every assay chamber would be fluorometrically calibratied separate from one another.

4.4 Cell Assay Design

With the device infrastructure, imaging routines, and fluid operations well characterized, the device would then be primed for performing cellular metabolic profiling. To transition to integrated assays, it was necessary to calculated metabolism estimates for our mammalian cell line, create custom blends of culture media suitable for fluorometric assays, and perform fluorometric calibration trails. Further, since these experiments will use mammalian cells as opposed to embryos, consideration was given to the problem of culturing adherent cells on PDMS surfaces.

4.4.1 Predictions of Cellular Metabolism

In order to determine the adequate concentration of metabolites to utilize for fluorometric calibration of media, it was desirable to know the expected consumption of glucose and pyruvate, and the production of lactate due to cell culture. Rates of changes in these metabolites are highly dependent on culture media compositions, temperature, pH and general culture technique, thus any predictions would have to be used as guidelines only when adapting these results to a microfluidic based construct.

In particular, relevant metabolism measurements reported by Barton were performed in macro scale dishes, and may not apply to cells cultured in confined volumes[109]. Across a range of culture media pH between 6.8 and 7.5, glucose consumption and lactate production values for HeLa cells were measured to lie anywhere in range of 0.2-0.8 mg / 1E6 cells / 24 h, and 0.1 - 0.4 / 1E6 cells / 24 h, respectively[18, 110]. DMEM media which will be used in these studies also has a range of pH values depending on the formulation and buffer strengths, but if we assume a

midrange pH of 7.2, approximate glucose and lactate changes are 0.41 mg / 1E6 cells / 24 h, and 0.16 mg / 1E6 cells / 24 h, according to Barton[109].

The cell sieve structures in the integrated device accommodate approximately 100 cells each[36]. Thus we may expect that ~1.7E-6 mg glucose will be consumed, and that ~6.7E-7 mg of lactate will be produced every hour, in each chamber. On a molar basis, these hourly differentials are equal to 9.42E-12 moles glucose, and 6.0E-12 moles of lactate. Further, the total available media volume is ~25 μl within the combined culture and bypass circuit. This suggests that the glucose concentration will drop by ~0.37 mM / h, and the lactate concentration will increase at ~0.24 mM / h. These metabolic rates were reported using a different culture media and approach, but provide a starting point to determine the sensitivity requirements of our detector.

In the serial metabolite detector from Chapter Two, expected physiological changes in metabolite concentration in embryo media samples were in the range of 0 - 0.5 mM, and the microfluidic platform was capable of detecting changes in the μM range. This resolution therefore should be sufficient for measuring the changes in nutrient levels of mammalian cells populations after even minutes of culture. Conversely, it would be possible to reduce the numbers of cells per culture chamber, with the tradeoff that it may that it may take longer to generate sufficient concentration changes in the media which can be measured. Perhaps with an optimized microfluidic system, it could be possible to use these fluorometric assays for single mammalian cell metabolic profiling in the near future.

4.4.2 Cell Media and Calibration

With approximations of metabolic rates completed, it is possible to compute and prepare a range of calibration standards suitable for on chip assays with culture periods from 0 to 24 h. The nominal concentrations of glucose, lactate and pyruvate in conventional high-glucose DMEM media are 25 mM, 0 mM and 1.25 mM. Custom media was prepared based on a formulation of low glucose media (Invitrogen, 11054-020) which was free of lactate and phenol red pH indicator (which would interfere with fluorometric measurements). For culturing purposes, glucose was supplemented to original DMEM levels of 25 mM glucose. A range of standards with known glucose, lactate and pyruvate concentrations based on the phenol red free media

would be used for fluorometric calibration. Contents of the four calibration standards are provided in Table 4.1. Since it was not possible to obtain DMEM media which did not contain phenol red without also including pyruvate, it was necessary to use an extrapolation calibration scheme. A linear calibration curve would be calculated for concentrations greater than 1.25 mM, although pyruvate will actually be consumed during metabolism.

As with previous metabolite specific assays, glucose, lactate and pyruvate were combined into single standards to reduce the number of required fluid input to the device. After reagents had been added and mixed, all media was passed through a 0.22 μm syringe filter prior to refrigeration.

Nominal	STD 1	STD 2	STD 3	STD 4	
glucose	25	20	15	10	mM
[180 g/mol]	225.00	180.00	135.00	90.00	mg/50 ml
lactate	0	2.5	5	10	mM
[112 g/mol]	0.00	14.01	28.02	56.04	mg/50 ml
pyruvate	1.25	1.50	1.75	2.00	mM
[88 g/mol]	5.50	6.60	7.70	8.80	mg/50 ml

Table 4.1: Metabolite concentrations in the media standards and fitted values

To assess sensitivity of the detector as well as develop analysis routines, numerous calibration assays were performed. Replicate assays were performed for the three metabolites of interest, across the aforementioned media standards. Each assay of a single calibration standard for a particular metabolite required approximately ten seconds for metering samples, 60 seconds for mixing, and another ten seconds to automatically image all eight chambers. An example calibration panel from an assay routine is presented in Figure 4.10.
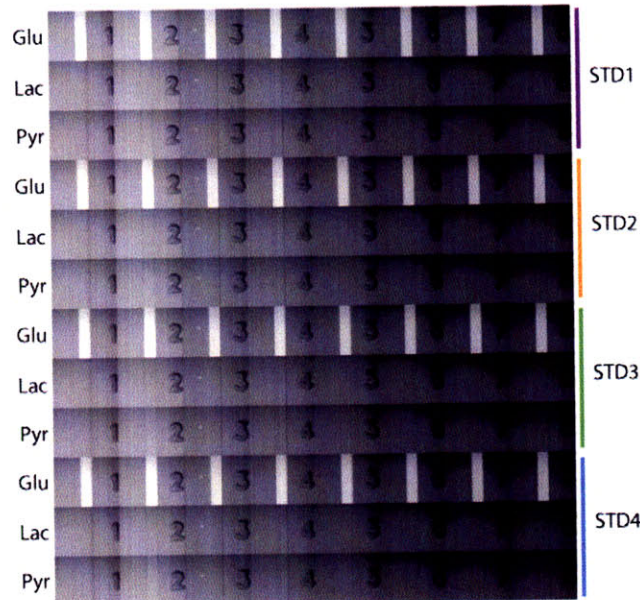
Figure 4.10: Montage of fluorometric images acquired during the detector analysis routines. Four calibration standards are assayed for glucose, lactate and pyruvate. The channel widths are 100 μm. While obvious fluorescence is only apparent in the glucose set of images, the 16 bit CCD camera used to acquire these images has a large dynamic range and acquires sufficient signal from all the channels. In all cases, the fluorometric measurement reported is the difference in intensity between inside the microchannel and surrounding background.

Due to the difficulties in obtaining sub milligram accuracy in adding G, L and P to aliquots of culture media, some discrepancies from nominal concentrations were experienced. Following several rounds of calibration, a correction scheme was used to determine which actual concentrations of metabolite are necessary to generate linear curves, as per Figure 4.11.
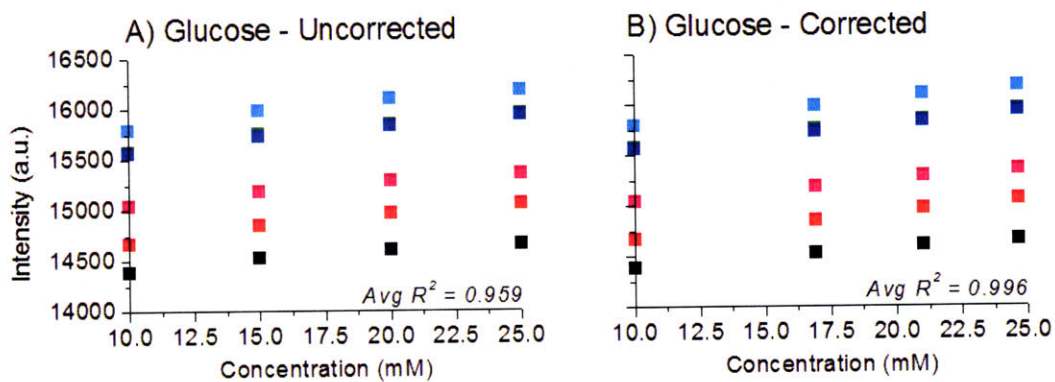
Figure 4.11: Correction of nominal to actual glucose concentrations in the calibration standards accounts for inaccuracies in metering sub milligram amounts of metabolite. The linear coefficient of determination averaged across all eight chambers is significantly improved.

In all cases, nominal values of metabolite in the media as received were not modified. Similar correction schemes were also tested for both the amount of lactate and pyruvate in media standards. Corrected values are summarized in Table 4.2.

Concentration (mM)	STD 1	STD 2	STD 3	STD 4	Avg R^2
Glucose - nominal	25	20	15	10	0.96
Glucose - corrected	25.64	21.02	16.92	10	0.99
Lactate - nominal	0	2.5	5	10	0.98
Lactate - corrected	0.00	3.59	5.01	9.72	1.00
Pyruvate - nominal	1.25	1.50	1.75	2.00	0.97
Pyruvate - corrected	1.25	1.52	1.78	1.97	0.99

Table 4.2: Nominal vs. corrected concentrations and resulting linear fits averaged over all eight assay chambers.

4.4.3 Culture Surface Treatments

A known challenge in microfluidics is the ability to culture adherent cell lines directly on PDMS surfaces. To circumvent these difficulties, "push down" valve geometries are most often used with mammalian cells such that culture in microchannels can occur in contact with a glass substrate. Since the performance of the device was found to be more repeatable using "push up" valves, it was decided that cell growth should be attempted directly on PDMS surfaces. It was also desirable to maintain use of the "push-up" valve geometries with the integrated device, since this was the same approach used for embryo culture with megavalves from Chapter Three.

As adherent cells are not capable of growing directly on PDMS, it is necessary to introduce an interstitial protein matrix, which can adhere to both the surface, and to cells[22]. The most popular adhesion layer is gelatin due to the simplicity of application[36], while more specialized matrices have been suggested specific to different cell lines. To assess suitability of various surface treatments, culture trials were performed with various culture dishes which were coated with a thin layer of 20:1 RTV PDMS. After complete curing and prior to surface treatments, all test plates were thoroughly rinsed with ethanol and dried at 90°C. In total, seven surface conditions were tested in replicate, using combinations of gelatin (GE), fibronectin (FI) or poly-L-lysine (PLL). Solutions of G, F and P were prepared in either DMEM media or PBS, and these solutions were spotted to the PDMS bottomed plates with a pipette. Gelatin was diluted to 2% by volume. Fibronectin and poly-L-lysine were both applied using concentrations of 20 μg / ml.

After a 12 h incubation period, the spot treatments were briefly rinsed with fresh media, and HeLa cells were then added in solution. The effectiveness of cell adherence in various regions of the culture plates was assessed several hours later, and the results are presented in Table 4.3. As a control, a PDMS coated device with no surface treatment was also tested, with no adhered cells observed.

PDMS treatment	Plate "pbs1"	Plate "pbs2"	morphology comments	Plate "media1"	Plate "media2"	morphology comments
GE	25%	30%	acceptable	0%	0%	n/a
PLL	15%	20%	marginal	5%	10%	poor
FI	75%	75%	very good	25%	20%	acceptable
GE + PLL	30%	40%	acceptable	0%	10%	poor
GE + FI	75%	75%	very good	10%	10%	acceptable
FI + PLL	30%	10%	poor	0%	20%	poor
GE + FI + PLL	35%	30%	poor	0%	0%	poor

Table 4.3: *Approximate percentages of cells adhered to PDMS after 2 h using various surfaces treatments. Two plates were tested for PBS based treatments, and two for media based. Each test spot was approximately 1 cm in diameter on a PDMS coated culture dish. Percentages were approximated by analyzing cell morphology in phase contrast images from each test spot.*

It is evident that media based treatments are not appropriate. Likely, the complex media mixtures contain many additional small molecules which preferentially adsorb to the PDMS, interfering with intended treatments. Either PBS based fibronectin, or fibronectin mixed with gelatin, both supported excellent cell growth directly on PDMS.

These treatments were then tested in situ, using spare detector devices. Ethanol cleaned devices were filled with mixtures of either gelatin, or gelatin mixed with fibronectin and incubated overnight. Devices were then rinsed with fresh media and allowed to equilibrate in the incubator for about 2 - 4 h prior to cell seeding. The contrast in cell proliferation when using two of these different treatments is presented in Figure 4.12.
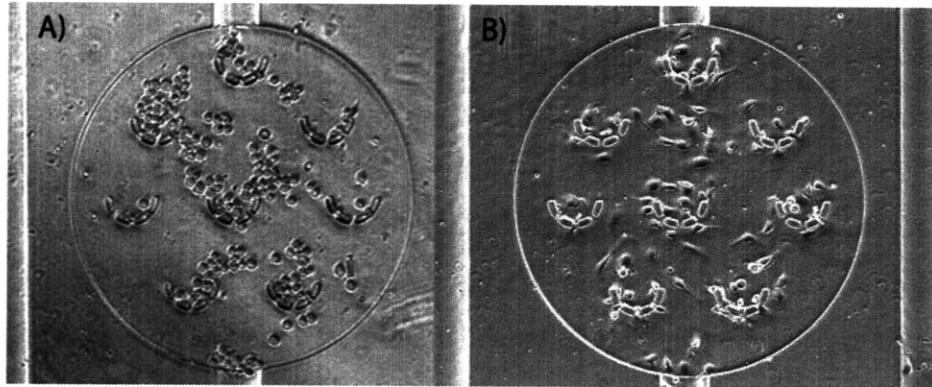
Figure 4.12: Cell culture on chip using two different surface treatments, approximately 2 h after seeding. The difference in morphology is apparent between A) non-adhered cells on gelatin vs. B) adhered cells on fibronectin treated PDMS. The diameter of the cell sieves is 800 μm.

With the protocols in place for establishing reliable cell culture in the devices, it would now be possible to combine detection and culture capabilities for metabolic profiling in a single device.

4.5 Cell Assays

Metabolic assays of HeLa cell lines were performed using the parallel device to assess accuracy and demonstrate utility of this platform. Control channels were all filled with sterile PBS to prevent osmolality shifts of media, and all devices were cleaned using an overnight soak with ethanol before use. Culture channels were treated with PBS based fibronectin for an additional night, followed by an equilibration period with fresh DMEM media for several hours before loading cells.

4.5.1. Cell transfer and device preparation

HeLa cells for assays were grown in 25 cm^2 culture flasks using filtered DMEM media supplemented with 10% FBS and 1% penicillin-streptomycin for several days in preparation for experiments. For harvesting, cells in the flask were first rinsed with warm PBS buffer to remove dead cells then incubated with 0.5 ml trypsin for at least five minutes. Although only two minutes of trypsin is usually required to passage the cells, a longer release treatment was helpful to prevent cell aggregation during loading without adverse affects on cell growth. Trypsin was neutralized and cells were resuspended by adding 2 ml pre-equilibrated DMEM media. To increase the density of cells for seeding, the cell suspension was transferred to Eppendorf tubes and centrifuged at 1000 g for 1 minute. The supernatant media was removed, and cells were

resuspended in approximately 250 μl media. Using sterilized Tygon tubing and stainless steel tubing, this suspension was transferred by a syringe and input to the microfluidic device for seeding. Control lines on the microfluidic device were actuated to select the desired input channel, and to isolate columns from one another (valve 13, Figure 4.2) during seeding. This ensures a direct flow of media containing cells from the input port, through all of the sieves, and then towards the waste port. Gentle pressure was manually applied on the syringe to ensure cell velocities did not exceed ~ 1 mm/s, and after about 3 minutes, most of the sieves in the culture chambers contained an adequate number of cells. Excess cells were removed with a rinse of clean media, and in some cases, a rinse with trypsin directed around the culture chambers. Care was taken to prevent the introduction of air bubbles into input wells on chip. After seeding, the entire device was placed back into an incubator to allow for the cells to adhere to the fibronectin treated PDMS and grow. Long gel loading pipette tips containing for media were placed at the input wells of the device to allow a slow gravity driven perfusion of media to feed the cells during culture in the incubator.

In some cases, profiling experiments were initiated several hours after seeding. In other trials, cells were cultured on the device for at least one or two days prior to experiments (it was established in culture trials that cell viability could be maintained for periods of more than a week on chip, providing media was refilled daily in the pipette tips). To perform experiments the device containing cells was transferred to a portable incubator on an inverted epifluorescent microscope (see Appendix D). Fluidic inputs for rinse buffers, enzyme cocktails, calibration standards as well as fresh pre-equilibrated media in Tygon tubing were connected to the device (following Chapter Two). All valve control lines were reconnected to external microsolenoids and the rotation correction for the motorized stage was established for automatic imaging.

The microscope incubator was used to maintain an environmental temperature of 37°C, and a sub chamber was placed directly over the device to provide premixed gas with 5% CO_2 and 21% O_2, ideally at 100% relative humidity. The microscope incubator and humidifier greatly improves the sustainability of cell culture on chip, but due to inherent system leaks and environmental fluctuations over the course of the experiment, the best culture was still achieved when devices are located in a real incubator. Nonetheless, the morphology of the on chip cells

was deemed suitable for proceeding with experiments using the current system. Cells were often mounted on the microscope for 12 h periods or longer during the course of assays routines. Along with the fluorometric imaging required for metabolic profiling, the cell sieves were periodically imaged to check the status of the cell samples.

4.5.2 Proof of principle glucose measurements

Using the integrated device, glucose measurements were performed on separate cultures of HeLa cells grown on chip. Cells were allowed to adhere on chip for at least six hours after seeding, then cultured in phenol red free media ("STD1", Table 4.1), which was loaded into both the sieve and bypass channels. Software routines were written to periodically recirculate media over the cells in the culture chamber, for 30 seconds every five minutes. This arbitrary recirculation was used to ensure a homogeneous concentration of metabolites throughout the chamber, although it may be necessary to revisit the effects of perfusion on metabolism in future studies. Four point glucose calibrations were performed using standards one through four, immediate prior to, and following, assays performed on cells. Typical results of glucose assays are presented in Figure 4.13.
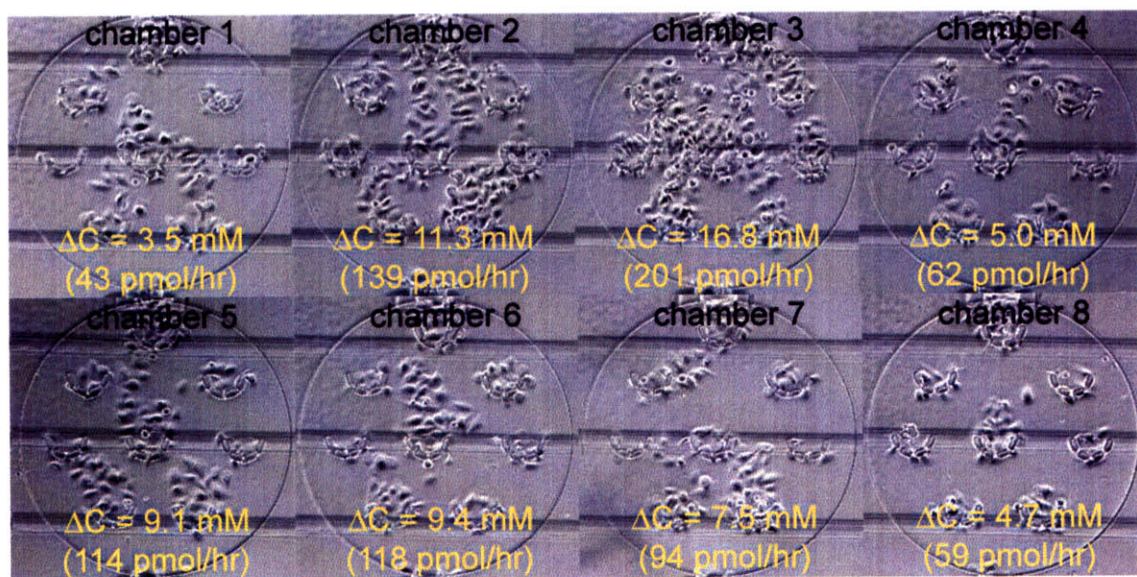
Figure 4.13: Glucose consumption of HeLa cells, reported as decrease in average glucose concentration in the chamber media, and the effective rate of substrate uptake. The quantitative results qualitatively agree with cell density. Measurements were performed in 90 minutes after replenishment with fresh DMEM media containing 25 mM glucose, 1.25 mM pyruvate and 0 mM lactate.

In this device there was some heterogeneity in cell density due to the seeding process, although this effect was useful for evaluation of results. The absolute values of glucose uptake alone were less meaningful than relative metabolism measured between chambers. As evident in Figure 4.13, the qualitative density of HeLa cells corresponds closely with the measured rate of glucose uptake. Each uptake measurement represents the average of two measurements taken after 90 minutes.

Degradation of enzyme generated fluorescence was observed over the course of routines, due to the warm incubator environment. This degradation was not a concern when using the standalone detector at ambient temperature, where it was possible to use the same cocktail overnight in long calibration experiments. As such, the normally refrigerated metabolite reagents were replaced in the Tygon tubing several times through the course of the long experiments. There exists a tradeoff between maintaining a warm device for cell culture, along with the use of temperature sensitive enzymes for assays. It was still possible to generate linear calibration curves even when the enzymes had been connected to the device for several hours, although the slope of calibration curves decreased continually, which introduces measurement uncertainty. This degradation reinforces the importance of frequent fluorometric calibration. Fortunately, calibration routines were fully automated in the software, and linearity could be verified regularly. In future work, it may be worth investigating approaches to either reduce the sensitivity of cocktails to temperature degradation, or in ways to keep reagents cool in tubing when attached to the incubating chip.

Some degradation in cell morphology was also observed over the course of extended experiments. Time lapse images from eight cell chambers over the course of a 22 h experiment are presented in Figure 4.14.
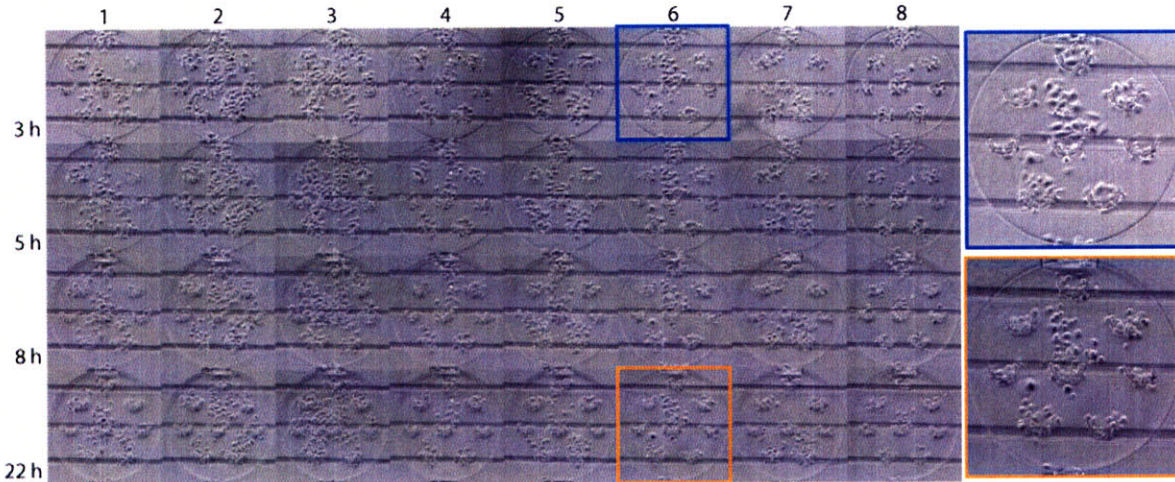
Figure 4.14: Cell culture in eight parallel sieves over the course of an extended metabolic assay. The labels on the left indicate the number of hours since cells were seeded onto the chip. Changes in cell morphology are illustrated in the insets. Diameter of individual cell sieves is 800 μm.

As observed in the images, changes in cell morphology occurred over the course of experiments. Degradation in cell culture conditions may be due to a combination reasons, including excessive driving pressure or fluid shear, and imperfect culture conditions on the microscope incubator. Every time that media was drawn from the chambers for assays, fresh media was provided to the chambers at a pressure of 3 - 4 psig, which may have stressed the adhered cells. During culture, and also prior to assays, media was regularly circulated through the culture sieve and bypass using the parallel peristaltic pumps, with fluid velocities in excess of 100 μm/s in the bypass channels. It is possible that the cells were adversely affected by frequent pressure fluctuations and it may be necessary to dampen the affects of mechanical agitation on biological samples by using either smaller valves, or longer bypass channels. Modification of device geometry may be useful to reduce necessary driving pressures for fluid transport. Alternatively, circulation and metering pumping protocols could be reexamined to reduce average fluid velocities over biological samples. Fortunately, the cell lines utilized in this research are robust and can withstand some adversity in culture conditions.

Further, the volumes sampled from the culture chambers were approximately 25% of the total available culture volume (~6 nl of a total ~25 nl in the culture loop). Thus it was necessary to perturb most of the fluid within the chamber for every sampling operation, and the discrete

- 113 -

actuations of peristaltic pumps displace a lot of fluid every cycle relative to this culture volume. If this integrated approach was adapted for embryo culture, the relative fraction of media sampled to total culture volume should be much lower. For example, if ~ 250 nl is used for embryo culture, it should still only be necessary to displace ~ 6 nl of media for measurement. It is believed that with adequate modifications of both culture channel geometry and protocols used for sampling, similar architectures can be deployed for integrated embryo assays, while also ensuring robust culture conditions.

Another approach which may be worth exploring is the addition of a sample staging area. In this approach, spent media could be transported to a downstream chamber all at once using gentle pressure as to not disturb the primary culture. Assays could be then performed in replicates using standard high-throughput protocols from this staging chamber, reducing the potential of disrupting cells or embryos with frequent microfluidic pumping. For future embryo culture, this may be the most desirable and least invasive approach.

4.5.3 Metabolic inhibition assays

Beyond simple consumption measurements, this architecture can also be utilized for studying the metabolism of different cell types or culture parameters in parallel. The multiplexor on the outlet of the device allows culture chambers to be addressed individually with custom media inputs. As a proof of this flexibility, metabolism of cancerous HeLa cells cultured on chip using standard media was contrasted to those cultured in media containing one of the most common glycolysis inhibitors, 2-deoxyglucose (or 2-DG)[35, 111, 112]. In these experiments the relative difference in glucose uptake and lactate output by use of inhibitor agents would be measured.

The conversion from glucose to pyruvate and ATP involves several intermediate steps. Consider the initial mechanisms of glycolysis in Figure 4.15, in the conversion of glucose to glucose-6-phosphate (G-6-P), followed by the conversion to fructose-6-phosphate.
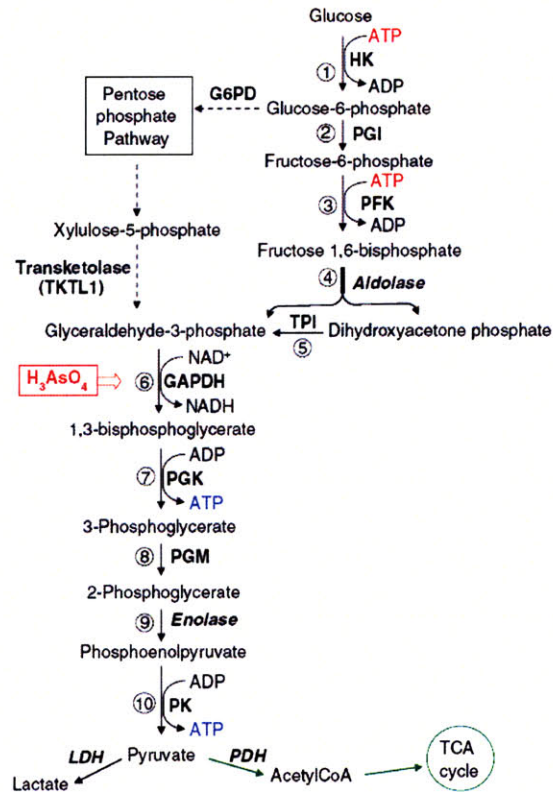
Figure 4.15: Glycolytic pathway (Adapted from Pelicano et al, 2006). Of specific relevance for the inhibition by 2-deoxyglucose are the phosphorylation of glucose to G-6-P by hexokinase (HK) and conversion of G-6-P to fructose-6-phosphate by phosphoglucose isomerase (PGI).

The ATP-dependent conversion of glucose to G-6-P is the rate limiting step in glycolysis, catalyzed by HK. In competition to glucose, when 2-DG is transported into a cell, it is phosphorylated by HK to 2-DG-P. However, unlike the phosphorylated version of glucose, G-6-P, 2-DG-P cannot be metabolized by PGI[35, 111]. 2-DG-P is accumulated in the cell and the result is a decrease in cellular ATP by this pathway. In inhibition experiments, since less HK is now available to convert standard glucose, it is expected that less lactate will be generated by the cells and this should be reflected in the microfluidic measurements.

The clinical effectiveness of this particular inhibitor is still under clinical investigation[35]. The effectiveness of 2-DG cannot completely offset the native physiological presence of glucose, and there are some side effects which need to be considered during high concentration inhibition treatments. Cancer cells are surprisingly robust, and cellular studies with 2-DG alone have not exhibited the full cytotoxic response *in vivo* as expected[112] suggesting that treatments using

multiple inhibitors to address multiple pathways simultaneously may be more effective. Conversely, it has been possible to detect changes in glycolytic activity from cell populations *in vitro* treated with such inhibitors, and most notably, a reduction in lactate output[113]. Thus, inhibition of glycolysis with treatments such as 2-deoxyglucose on cervical cancer HeLa cells should serve well as a proof-of-principle model for an integrated metabolomics tool.

In these experiments, cells were seeded on the device and grown overnight on chip in the standard incubator. The following day, the device was transferred to the microscope incubator for monitoring, and reservoirs were connected containing either standard DMEM media, or media supplemented with 5 mM 2-deoxyglucose (D6134-1G, Sigma Aldrich). Media was addressed individually to each culture chamber to initiate inhibition. To ensure cell viability and uniformity, four of the eight chambers on chip were treated with a live / dead cell stain (L-3224, Invitrogen) at the onset of the experiment, while four were reserved for post experiment counting. The cell densities on chip are presented in Figure 4.16.

chamber 5
DMEM

chamber 6
DMEM

chamber 7
2DG
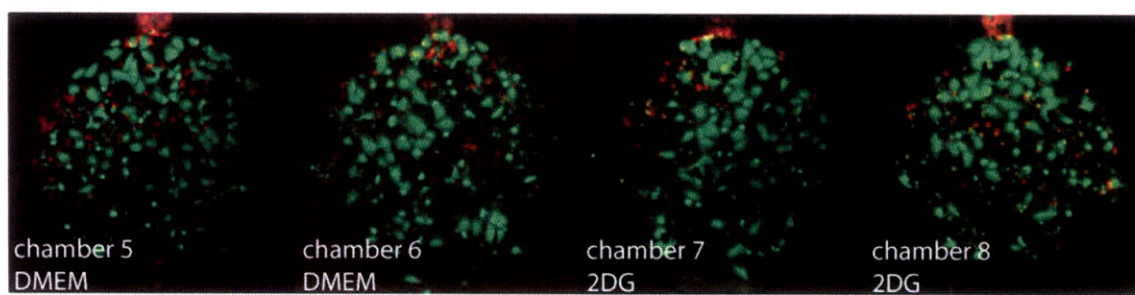
chamber 8
2DG

Figure 4.16: Live/dead stain was utilized at the initiation of the inhibition culture experiment to assess cell quality and density uniformity across chambers (live = green, dead = red). Only four of eight chambers were treated with stain before the experiment. In this experiment, alternating pairs of chambers were cultured using either regular DMEM media, or DMEM with 5 mM of 2-deoxyglucose.

Culture was performed for four hours on chip, with intermittent recirculation every several minutes (slow 250 ms duty cycle peristaltic pumping for 60 seconds, once every 10 minutes). Assays for glucose and lactate were performed by sampling media from the bypass and sieve channels, with four point calibration performed immediately before and after media assays. The results are summarized in Figure 4.17.
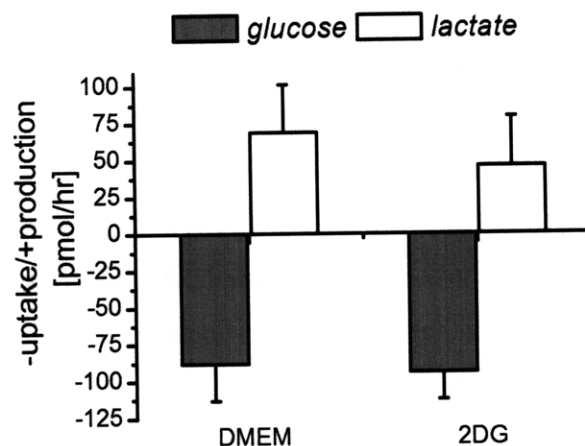
Figure 4.17: Results of glycolytic inhibition experiments. Glucose and lactate measurements were performed on four cultures which were cultured in DMEM media in contrast to two others cultured in media supplemented with 5 mM 2-deoxyglucose. Error bars represent one deviation on duplicate measurements for each chamber. After four hours, the average glucose uptake is approximately equal, but the production of lactate has been hindered. This indicates that glycolysis had been moderated by 2-DG.

These measurements of glycolytic inhibition of HeLa cell lines by 2-deoxyglucose are in general agreement with the reported observations of Barban and Schulze[111]. In their work, media containing equal concentrations of glucose and 2-deoxyglucose (both at 5 mM) was found to hinder lactate production almost immediately, while glucose uptake did not lag in 2-DG media until approximately 12 hours of exposure. Had measurements been performed several days after culture, significant decreases in both glucose uptake and lactate production would be expected. These results also verify the specificity of metabolite measurements using the integrated platform. Roughly speaking, it was also noted that the overall glucose uptake was slightly lower than in the previous studies on a per cell basis. The average glucose uptake may have been reduced by including some measurements from cells treated with live/dead stain prior to the experiment. Further, the one entire day of culture on chip to settle cells before starting inhibition experiments may have resulted in culture with slightly lower metabolic requirements. This alludes again to the importance of being able to run many cultures in parallel on a single platform, such that relative differences can be characterized carefully, even when absolute uptake values may vary between cell populations. The ability to seed approximately equal cell numbers on chip for integrated assays by the use of sieves is also critical[108], and in future experiments, it may be necessary to refine loading protocols further to yield similar populations for every experiment, avoiding the necessity of counting cells every run to normalize results.

There are a wide variety of alternative agents suitable for use in future inhibition studies, which would also serve as interesting test cases for the integrated metabolomics device. Potential inhibitors include phloridzin to regulate glucose uptake, alpha-chlorohydrin to modify glycolysis, or pentachlorophenol to stunt oxidative phosphorylation. As the fluorometric reaction of glucose in this research is converted using hexokinase (Appendix A), however, it may be necessary to perform additional trials to confirm the linearity of calibration, since hexokinase may inadvertently be depleted by converting inhibitors as well (i.e. 2-DG to 2-DG-P).

4.6 Conclusions and Contributions

In this chapter, the essential functionalities for culture and detection required for a microfluidic metabolomics tool were combined to a single platform. The architecture developed was scalable, and allowed several cell cultures to be assayed in parallel using a variety of media inputs and metabolite reagents. The advantages of automatic fluorometric calibration and sensitivity were adapted directly from the standalone microfluidic detector of Chapter Two. The lessons learned from embryo culture in Chapter Three provided a systematic basis debug culture issues early and provide support of standard mammalian cells.

While several approaches for monitoring changes of glucose and lactate have been demonstrated by a number of research groups in the past, none have offered the flexibility of this integrated device. Previous microfabricated approaches often used metabolite specific electrodes for detection either dipped directly into culture media containing samples, or near an outlet port of the culture which necessitates constant bleeding of media for detection. Technically these systems do provide dynamic measurement of growth conditions, but none offer the flexibility of studying multiple metabolites in parallel, or demonstrated the capability to modify culture conditions upstream based on current metabolic conditions. The non-invasive approach demonstrated in this chapter open avenues to implement feedback driven culture, and can support many different cell lines on a single chip.

All of the infrastructure, including software and imaging routines, were developed to ensure this platform is tractable to use in standard cell research. Arguments were provided to ensure that detection limits and sensitivity covered the physiological range of interest for the cell populations that would be contained on chip. Scaling up this integrated device in the future, to accommodate larger culture volumes or many more culture chambers, is simple based on the architecture proposed in this work.

Using the integrated device, glucose profiles were first captured from parallel cultures of HeLa cervical cancer cell line, with qualitative cell densities correlating closely with reported nutrient uptake values. As a further proof of applicability for this device in the fields of cancer research, metabolic inhibitors were utilized to modify the nutrient utilization of these cancer cell lines. It was possible to detect reductions in lactate generation when glycolytic pathways were regulated using low concentrations of 2-DG. As many replicate experiments would be required to determine the effects of different inhibitor concentration and application strategies, the economies of scale through parallel processing with the proposed architecture is evident. There are many avenues for research with an integrated microfluidic tool, and the goal of transitioning to hands off embryo metabolomics in the future should be possible with this unprecedented approach.

(This page intentionally left blank)

Chapter Five - Vertically Integrated Microfluidic Architectures

5.1 Introduction

Although state-of-the-art microfluidic devices contain complex channel networks with hundreds or thousands of channels, designs are inherently planar due in part to the fabrication process of soft-lithography. In this chapter, a new design paradigm is described which will allow for unprecedented assay densities in microfluidic constructs. The concept is based on enabling numerous individual planar microfluidic networks to be operated in parallel within integrated vertical stacks.

5.1.1 Limits of Existing Architectures

To accommodate more features in a microfluidic construct, a designer must either increase the footprint of the device, or decrease the size of individual features. Unfortunately, there are fundamental limits to both of these routes. As the spatial area of devices increase, it becomes difficult to monitor multiple channels or samples in parallel. Motorized stages on microscopes have alleviated this limitation for the most part in the microfluidics community, so allow simultaneous monitoring of multiple regions beyond a fixed field of view. Chips with footprints greater than several inches in length, however, necessitate specialized optical readers, such as those used for fluorescent analysis of high density 384 or 1532 well plates. Device footprints are also limited by the means of fabrication. Microfluidic molds used for soft-lithography replica casting are most commonly prepared using photoresist patterned on 3" or 4" diameter wafers. It is certainly possible to cast larger devices, although manual manipulation of larger chips increases potential for defects or debris during assembly, compromising performance.

There are also limits to the miniaturization of microfluidic features. In the semiconductor industry, photolithography resolution governs the smallest features (such as transistors gate widths on a processor) which can be reliably fabricated. The ability to form small features in the microfluidics field is not the limiting factor; PDMS replica casting is capable of reproducing features accurately to the molecular level. For example, Hua et al have demonstrated PDMS casting fidelity off individual carbon nanotubes with diameters of 4 nm for nano imprint lithography[114]. However, there are three important reasons which limit extreme miniaturization of channels for higher density assays.

First, hydraulic resistance increases dramatically as channel dimensions decrease, and the necessary driving pressures for obtaining desired flowrates becomes prohibitive. Analogous to Ohm's law, an expression for pressure driven flowrates can be expressed as $\Delta P = QR$, where ΔP is the driving pressure differential through a length of channel, Q is the fluid flowrate and R is the hydraulic resistance. For a simple case of a square channel (width = height = L), the resistance term increases with L^{-4}. Halving the dimensions of a square channel decreases the flowrate by a factor of 16 for a given input pressure. This is a well known tradeoff in microfluidic systems. Fortunately, fluids driven by electro-osmosis (EO) do not suffer this setback, and the use of electric fields to transport fluid increases in efficiency with miniaturization[115-119]. At the same time, not all samples can be transported using EO or alternating current electro-osmosis (ACEO)[115, 117, 120]. EO requires high voltages, on the order of ~kV per centimeter of channel length, which can result in adverse hydrolysis or Faradiac reactions in solutions of high electrolyte strength. Thus EO is not suitable for routine analysis of many biological fluids (inherently strong electrolytes) and this remains a reoccurring technical barrier with these fluid transport options.

The second limiting factor involves the integration of sensors or actuators in microfluidic channels. Many valve strategies (Section 3.5.1), and in particular those fabricated using multilayer soft lithography, do not scale well with miniaturization due to high actuation pressures[60, 121]. The PDMS membrane between the flow and control channels may be considered as a dually supported beam undergoing deflection due to application of a uniform pressure[121]. Based on a deflection model developed by Kartelov, necessary sealing pressures for a valve

increases quickly with smaller channel widths, as presented in Figure 5.2. For reference, common valve widths in many microfluidic devices are ~100 μm, used for sealing a ~100 μm wide channel.
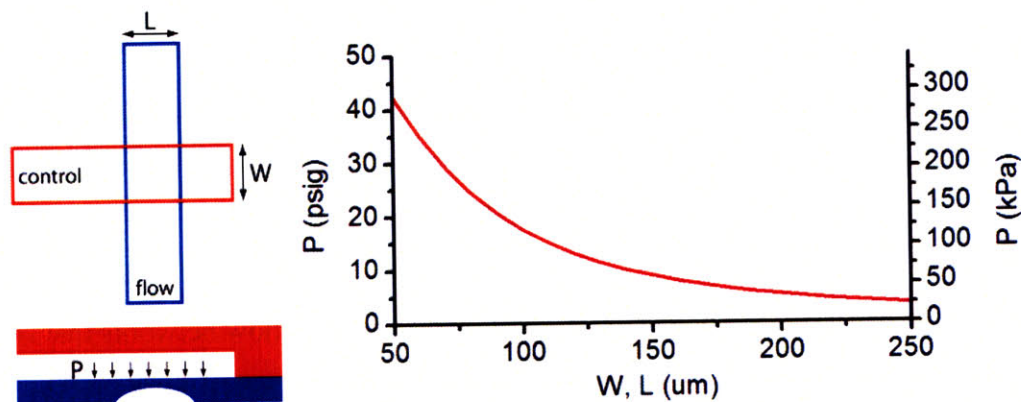
Figure 5.2: Approximate actuation pressure scaling as a function of valve geometry. For a valve with equal lengths and width used to seal a flow channel, the required control pressure increases dramatically with miniaturization. This valve scaling model was developed by Kartelov et al (2007). In this calculation, dimensions of the flow channel height and interlayer PDMS membrane are each 20 μm.

While valves have been fabricated with dimensions less than 10 μm wide, the actuation pressures required become very high and increase the potential for device rupture. In addition, standard microsolenoids used to control microfluidic devices are often rated to ~20 - 25 psig.

With sufficient pressures for valves, and ability to transport fluid in nanometer scale channels, there are no limits to microfluidic miniaturization. However, the third limiting factor to channel scaling involves physical dimensions of the samples of interest. It is certainly possible to produce submicron scale channels with existing technology, but these will not be suitable for accommodation all biological samples of interest. Selected examples include bacteria (~1 μm), yeast (~3-5 μm), mammalian cells (~10 μm), or even embryos (~100 μm). In certain devices, such as those used for the separation of DNA and protein solutions, miniaturization of channels is necessary and increases efficiency of these systems[122, 123]. For the remaining microfluidic networks used for studying cellular biological systems (particularly in this thesis) channels must remain on the scale of the samples.

5.1.2 The Concept

Vertically integrated devices increase density of microfluidic assays while avoiding the aforementioned limits to miniaturization. These architectures can conserve use of "large" channels as well as limit the necessary footprint of devices. To achieve increases in device complexity, individual planar networks of channels are assembled above one another within the volume of a microfluidic chip. New approaches to addressability and optical readout enable the planes of a stacked microfluidic system to be addressed individually. In colloquial terms, the transition would to the new design technique be analogous to performing experiments in apartment buildings as opposed to standard bungalow chips.

It is possible to layout microfluidic devices comprised of multiple flow networks that share common flow and control inputs to significantly scale up channel capacity without requiring a larger device footprint or excessive devices connections. Interconnects to actuate control lines are common through all layers, such that only one port must be punched when assembling PDMS chips, and only one control line must be connected to pressurize all valves arranged above one another. Vertical multiplexors can be arranged to enable layer by layer addressability, similar to the way that planar control multiplexors allowed an exponentially large number of control lines to be controlled with a minimum of control valves. While control valves for planar multiplexors are identical throughout the stack, vertical multiplexors are unique on every layer to provide addressability. This concept is illustrated in Figure 5.2.
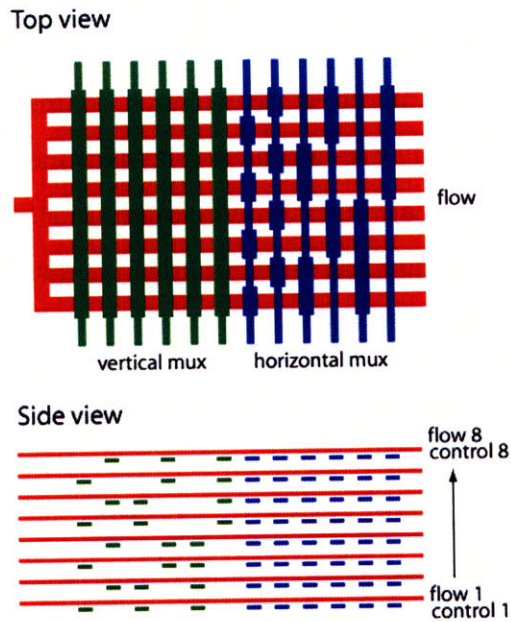
Figure 5.2: Schematic of an eight layer vertical multiplexer, each with a corresponding set of control lines. Control of N channels requires $2\log_2 N$ control lines as with standard multiplexers, but networks may be designed in more compact devices. The above configuration, for example, allows 64 channels to be controlled in a footprint of only 8 channels. Only one interconnect from the left is required to the chip to access all 64 lines.

There are several advantages in increasing the channel density of devices by using vertical integration. First, the manufacturing process is more robust against fabrication errors. On a device consisting of several cm^2, the possibility of experiencing a point defect on a photoresist mold increases. If there are several thousand channels on a single layer, one or two defects on a layer may render a device unusable. Using a stack of several slightly less complex devices, clean castings are easier to select or reject from subsets of larger molds when building up vertical structures. The tradeoff is that precautions are necessary to avoid introducing debris between layers of the chip during assembly.

In long term cell and bacteria culture experiments, more samples can be contained in a single device. For example, an eight layer device can contain the samples previously studied using eight separate chips. Containing more samples on multiple layers of a device can potentially alleviate concerns whether all samples were cultured under identical conditions, and improve consistency in comparing experiments. It would, however, still be worthwhile to quantify spatial environmental variations that could adversely affect culture through the depth of the PDMS, by

the use of heat and gas transfer models. Further, if many different chips are cultured concurrently, control lines would have to be reconnected from device to device to run experiments, while with vertically integrated architectures, control lines remain connected to the same substrate at all times. The only tradeoff in complexity is the additional control valves used to address fluid samples to appropriate layers, while designs of all flow layers is unchanged. Additional functionality could be introduced with internal interconnects to transfer or merge fluid between adjacent layers in arbitrary locations throughout the assembly[124]. It would also be possible to increase the throughput of multilayer soft-lithography peristaltic pumping, by merging several parallel streams towards a single channel or connection port.

5.1.3 Optical Considerations for Vertical Microfluidics

As numerous networks are stacked above one another within transparent PDMS substrates, it may become more challenging to resolve and monitor individual samples within a stack. With the use of appropriate device design and optical instruments, it should be possible to alleviate these difficulties and monitor samples independently from one device layer to the next.

Confocal microscopes are specifically designed for performing three dimensional optical scans through thick samples, and to resolve features independently at different focal depths. This would be a particularly valuable tool for observing experiments simultaneously through the depth of a device with N device layers, each separated by a distance dz. However, even a standard microscope used in most research labs with a decent selection of objectives should be capable to resolve features independently on different layers. An ideal microscope objective would have long working distance (LWD) and a high numerical aperture (NA). The working distance allows observations to be made several millimeters deep into a transparent (presumably PDMS device), and the depth of focus (DOF) is inversely related to high NA values[125]. A shallow DOF ensures only those features of interest are in resolved in the field of view. For example, a high quality 20x objective (Olympus) with ~7.6 mm LWD and 0.45 NA has a nominal DOF of ~ 3-6 μm for collecting fluorescence in the range of ~550 nm. If the layers are separated by several hundreds of microns, vertically integrated microfluidics should be ideal for independent fluorometric assays even for lower values of dz. There are additional optical

analysis tools, such as confocal reconstruction and simple background subtraction, which can be used to improve fluorometric assays in a three dimensional space.

Another option to further improve observation between individual chambers is to purposely offset successive layers during assembly. In this manner, samples contained in chambers on a lower layer will not interfere with observation through to channel above, either using fluorescent or brightfield observations. The principle of offset alignment is presented in Figure 5.3, where, for example, four sample types are loaded into four chambers on unique device planes.

load chambers   overlapping alignment   offset alignment
                 (4 samples, 4 layers)
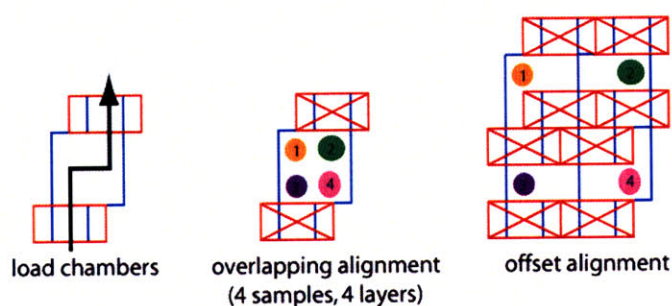
Figure 5.3: Offset alignment may be used to simplify the observation of samples in stacked storage chambers. Here, blue outlines represent a flow channel, and red outlines represent control valves used to isolate samples within the chambers. Since PDMS is transparent, chambers containing four different cell types may appear to occupy the same section of channel when observing with a deep depth of focus. This ambiguity is resolved to an extent by offsetting pairs of flow and control lines during assembly of successive layers.

With high NA objectives, it would be possible to resolve which sample is stored on individual planes, but the offset technique may be useful for further reducing background (such as fluorescence emitted) from samples in adjacent layers. Since the offset required (~ 100 µm), is small relative to the typical punch diameters used to create interconnect ports for fluids to the chip (~ 500 µm), there is some tolerance in alignment of adjacent flow layers which maintaining connectivity to all layers.

5.2 Applications of Vertical Architectures

There are fields of microfluidic research which increase in utility with the ability to manage more samples in parallel. Application such as protein crystallization, emulsion based

microfluidics and high-throughput screening are examples which often necessitate complex device networks, and may benefit in scalability from vertically integrated architectures.

5.2.1 Protein Crystallization

One of the most difficult and perennial problems in structural biology is to identify the structure of proteins. Significant computation progress has been made to predict the most likely configurations which proteins are folded. Most of the work to identify or verify the true structure (and thus protein function) is still performed experimentally. One of the most popular approaches is X-Ray diffraction, which may be used to examine the protein structure of pure protein crystals. However, discovering the necessary conditions to nucleate and grow crystals from microliter volumes of highly purified protein solutions for diffraction studies is far from trivial. Little information is usually known in advance of the appropriate buffers and complementary salts required to be mixed with a protein to yield a crystal, which is why high-throughput trial and error experimentation is commonplace.

Microfluidics has made fundamental contributions to structural biology in this regard, and is arguably one of the most prolific success stories of implementing microchips in pharmaceutical settings[126, 127]. Devices have been demonstrated which perform multiplexed reactions of different buffers with purified protein. Hundreds and thousands of conditions may be tested without user intervention, either serially or in parallel, to identify likely conditions to nucleate protein crystals. The growth of proteins also favors chambers of small length scales, where delicate sample are protected from the outside laboratory environment and in particular, fluid turbulence[128, 129]. Diffusion limited mixing allows proteins to grow, either during incubation on chips or in external capillaries, for days or even weeks[128, 130]. To accommodate additional parallel reactions and enable a wider array of screening conditions, the current generation of devices is limited only by available storage cells[128, 131]. VLSI may be aptly suited for these high-throughput screening applications. In addition to simply screening for protein crystallization conditions, there are opportunities for kinetic optimization of growth rates by controlling osmotic shifts through the numerous interlayer PDMS membranes during incubation[127, 129]. Conversely, if there are concerns about water or solvent diffusion between samples located on separate planes, it is possible to increase the interlayer thickness, or coat the PDMS surfaces with impermeable barriers such as Parylene.

5.2.2 Droplet based microfluidics

Miniaturization of chemical reactions and biological assays into emulsion formats has been a rapidly developing area of interest in recent years[22, 83, 132, 133]. Aqueous reagents may be dispensed into an immiscible oil phase as droplets to separate reactions in many containers. This avoids cross contamination of reaction products, and may allow rare samples of interest to be amplified and sorted from bulk library solutions. In addition, microfluidic emulsion technology has been realized as a valuable route for particle and microgel synthesis where monodispersity and dimensional control is of primary importance[134, 135]. A key limitation of these microfluidic processes is the production rate of emulsions depending on fluid properties of both fluid phases, operating conditions and device geometry. For a given set of conditions, there is a limit on microfluidic water-in-oil droplet production (typically ~ 100 - 1000 Hz) before the onset of instabilities leading to polydispersity or droplet coalescence. It has been suggested that bottlenecks can be overcome by operating several separate devices in parallel, although this requires user multitasking to set up more chips, and additional hardware such as syringe pumps to pump fluid for each device[136].

Several options have been developed to circumvent limitations in production rate. By using a microfabricated manifolds bonded on top of a microfluidic device, parallel droplet production was demonstrated from four inline droplet nozzles with good monodispersity[137]. This allows essentially four microfluidic droplet devices to be driven at one using single input for aqueous and oil phases. Pseudo three dimensional methods have been proposed for microfluidic emulsification by sandwiching two patterned slabs of PDMS together in order to flow focus an aqueous stream into a surrounding oil phase which effectively lowered overall fluidic resistance while still enabling small emulsions to be produced[138]. A circular three dimensional droplet nozzle has also been fabricated using etched silicon which was found to enable higher droplet rates by more than an order of magnitude[88]. Impingement devices with droplet nozzles arranged in symmetric bicycle spoke patterns have also been used to produce many droplets in parallel[139].

Vertically integrated architectures may also be useful for increasing droplet production rates. Rather than producing emulsions with one planar set of channels, it may be possible to prepare stacks of nozzles within a microfluidic device. Common ports for inputs and droplet collection

reduced the number of external connections required. It remains to be seen whether monodispersity can be ensured from one layer to the next due to subtle differences in hydraulic resistance, although design of larger connection wells relative to channel dimensions can reduce this issue.

5.2.3 Microfluidic LSI

One of the fundamental advantages of vertically addressable architectures is the capacity to increase feature density on chip without requiring a prohibitively large device footprint. General resources to store and retrieve multiple fluid samples on chip is useful for screening applications, and allows more experiments to be prepared on a single chip while reducing the time spent in configuring multiple smaller chips in parallel.

Consider the pioneering device which was used to demonstrate microfluidic large scale integration (LSI), where 1000 fluidic storage chambers were located in an area of ~20 mm x 20 mm, while the total device footprint was about ~25 mm x 25 mm. As a rough approximation, to increase this feature number by eight fold conserving a similar architecture would require a footprint of ~3425 mm^2, or edge lengths of ~59 mm (approximately the largest device which could be cast using a 3" wafer, a typical mold substrate for casting devices). With a 16 fold increase in the number of features, the edge lengths approach ~81 mm. Over such large areas, the possibility increases of introducing a point defect in either the mold, or in the device. Further, many instruments such as microscope stages, cannot accommodate samples with edge lengths exceeding two or three inches. The use of vertical multiplexers could be used to obtain ten-fold or more increases in the numbers feature, while maintaining conventional postage stamp sized footprints if desired. For reference, the original microfluidic LSI is reproduced in Figure 5.4, as well as some simplifications to the geometry used in the present research.
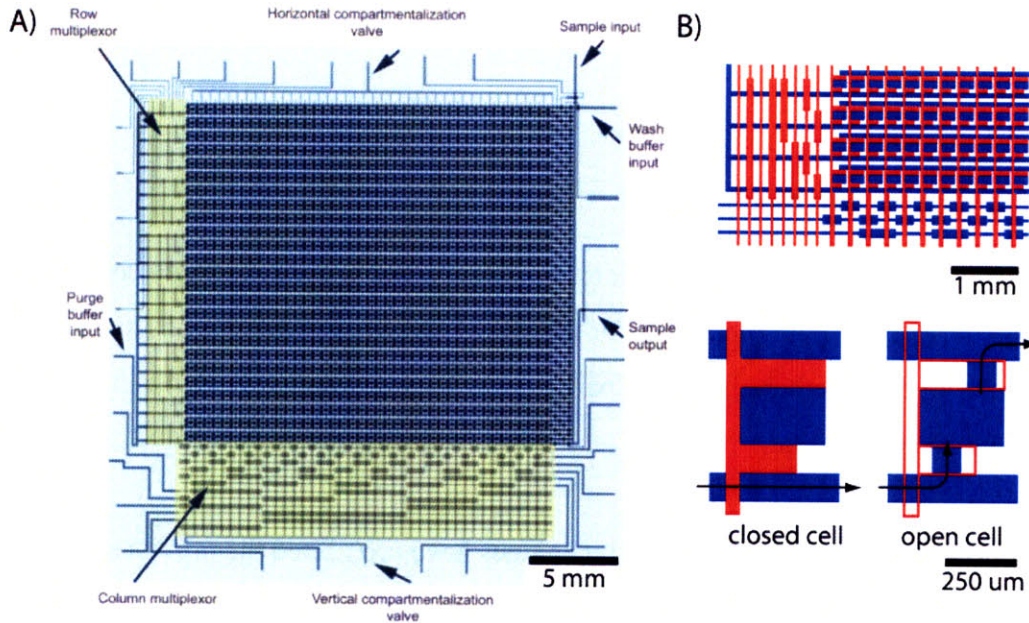
Figure 5.4: A) Example of a complex microfluidic storage architecture utilizing planar multiplexors (Adapted from "Microfluidic Large Scale Integration", Thorsen et al, 2002). The device contains 1000 storage chambers in an area of approximately 25 mm by 25 mm. B) Modified geometry based on LSI suitable for integration with vertical multiplexing. Serial architectures allow samples to pass through storage bins when column valves are open. Chamber dimensions are 200 μm x 300 μm.

Again, consider the eight layer device, which may have necessitated a total footprint of ~3425 mm^2 (59 mm x 59 mm). By implementing vertical multiplexing, this complexity could also be achieved while conserving the original (25 x 25) mm^2 total device footprint and the same feature sizes.

Another interesting application is the use of VLSI to create high resolution microfluidic displays. If pixels are offsets from one layer to the next (similar to Figure 5.3), there will be no apparent empty space between storage cells, and the total display will appear to be continuous is colored dyes are used in every cell. Rather than monitoring an apparent 16 x 32 storage array through 4 levels, for example, offset alignment allows all 16 x 32 x 4 (2048) "pixels" to be observed at once in a 32 x 64 grid. Further, with vertically overlapping pixels, there is the option to mix complex combinations of colors. A chamber filled with yellow, backed by a chamber filled with blue, may appear green when backlit. This is not intended to suggest microfluidic devices would

ever replace LCD displays, but only illustrate the interesting side effects when working with complex transparent devices.

5.3. Manufacturing Process

To realize vertically integrated microfluidics, it is necessary to create a single composite device from many individually patterned layers of PDMS. There are several options available to bonding these layers together, each with particular advantages and drawbacks in terms of robustness and required time.

Limitations of existing PDMS assembly techniques have prohibited the previous development of such systems. If standard techniques had to be used, the assembly time scales linearly with the number of layers, and as such, a ten layer device would take at least ten times as long to manufacture. The last thing microfluidic researchers desire is more time spent fabricating devices. In this section, a unique thermal-plasma approach is devised, where the forgiving nature of thermal bonding is combined with the parallel processing nature of plasma bonding, to allow the fabrication of vertically integrated microfluidic systems with PDMS.

5.3.1 Thermal Bonding for Assembly

Thermal bonding is the most common approach of bonding separate flow and control layers to one another in MSL microfluidics[25]. Thermal bonding has the advantages of forgiving processing for high accuracy alignment, but is slow for creating devices consisting of multiple layers. In standard thermal bonding, complementary layers, one containing an excess of PDMS curing agent, and the other a deficit, are partially cured on separate molds (typically for ~15 minutes at ~80°C). After this initial cure, the thick layer containing the top channel network can be removed from the first mold, and aligned to the second layer of PDMS. To promote bonding, the two layers are then baked for several hours to create a single device containing two channel networks. The thick layer is normally cast two ~ 5 mm thick to simplify handing and to allow sufficient engagement for tubing to be plugged into the chip. Alignment error of alignment between flow and control layers is generally < 25 μm, and often < 10 μm for researchers experienced with PDMS assembly. Since bonding is not initiated until two separate layers have been baked together, this process is forgiving if adjustments between layers must be made during

the alignment process. However, there is dependence on total PDMS curing time which complicates assembly for vertically integrated devices.

With careful control of process parameters, it is possible to repeat this step to bonds with a third layer, and so on. In this technique, the first two layers are subsequently baked for a short period (~ 15 minutes at 80° C) while a third layer of PDMS is also cured on a separate mold. Alignment is performed again, before a subsequent bake. This thermal technique requires a unique mold for every layer, and the assembly time linearly increases with the number of device layers. With a minimum of 20 minutes required per layer pair (baking + alignment time), it would be intractable to use this technique for a very complex VLSI device.

5.3.2 Plasma Bonding for Assembly

Plasma bonding is also an attractive method for multilayer bonding[9, 36]. Traditionally, plasma bonding is reserved for the final assembly process to seal a PDMS device to a glass slide, since this process yields a covalent bond between mating surfaces, and is irreversible. In this process, a sample is placed inside of a vacuum chamber and exposed to a reactive radio frequency (RF) air or oxygen plasma. The cleaned sample surfaces are rendered hydrophilic and can be readily bonding to treated glass[9]. Plasma can also be used to bond together separate layers of PDMS, but is simply unforgiving for novice microfluidic practitioners, since the alignment between critical features must be perfect on the first try.

Plasma bonding is a serial process, although large plasma chambers are capable of accommodating multiple samples at once. Treating and bonding of already cured PDMS surfaces to one another requires only several minutes (~ 1 min to pump down the vacuum the plasma chamber + 30 sec plasma treatment + ~ 1 min for alignment). Unlike the thermal bonding approach for vertically integrated architectures, a unique mold would not be required for every microfluidic layer. The multiple device patterns could be arranged on a single mold with several plasma steps used to combine the separate levels together.

With plasma bonding, wafers for flow and control features were coated with PDMS and fully baked in the oven overnight. For device assembly, a blank piece of PDMS was used as a master, and successively bonded to features on the flow and control wafers to build up the device height.

With additional layers, alignment was increasingly difficult and it became challenging to visualize complementary features through the master.

There are several concerns when using a plasma treatment to assemble all layers of a vertically integrated device. Every time that a sample must be transported into a vacuum chamber, treated and aligned, the potential for introducing debris to the devices increases. Since the plasma bond is permanent, care must be taken to work in a clean environment and remove any potential debris (with a nitrogen flux, or similar) immediately prior to bonding. The strength of the plasma bond can also introduce difficulties. To create MSL valves, the interstitial layer of PDMS between flow and control layers is typically ~15 - 20 μm to facilitate valve deflection at low actuation pressures. In plasma bonding, if is possible to inadvertently collapse this membrane to the adjacent PDMS layer, sealing the channel and rendering the valve and device unusable. It may be necessary to increase the thickness of valve membranes at the expense of low valve operation pressures if plasma bonding is used to assemble an entire device.

5.3.3 Hybrid Thermal-Plasma Assembly

Using either the thermal or plasma assembly approaches, it was possible to assemble prototype vertically integrated devices. Unfortunately, it was difficult to find a balance among all the parameters which govern device performance. The thermal bonding approach accurate, but extremely slow, and the resulting bonding between uppermost layers was not robust. The plasma bonding approach was rapid, but it was difficult to ensure correct feature alignment, and to prevent collapse of valves and channels it was necessary to increase PDMS thickness to the point that some valves could not close.

A preferred protocol was developed to significantly improve the assembly process, combining benefits of both thermal and plasma bonding. Thermal bonding would be used as the first step to ensure accurate and forgiving alignment between complimentary flow and control layers. As an example, consider a device featuring four flow layers, and four control layers. The control mold used for such a four layer device with a vertical multiplexor is pictured in Figure 5.5.
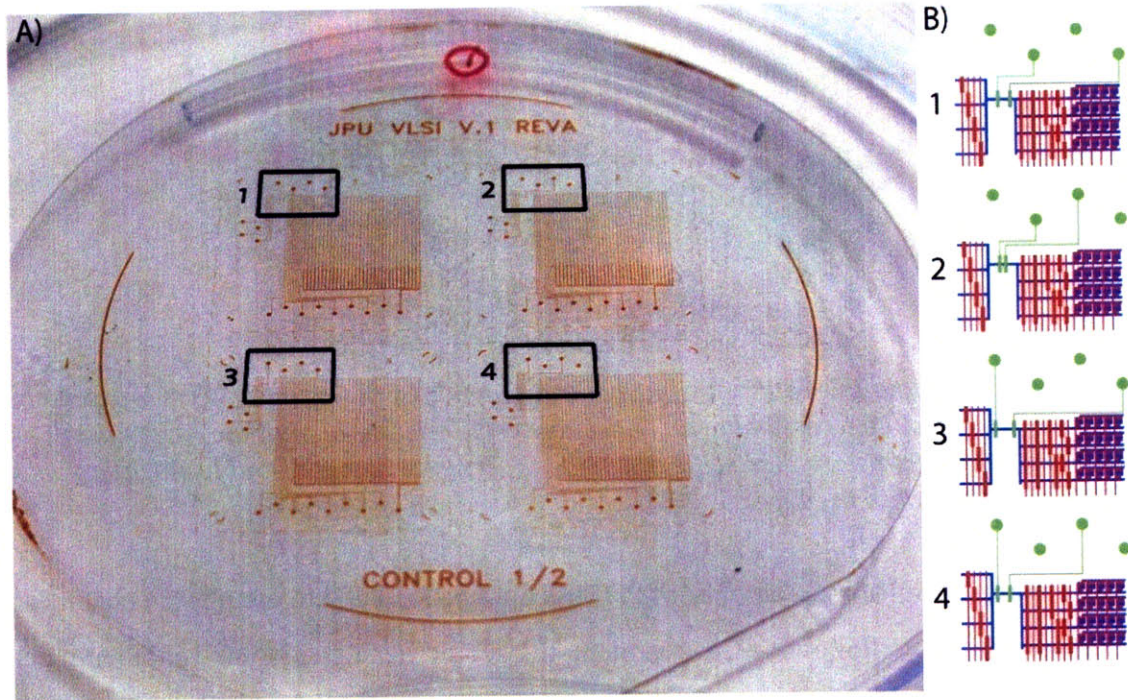
Figure 5.5: Control mold layout for a single VLSI device patterned on a 4" quartz wafer. A) The patterns for all four layers are identical with exception to the annotated regions. B) VMUX valves (in green) are selectively connected to enable individual layer addressability using common ports in the final assembly.

With bottom actuated valves, a set of flow layers would be spun coat to ~ 500 μm thick (~130 rpm for 60 seconds, 5:1 PDMS), partially cured, and bonded to a control wafer containing the valve features (20:1 PDMS). Layers which are several hundreds of microns thick are delicate, but can still be picked up and aligned by hand to the second wafer. After all four films have been aligned to their respective features on the second mold the control wafer is baked for least several hours at 90°C to complete bonding of the flow and control layers. This process creates essentially four sub-assemblies of a complete vertically integrated device, which can be removed from the mold individually. Next, a plasma treatment would be used to bond these four sub assemblies together. A simple rack for the plasma vacuum chamber was prepared which would allow both sides of a sub-assembly to be treated by plasma at the same time, pictured in Figure 5.6.
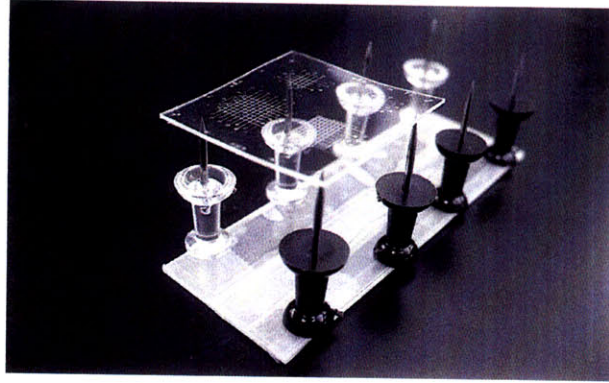
Figure 5.6: A "bed of nails" holder for plasma treating both sides of a PDMS sub-assembly. In this manner, it is possible to assemble an entire device consisting of multiple layers using only one rate limiting plasma step. For scale, the slide is 25 mm x 75 mm. Double sided tape is suitable for holding tacks in place.

Using this approach, all sub-assemblies of PDMS could be loaded into the plasma chamber and treated simultaneously. Following the treatment, they could be aligned to one another under a microscope. The alignment tolerance of this secondary step is more forgiving, since all critical alignment has been completed in the thermal stage. It is only necessary to align the sub-assemblies within ~ 100 μm on one another, such that a common interconnect punch (~500 μm diameter) would make contact through all the layers. The assembly process is presented in Figure 5.7.
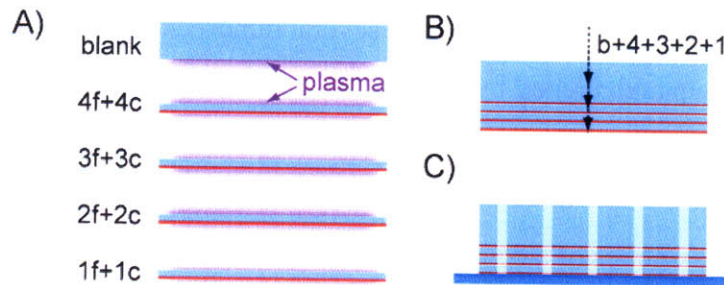
Figure 5.7: Assembly schematic for a vertically integrated device. A) Sub-assemblies consisting of complementary flow and control layers (shown in blue and red, respectively), as well as a blank layer of PDMS are all exposed to plasma (The base assembly "1f+1c" is placed on a glass slide in this step ensuring only the top surface is treated, while the remaining assemblies are placed on the bed of nails from Figure 5.6). B) The sub-assemblies are sequentially aligned to one another under a microscope, resulting in permanent bonds C) Interconnects are punched in one step, and the device is bonded to a clean glass slide with a final plasma treatment.

An eight layer device would require eight flow and eight control designs. The design modifications necessitated on every control layer are minor, but bookkeeping is required during mask layout and chip fabrication. This complexity issue is inherent in the addressability approach, but the additional work to fabricate one or two extra molds is not significant.

Also, there are some limitations to manual assembly; most notably that alignment becomes progressively more difficult as the number of layers is increased. Alignment problems could also be compounded by previous errors on lower planes. It may be necessary to reduce the density of features and increase the spacing between adjacent features to ensure consistent assembly for every layer.

The hybrid thermal-plasma process was found to be the most direct way to assemble vertically integrated devices using standard equipment available in most microfluidic laboratories. At the same time, it may be possible to further improve and automate this process to reduce the potential for defects or valve failure. Alternative bonding approaches using corona RF systems have recently been investigated to take advantage of the strength of reactive plasma treatments with the forgiving nature of thermal bonding[140], and these may find application with vertical assembly. To improve alignment, semi-automatic PDMS bonding systems integrating optical feedback have also been demonstrated, which could be used for both thermal and plasma processes[36, 141]. These examples illustrate the range of approaches available to create complex stacked devices, and may help simplify high-throughput assembly of vertically integrated chips devices in the future.

5.4 VLSI - Vertical Large Scale Integration

To demonstrate the ability of vertical architectures to enable unprecedented sample addressability in microfluidic constructs, several storage arrays were designed and tested. An example VLSI device is presented in Figure 5.8. This design was motivated by the original microfluidic LSI device of Thorsen et al containing 25 x 40 = 1000 chambers with a footprint of approximately one inch squared[66].
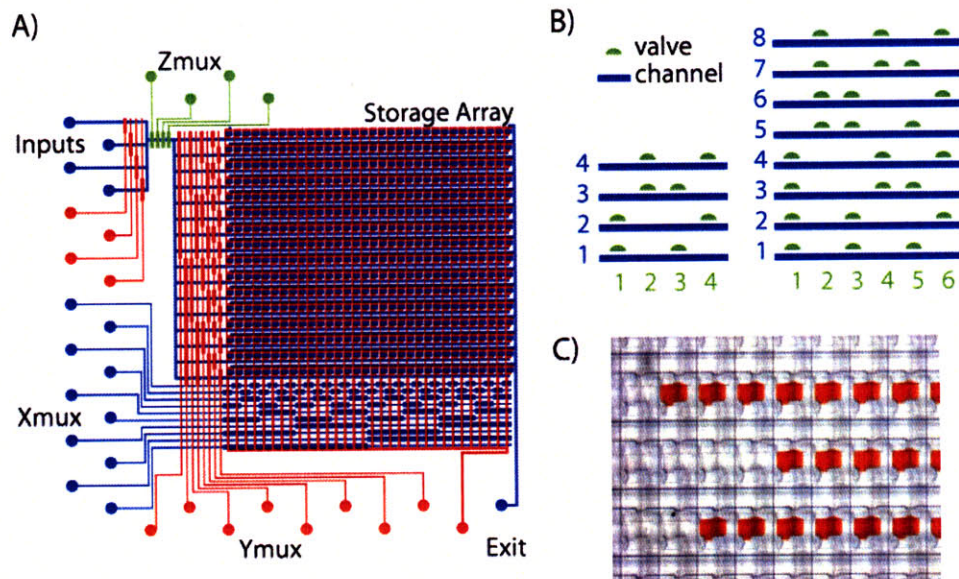
Figure 5.8: Schematic of a stacked storage device (VLSI 1 = 2048 chambers) realized by vertical multiplexing. Repeated levels of storage chambers may be successively stacked on top of one another to yield significantly more complex devices with multiple planes while utilizing common interconnects. A) The vertical multiplexer (or Z mux) is denoted in green. Flow and control channels are in blue and red, respectively. B) Schematics of four or eight layer multiplexors to enable layer by layer addressability. C) Sample manipulation within a storage array. Red food dye was loaded into storage bins, with dimensions of 200 μm x 300 μm.

To demonstrate VLSI, two different architectures (denoted "VLSI 1" and "VLSI 2") were developed of varying complexity while conserving approximately the same device footprint (~25 mm x 25 mm). VLSI 1 contained a total of 16 rows, 32 columns and 4 layers, for a total of 2048 individually addressable chambers.

Flow channels were 25 μm tall, and 100 μm wide. The control wafer was fabricated using a two step photolithography process, with a base layer of 10 μm hard baked positive photoresist to create rounded channels, followed by a layer of 10 μm tall SU8 to create valves. All molds were treated with fluorinated silane prior to casting, and devices were prepared using RTV 615 type PDMS. This architecture was particularly useful for debugging fabrication protocols of vertical devices, as well as some of the operational issues for a three-dimensional storage array. It was found that interlayer thicknesses of greater than several hundred microns are preferable for sample resolution as well as for alignment in thermal bonding.

After of the assembly and operational issues had been experienced and resolved using VLSI 1, a more complex architecture was devised. VLSI 2 featured 32 rows, 64 columns and 8 layers for a total of 16384 independently addressable chambers, illustrated in Figure 5.9.
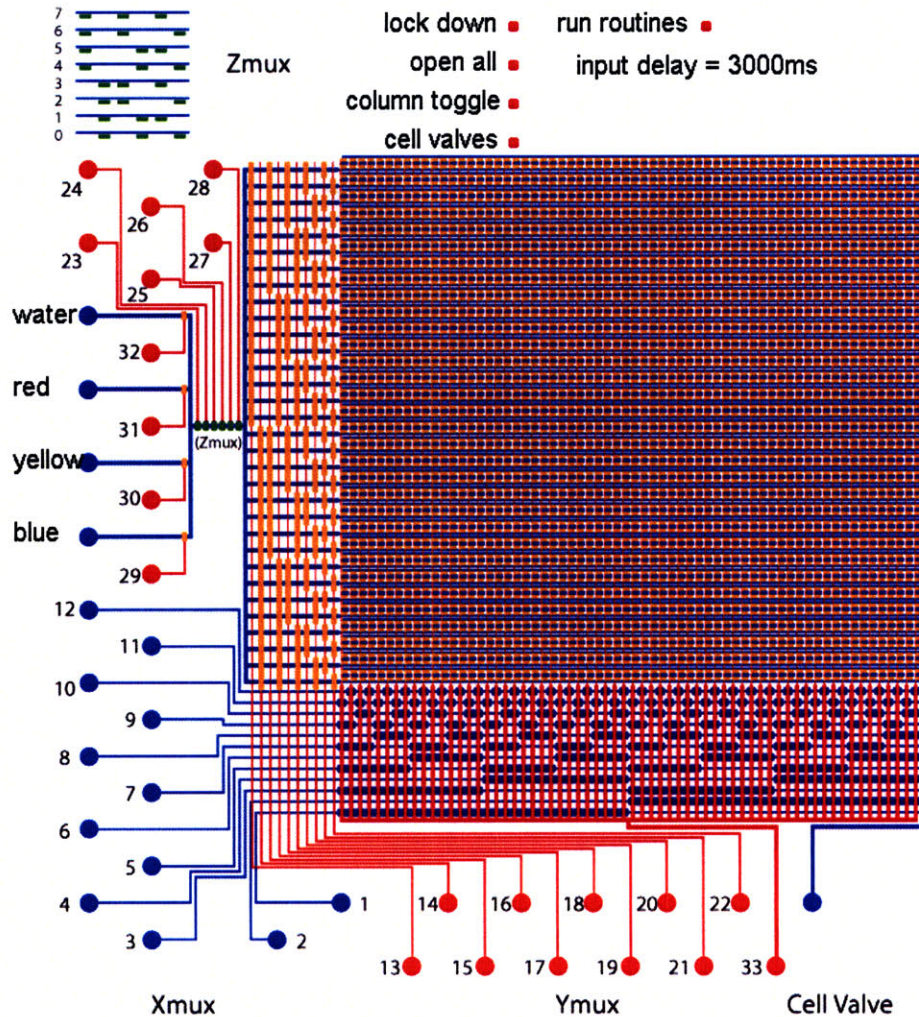
Figure 5.9: Software interface for VLSI 2. The device contains a total of 32 rows, 64 columns and 8 layers, for a total of 16384 individually addressable chambers with a total footprint of less than 25 mm x 25 mm. Valves used for vertical addressability are in green. Flow and control channels are in blue and red, respectively.

Interestingly, introduction of this architecture follows growth rates postulated by a co-founder of Intel Corporation, Gordon Moore, commonly known as "Moore's Law". According to Moore's Law, the storage capacity of silicon-based integrated circuits doubles approximately every 18 months, a trend which has persisted since around 1970. Since the arrival of the original LSI device in 2002, the storage capacity should have doubled four times, and this is precisely the

case. Only, instead of miniaturizing features to accommodate the complexity as is the case in the semiconductor industry, the designs are been fabricated using vertical integration. The VLSI 2 device is presented in Figure 5.10.
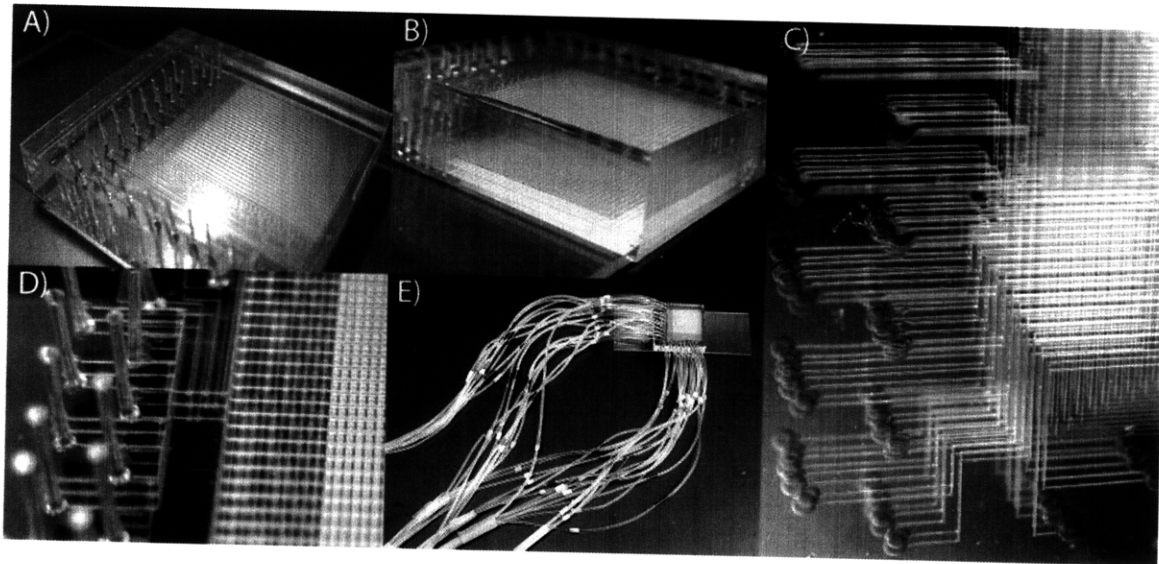
Figure 5.10: The VLSI 2 device A) An isometric view of the device bonded to a glass slide with B) separate planes visible. The total device thickness is approximately 5 mm. C) Multiple planes after plasma bonding of sub-assemblies, prior to punching interconnect ports D) A side view of a vertical multiplexor, with three of eight layers assembled E) The chip connected to 33 external control lines for operation.

A VLSI 2 device contains 34104 valves, and is the most complex device reported to date in the literature with fully addressable storage.

5.5 Vertically Integrated Cell Assays

Beyond demonstrating the capability to increase the fluidic storage capacity of microfluidics, vertical integration was also applied to pertinent biological applications. Specifically, new microfluidic architectures are implemented for cytotoxicity assays on multiple, independent planes. Such applications are intended to demonstrate the applicability of vertical integration for fluorometric measurements and management of cells within a multilayer construct.

There are several reasons to perform cellular assays in a vertical device. First, it is possible to perform replicate runs of an experiment on a single device without requiring additional hardware. By repeating protocols and measurements from one layer to the next, it is possible to

support quantitative data with statistically information. Without vertical integration, it may be necessary to repeat experiments using several different devices. Another advantage of vertical integration is that replicate samples can be contained on a original device, ensuring all samples were treated under identical conditions.

By performing cytotoxicity assays in stacked, it is demonstrated that this approach is not only feasible, but may find several applications for scaling up the complexity of biological and chemical assays. In this chapter, we develop two approaches to using vertically integrated microfluidics for cell assays. In one approach, we extend a well characterized planar system for toxicity assays, and in another, we demonstrate a convergence of the addressability of VLSI with cell culture.

5.5.1 Non-planar Row/Column Cytotoxicity Screening

Recently, high density channel arrays were demonstrated for cell toxicity assays using multilayer soft lithography[36]. With this architecture (Figure 5.11), it was possible to culture different cell lines in parallel then expose each to a variety of stimulants or toxins. The affect on cells was assessed at the endpoint of the experiment with standard live/dead fluorescent dyes.
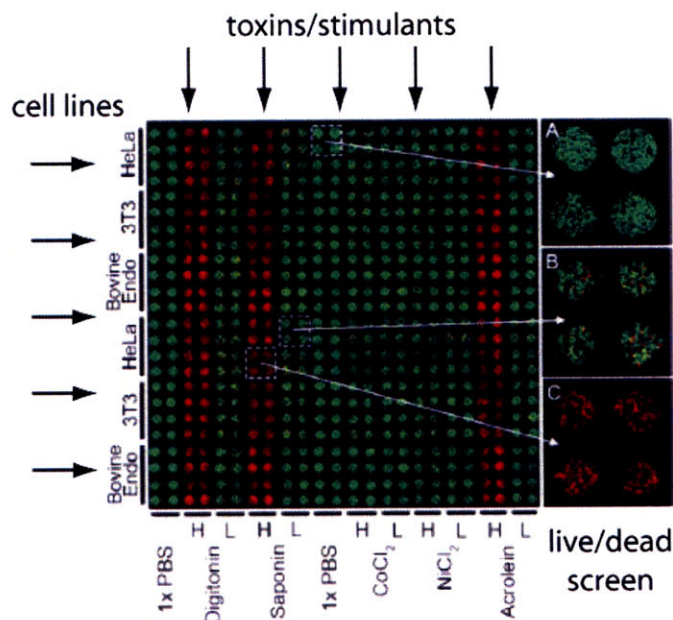
Figure 5.11: A microfluidic device with 24 x 24 = 576 chambers for high-density cell toxicity assays. Cells are seeded into chambers across rows, and integrated valves allow the delivery of toxins to individual columns. Using a live/dead cell screen (live = green, dead = red), the toxicity of chemicals can be characterized in parallel. Figure adapted from Z. Wang et al (2007).

Cells are seeded into chambers using the sieve traps previously described[108] (also refer to Figure 4.12), and MSL valves were arranged to direct flow along rows or columns. Motivated by these effective assays designs, a vertically integrated approach to row column assays was developed as presented in Figure 5.12. These devices were fabricated using bottom actuated valves using RTV 615 PDMS, and assembled using the hybrid thermal-plasma method.
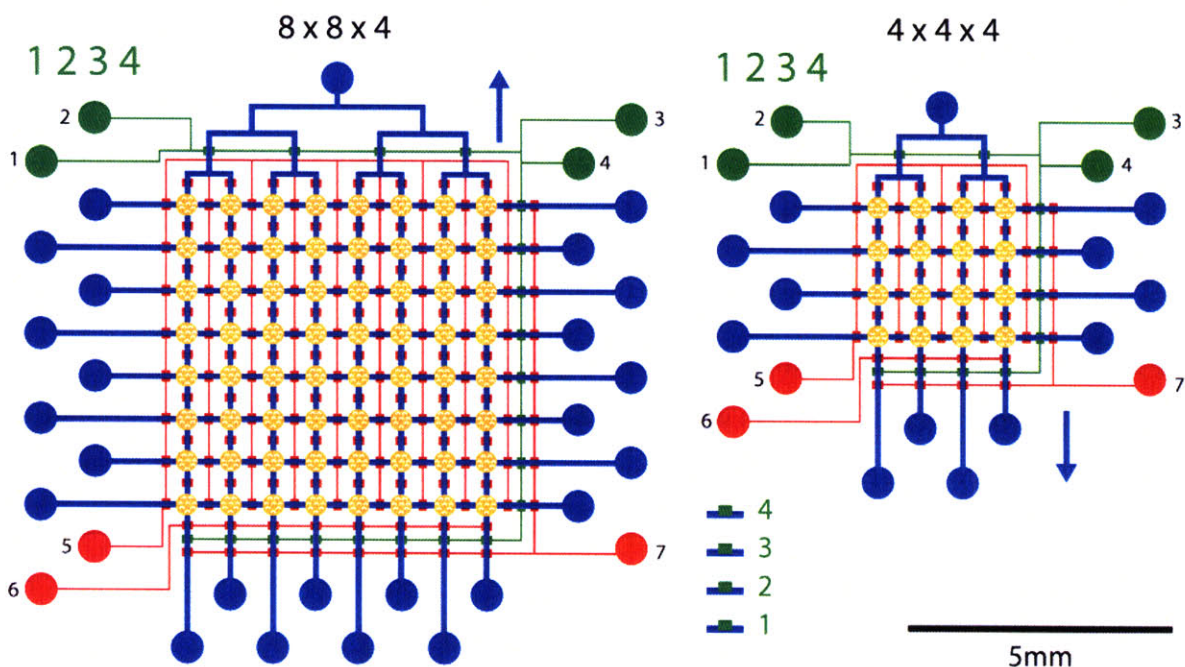
Figure 5.12: Two row/column architectures for cell toxicity screening, motivated by the assays demonstrated by Wang (2007). Both devices use only seven control lines to direct stimulants/toxins to cells on four independent device layers. Control lines used for vertical addressability appear in green. Valve five is used for cell seeding, valve six for toxin screening and valve seven for device pretreatment. These scalable architectures are also designed with row/column spacing equal to the diameters of the cell sieves, to enable offset alignment during assembly.

While these proof-of-concept devices contained less samples that the architectures demonstrated by Wang, the density of assays per device area could now be increased substantially without reducing the size of the cell culture chambers. Since these devices contained only four flow layers, standard valve arrangements were used rather than vertical multiplexors to provide addressability.

Returning to earlier discussion regarding optical independence between layers, it was necessary to first assess whether cytotoxicity screening could be confidently completed using fluorescent dyes without affecting the results in adjunct levels. A simple fluorometric study was thus performed with a row column device. In this experiment, a strong fluorescent sample (0.1 mM Rhodamine 6G) or water was flowed into cell culture chambers. While imaging on one plane, it would be interesting to determine whether the presence of a fluorescent sample out of the focal plane would affect intensity measurements. Imaging trials from within intermediate layers using either dye or water as mock samples was performed, and the results are summarized in Figure 5.13.
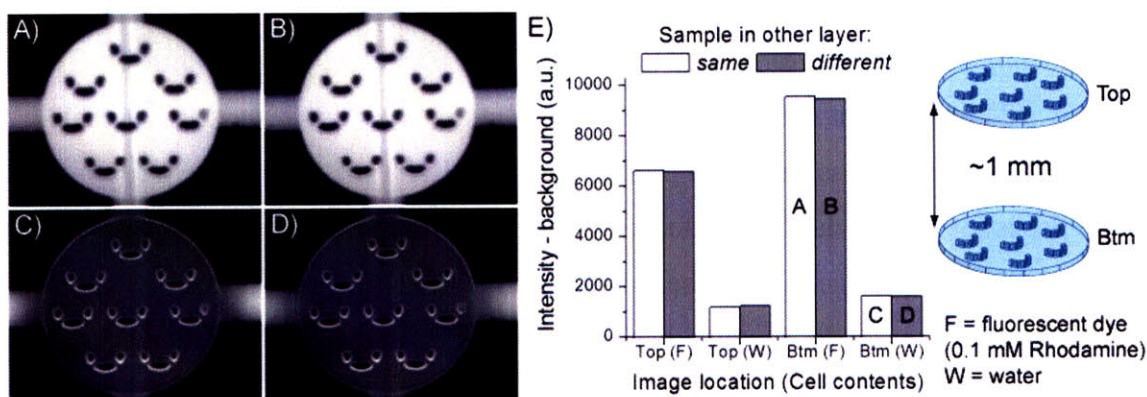
Figure 5.13: Assessment of fluorometric independence. Fluorescent dyes were imaged in cell culture chambers at 20x magnification (0.2 second exposures) with either A) dye, or B) water in the adjacent chamber. Similarly, water was imaged in chambers when either C) dye, or D) water was stored in behind. E) by subtracting the background contribution of intensity, it is shown that the fluorescent signal from within a culture chamber is essentially independent of a same either in front or in behind. It is also noted that samples located deeper into the stack may exhibit lower intensity. As such, quantitative calibration of fluorescence should be performed for every plane. Culture chambers are 400 μm in diameter, and ~25 μm deep.

Fortunately, the measurements of Figure 5.13 represent a worst case scenario for potential fluorometric assays for several reasons. The sample chambers covered almost the entire camera field of view, and contained a concentrated solution of Rhodamine 6G. Images were acquired manually with an inverted epi-fluorescent microscope, and background was subtracted manually during post processing with ImageJ software. Confocal systems (specifically designed to remove background noise between optical planes) would be expected to provide superior results. To improve signal to noise ratio, it is straightforward to increase the interlayer thickness between

flow layers in future devices. Further, these cell chambers were located directly above one another, whereas the "offset" approach (Figure 5.3) could also alleviate intensity interference issues, particularly with detection chambers with smaller volumes. Nonetheless, under these experimental conditions, it was demonstrated that it is possible to perform measurements in overlapping planes independent of the sample contents in the neighboring layer. In the case of cell assays, only cells would be dyed, resulting in significantly lower background fluorescence. Fluorescence in these assays will also be used for binary cell responses (live vs. dead), and quantification of intensity is of secondary importance.

For cytotoxicity assays, four layer devices ("4x4x4" of Figure 5.12) were prepared using the thermal-plasma approach. The distance between sample layers was approximately 500 μm. To promote biocompatibility and cell adherence, channels were cleaned with a 24 h soak in ethanol, followed by a 24 h treatment with fibronectin/PBS solution. This was necessary for enabling cell growth on PDMS surfaces, as described in Section 4.4.3. HeLa cells were grown to confluence in culture flasks for several days, collected, and seeded into the device sieves. Software control of the layer valves allowed cells to be seeded one layer at a time. After seeding, cells were incubated for at least 6 h prior to cytotoxicity experiments, with a gentle perfusion of fresh media.

Proof of principle assays were performed a challenge of a dilute solution of histamine flowed through the device, which had the intended effect of killing a fraction of cells. Histamine at a concentration of 0.1 mM in PBS was input to chambers containing cells on all four layers, and incubated for 20 minutes. Cells were then treated with a live/dead stain (L-3224, Invitrogen), prepared with calcein AM and ethidium homodimer-1 (EthD-1), both at 2 μM in PBS. The 16 individual chambers on each layer were automatically imaged one at a time using routines written in JAVA to synchronize the camera and motorized stage. Fluorescent scans were performed twice for each layer, once for live cells under a FITC filter set, and once for dead cells using a RHOD set. For multiple layers, the microscope is refocused between scans (it is possible to automate this step on microscopes with motorized focus features). The results of the cell assays are presented in Figure 5.14.
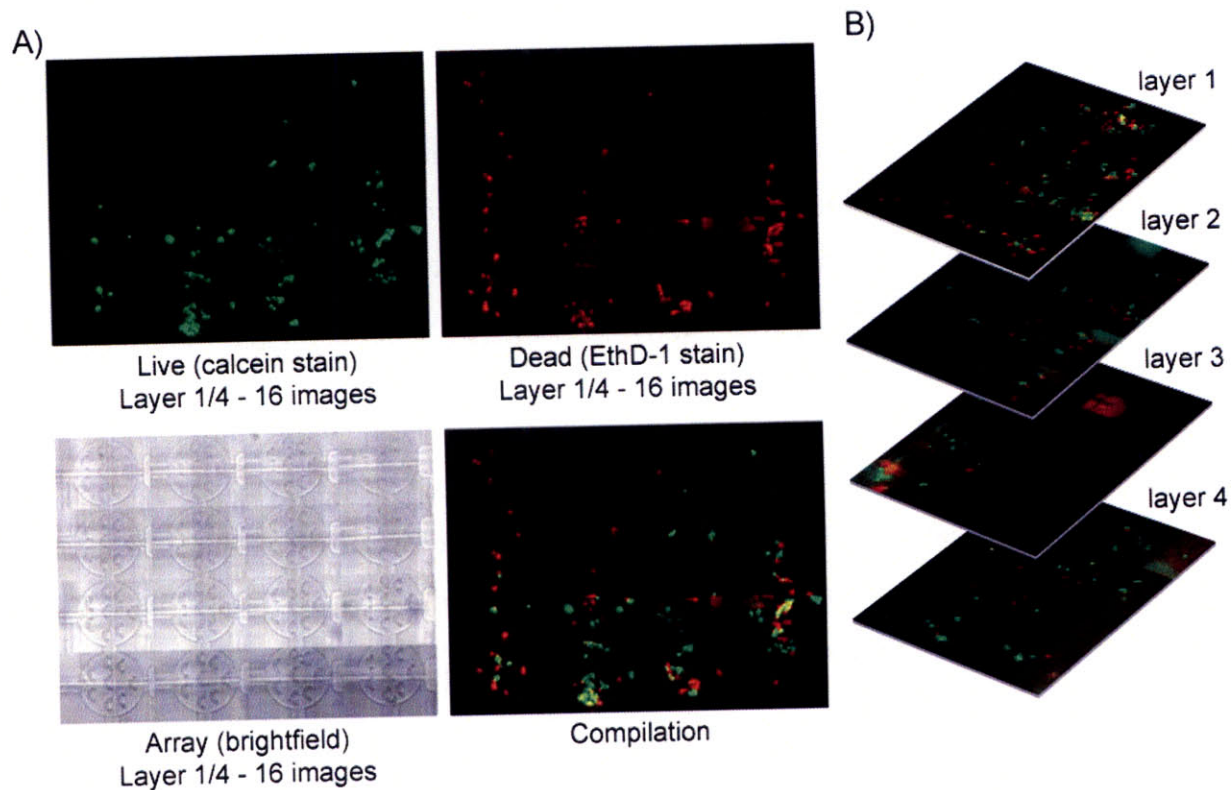
Figure 5.14: Live/dead cell assays performed using a vertically integrated architecture. A) The cell chambers contained HeLa cells which were treated with a histamine solution. Each of four layers contains 16 cell chambers. Live and dead images were captured through FITC and RHOD filter sets at 20X magnification, with exposure times of 0.2 seconds. B) The fluorescent results from one layer to another are independent.

The viability stains indicated that approximately half of the cells in the chambers had been killed by this particular histamine treatment. To preclude the possibility that some cells may have been dead prior to the assays, due to the seeding process or sub-par culture conditions, a live/dead stain could also have been preformed prior to the application of toxins, although these stains can adversely affect the health of the cells over several hours (this represents another advantage of vertical integration - if desired, it would be possible to perform pretreatment viability assays on a spare layer). Images from one layer to another did not exhibit interfering fluorescence. The results of this assay demonstrate that it is possible to increase the density of microfluidic toxicity assays using the concept of vertically integrated architectures. While high density cytotoxicity screens have been performed using planar devices in the past, the stacked device allows additional assays to per performed without necessitating additional hardware or handing on control lines. In the future, a wide variety of biologically relevant substrates and cell lines could

be combined on a single device, and replicate experiments on separate layers can be used to explore the effects of different treatment times.

5.5.2 Independently addressable chambers in three dimensions

By combining the ability to culture and assay cells in a three dimensional construct, with the addressability of VLSI, new architectures were conceived to extend the capability of microfluidic toxicity assays. Such devices extend the flexibility of row/column cytotoxicity protocols, by providing independent addressability of cell culture chambers.

In row/column assays, it is not possible to direct toxins to a specific culture chamber, and it is necessary to flow reagents over all cells in a row. Rather than connecting all cell chambers along a single flow channel, culture channels may be patterned containing bypass lines, as illustrated in Figure 5.15. This approach prevents cross contamination enables individual addressability.
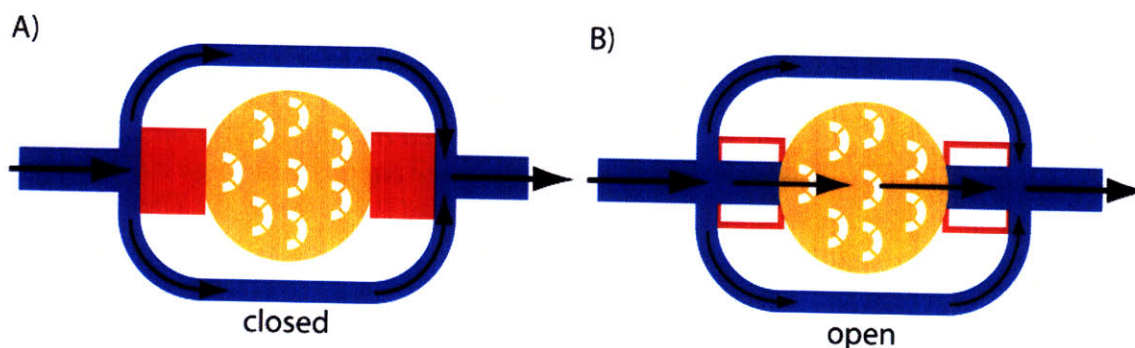
Figure 5.15: A serial method for storage chamber addressability, in contrast to the parallel architecture utilized for previous large scale integrated devices. Although this concept requires slightly more area, it is advantageous for cell signaling as cross contamination between chambers can now be avoided with adequate flushing of reagents. A) When chamber valves are actuated together (in red), flowing fluid passes around a chamber by via symmetric bypass channels (in blue). B) In the open state fluid will still flow though bypass channels, but due the ratios of hydraulic resistance, the majority of fluid flow will be directed through the storage cell. Typical widths for bypass channels are 25 μm, while the centerline flow channels are 100 μm.

In the row/column device, an entire column was dedicated to use of a specific reagent. It was not possible to rinse out this well for application of a second reagent without additional contamination of samples. By providing bypass channels, cross contamination between reagents is avoided, which is particularly useful if channel multiplexors are used to manage inputs. Using

this cell sieve design with bypass channels a modified VLSI device was implemented, illustrated schematically in Figure 5.16.
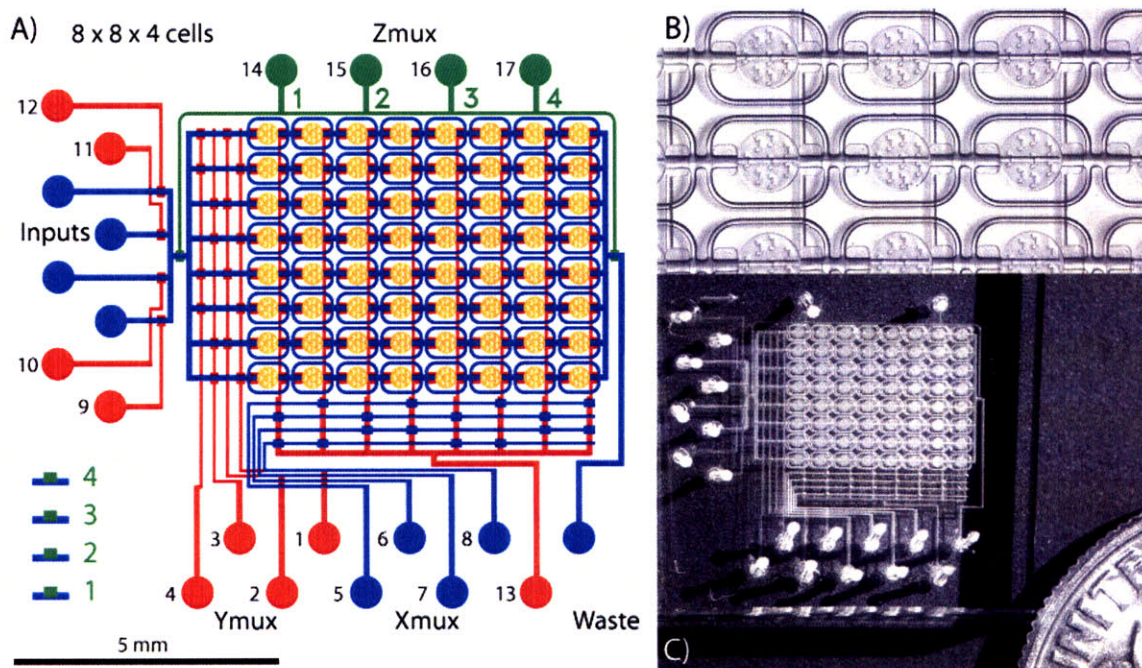
Figure 5.16: A cell toxicity device architecture utilizing both VLSI and the serially addressable chamber techniques. The device contains a total of 8 rows, 8 columns and 4 layers, for a total of 256 individually addressable chambers with a total footprint of less than 12 mm x 12 mm. Cell sieves (denoted in orange) have diameters of 400 μm. Valves used for vertical addressability are in green. Flow and control channels are blue and red, respectively. B) Detailed view of fabricated cell sieves. Shadows from out of plane features can be observed. C) Photograph of a two layer device during assembly, placed next to a U.S. dime for scale.

In this design, 256 independently cells could be observed in an area of approximately 7 mm x 7 mm. Fluid addressability and sample management is controlled using BioStream software routines (in a similar manner to the devices described in Chapters 2 and 4). The union of VLSI and cell culture offers unprecedented assay densities. While this architecture has been driven by the objective of cytotoxicity screening, there are other key applications including metabolic profiling and protein crystallization which can benefit from this new scalability.

5.6 Conclusions and Contributions

In this chapter a new paradigm for microfluidic device engineering has been introduced to implement unprecedented feature densities on chip which circumvents previous limitations with

device size and miniaturization. The concept of vertically integrated microfluidics could have utility in a wide variety of applications where it is necessary to increase the capacity of parallel assays on a single device. The key challenges of vertical addressability, layer fabrication, and optical readout were reviewed and solutions were proposed.

Design and fabrication rules were developed to allow vertically integrated microfluidics to be manufactured using variations of existing PDMS processing steps, with widely available equipment. These processing steps were devised to ensure that the fabrication of vertical devices is practical, and that the fabrication time does not prohibitively scale with the number of layers in the device.

High density storage devices were developed using the concept of vertical multiplexing. Device leveraging vertical multiplexing to yield independently addressable storage chambers in three dimensions represent the most complex example of integration reported to date. These devices used standard valve and channel sizes, while maintaining a device footprint of approximately one inch squared. Interestingly, the increase in complexity was found to scale closely with the rate predicted by Moore's Law.

Finally, vertical integration of microfluidics was proposed for several biologically relevant applications. The first three dimensional cytotoxicity screening devices using a row & column format were demonstrated, with optically independent results between layers. New architectures for independently addressable cellular assays have also been provided. Non-planar devices were found to be biologically compatible and will allow replicated data sets to be acquired on a device, while avoiding the complications of setting up many separate chips. It is believed that the concept of vertical integration will play a major role to manage complexity as more ambitious microfluidic challenges are addressed in the future.

Chapter Six - Conclusions and Outlook

6.1 Contributions

This thesis has addressed a wide range of technical challenges necessary to apply the benefits of microfluidic technology for metabolic profiling of biological systems. Both application-driven and fundamental design contributions to the engineering field were developed, which should be of interest to a broad audience in the areas of automation, device design and cell culture.

First, the flexibility of multilayer soft-lithography was applied to automate the process of single embryo profiling, in the form of a scalable and high-throughput microfluidics-based tool. Such approaches should simplify the non-invasive acquisition and analysis of critical data in culture studies to better understand the relationship between nutrient utilization and sample viability. Continued efforts to simplify measurement techniques may increase adoption of metabolism-based embryo selection metrics to a wider community in assisted reproductive medicine.

It was demonstrated that it was possible to resolve biocompatibility issues and successfully perform embryo culture in microfluidic environments by revisiting existing microfabrication processes. To date, the conditions necessary to sustain healthy embryo culture in closed chambers on chip have not been documented. In contrast to previous microchannel systems, our devices were produced entirely with PDMS. Development of the largest displacement MSL valves to date was crucial to achieve culture in sealed volumes, and to provide unprecedented regulation of flow in culture systems. Microfluidic embryo culture with tools similar to those introduced in this thesis will be applicable to pursue open questions in the field of embryology by enabling precise control of media volume and composition.

Microfluidic channels with integrated valves, that have been demonstrated to be compatible in embryo culture, were a major step towards integrated metabolomic analysis. To establish the feasibility of an end-to-end solution for IVF, the functionalities of culture and detection were combined to a single platform for mammalian cells. A microfluidic device and supporting instrumentation was automated to support multiple cell cultures in parallel while performing non-invasive metabolic assays. Automatic, real time metabolite monitoring may enable the ability to dynamically modify and optimize culture conditions *in vitro*. By moving towards single embryo culture and real time analysis with a single platform, parameters affecting embryo viability may be studied and understood with unprecedented accuracy.

As an extension to the culture and detection methods developed in this thesis, a new paradigm for microfluidic device engineering was presented which will allow an unprecedented number of assays per chip to be performed. Vertically integrated microfluidics ensures more features on chip without undesirable miniaturization of channels while also minimizing the necessary footprint area of a device. The key challenges of vertical addressability, layer fabrication, and optical readout were reviewed and solutions were proposed. Leveraging vertical integration, the largest number of independently addressable chambers on a device was demonstrated. In the context of biological relevance, the first three dimensional cytotoxicity assays were performed. It is believed that the conception of vertical integration will play a major role to manage complexity as more ambitious microfluidic challenges are addressed in the future.

6.2 Future work

There is a significant breadth of studies which can be pursued in both the metabolism and microfluidic fields using the tools developed in this thesis. In this section, potential short and long term projects are overviewed with the desire to initiate discussion for research by others.

For the microfluidic metabolite detector, with the fundamental operation already established, adoption by other groups may be accelerated by efforts to make the devices more accessible and easier to use. Next generation devices should also be scaled up to accommodate more samples. By adding two or four more control lines, it would be possible to increase the number of fluidic

inputs from 16 to either 32 or 64. While calibration would be required to determine the new minimum sample size for analysis, the advantages of throughput would be significant. It would also be worthwhile to revisit image analysis routines (currently based on ImageJ through BioStream JAVA software) to automatically compute linear regressions and slopes. By implementing more frequent calibration, it should be possible to implement error checking routines to ensure the metabolite enzymes have not degraded through the course of long experiments. Looking forward, application of this detection platform to analyze hundreds of culture samples could play a key role in illuminating the relationship between nutrient utilization and developmental viability.

With regard to embryo culture, it is important to pursue continued experiments to compare microdroplet culture with closed volumes on chip. Although several rounds of cell count data have been obtained using the open channel microfluidic devices, no groups to date have demonstrated sub-microliter embryo culture in microfabricated environments. A trial with at least 50 embryos cultured in each of the 125 nl, 250 nl and 500 nl chambers, corroborated with cell count data, would provide further insights to advantages and disadvantages of microfluidic culture in contrast to existing microdroplet techniques. The outcome of these trials would also provide importance information in the push for integrated metabolomic analysis of embryos.

Work should be continued to streamline the operation of the integrated detector device. Preliminary metabolic results from HeLa cell lines has been very promising, particularly the results obtained with metabolic inhibition. The architecture developed in the present work utilized eight parallel chambers. To demonstrate the economies of scale with this integrated metabolomics approach, it may be necessary to scale up the capacity further to accommodate additional cell lines and culture protocols. Currently, the ~25 nl recirculation chambers allow only about three or four measurements to be measured before all the media must be replaced. On future designs, these culture volumes may be increased to enable additional non-invasive assays to be performed every measurement cycle. The sensitivity characterized using the standalone detector suggests that dilution of metabolite signals should not adversely affect accuracy of fluorometric assays. To improve longevity of cell lines during long term assays, the widths of valves used for peristaltic pumping over cell cultures should be decreased to reduce flowrates

and minimize shear stress on cells. Beyond the investigation of metabolic inhibitors with different cell lines, it would be interesting to integrate the mixers necessary to formulate custom compositions of fresh media upstream of culture in response to current metabolic measurements in cell chambers. This would minimize the number of external inputs to provide different compositions of media for all chambers, and also prove as a proof of principle experiment for feedback driven cell culture.

With respect to vertically integrated microfluidics, only a limited number of experiments have been completed to date to fully convey the strength of this design approach. It was reviewed that one of the key applications demanding expanded storage densities was for protein crystallization. It would be interesting to revisit this field with vertically integrated devices to assess how well crystals can be observed through various channel layers. Using a microscope with a motorized focus, it would also be of interest to utilize vertical integration for metabolic measurements. In this approach, it is conceivable that integrated metabolite analysis devices can be operated in parallel on separate layers of a single device.

References

1. Bromer, J.G. and E. Seli, *Assessment of embryo viability in assisted reproductive technology: shortcomings of current approaches and the emerging role of metabolomics.* Current Opinion in Obstetrics & Gynecology, 2008. **20**(3): 234-241.
2. *Assisted Reproductive Technology (ART) Report.* 2005, United States Department of Health and Human Services.
3. Pearson, H., *Safer embryo tests could boost IVF pregnancy rates.* Nature, 2006. **444**(7115): 12-13.
4. Lane, M. and D.K. Gardner, *Selection of viable mouse blastocysts prior to transfer using a metabolic criterion.* Human Reproduction, 1996. **11**(9): 1975-1978.
5. Dickey, R.P., *The relative contribution of assisted reproductive technologies and ovulation induction to multiple births in the United States 5 years after the Society for Assisted Reproductive Technology/American Society for Reproductive Medicine recommendation to limit the number of embryos transferred.* Fertility and Sterility, 2007. **88**(6): 1554-1561.
6. Gardner, D.K., M. Lane, J. Stevens, T. Schlenker, and W.B. Schoolcraft, *Blastocyst score affects implantation and pregnancy outcome: towards a single blastocyst transfer.* Fertility and Sterility, 2000. **73**(6): 1155-1158.
7. Gardner, D.K. and W.B. Schoolcraft, *Elimination of high order multiple gestations by blastocyst culture and transfer.*, in *Female infertility therapy: current practice*, Z. Shoham, C. Howles, and H. Jacods, Editors. 1998. p. 267-274.
8. Schweitzer, S., *Massachusetts, land of twins*, in *Boston Globe*. 2008: Boston.
9. Martin, J.A., B.E. Hamilton, P.D. Sutton, S.J. Ventura, F. Menacker, S. Kirmeyer, and M.L. Munson, *Births: Final Data for 2005*, in *National Vital Statistics Reports*. 2007, Centers for Disease Control and Prevention (CDC).
10. Sundstrom, P. and P. Saldeen, *Early embryo cleavage and day 2 mononucleation after intracytoplasmatic sperm injection for predicting embryo implantation potential in single embryo transfer cycles.* Fertility and Sterility, 2008. **89**(2): 475-477.
11. Gardner, D.K., W.B. Schoolcraft, L. Wagley, T. Schlenker, J. Stevens, and J. Hesla, *A prospective randomized trial of blastocyst culture and transfer in in-vitro fertilization.* Human Reproduction, 1998. **13**(12): 3434-3440.
12. Gardner, D.K., P. Vella, M. Lane, L. Wagley, T. Schlenker, and W.B. Schoolcraft, *Culture and transfer of human blastocysts increases implantation rates and reduces the need for multiple embryo transfers.* Fertility and Sterility, 1998. **69**(1): 84-88.
13. Gardner, D.K. and H.J. Leese, *Noninvasive Measurement of Nutrient-Uptake by Single Cultured Preimplantation Mouse Embryos.* Human Reproduction, 1986. **1**(1): 25-27.
14. Gardner, D.K. and H.J. Leese, *Assessment of Embryo Viability Prior to Transfer by the Noninvasive Measurement of Glucose-Uptake.* Journal of Experimental Zoology, 1987. **242**(1): 103-105.
15. Rieger, D., *Metabolic Pathway Activity*, in *A Laboratory Guide to the Mammalian Embryo*, D.K. Gardner, M. Lane, and A.J. Watson, Editors. 2004, Oxford University Press. p. 154-164.
16. Mroz, E.A. and C. Lechene, *Fluorescence Analysis of Picoliter Samples.* Analytical Biochemistry, 1980. **102**(1): 90-96.
17. Leese, H.J., J.D. Biggers, E.A. Mroz, and C. Lechene, *Nucleotides in a Single Mammalian Ovum or Preimplantation Embryo.* Analytical Biochemistry, 1984. **140**(2): 443-448.
18. Leese, H.J. and A.M. Barton, *Pyruvate and Glucose-Uptake by Mouse Ova and Preimplantation Embryos.* Journal of Reproduction and Fertility, 1984. **72**(1): 9-13.
19. Squires, T.M. and S.R. Quake, *Microfluidics: Fluid physics at the nanoliter scale.* Reviews of Modern Physics, 2005. **77**(3): 977-1026.

20. Walker, G.M., H.C. Zeringue, and D.J. Beebe, *Microenvironment design considerations for cellular scale studies.* Lab on a Chip, 2004. **4**(2): 91-97.
21. Dittrich, P.S., K. Tachikawa, and A. Manz, *Micro total analysis systems. Latest advancements and trends.* Analytical Chemistry, 2006. **78**(12): 3887-3907.
22. El-Ali, J., P.K. Sorger, and K.F. Jensen, *Cells on chips.* Nature, 2006. **442**(7101): 403-411.
23. Suh, R.S., N. Phadke, D.A. Ohl, S. Takayama, and G.D. Smith, *Rethinking gamete/embryo isolation and culture with microfluidics.* Human Reproduction Update, 2003. **9**(5): 451-461.
24. Lucchetta, E.M., J.H. Lee, L.A. Fu, N.H. Patel, and R.F. Ismagilov, *Dynamics of Drosophila embryonic patterning network perturbed in space and time using microfluidics.* Nature, 2005. **434**(7037): 1134-1138.
25. Unger, M.A., H.P. Chou, T. Thorsen, A. Scherer, and S.R. Quake, *Monolithic microfabricated valves and pumps by multilayer soft lithography.* Science, 2000. **288**(5463): 113-116.
26. Hickman, D.L., D.J. Beebe, S.L. Rodriguez-Zas, and M.B. Wheeler, *Comparison of static and dynamic medium environments for culturing of preimplantation mouse embryos.* Comparative Medicine, 2002. **52**(2): 122-126.
27. Quinn, P., *The development and impact of culture media for assisted reproductive technologies.* Fertility and Sterility, 2004. **81**(1): 27-29.
28. *Vitrolife AB Sweden - Fertility Products.* [http://www.vitrolife.com/fertility.]
29. Lane, M., D.K. Gardner, M.J. Hasler, and J.F. Hasler, *Use of G1.2/G2.2 media for commercial bovine embryo culture: equivalent development and pregnancy rates compared to co-culture.* Theriogenology, 2003. **60**(3): 407-419.
30. Pool, T.B., *An update on embryo culture for human assisted reproductive technology: Media, performance, and safety.* Seminars in Reproductive Medicine, 2005. **23**(4): 309-318.
31. Gopichandran, N. and H.J. Leese, *The effect of paracrine/autocrine interactions on the in vitro culture of bovine preimplantation embryos.* Reproduction, 2006. **131**(2): 269-277.
32. Balagadde, F.K., L.C. You, C.L. Hansen, F.H. Arnold, and S.R. Quake, *Long-term monitoring of bacteria undergoing programmed population control in a microchemostat.* Science, 2005. **309**(5731): 137-140.
33. Gu, W., X.Y. Zhu, N. Futai, B.S. Cho, and S. Takayama, *Computerized microfluidic cell culture using elastomeric channels and Braille displays.* Proceedings of the National Academy of Sciences of the United States of America, 2004. **101**(45): 15861-15866.
34. Watkins, A.J., T. Papenbrock, and T.P. Fleming, *The preimplantation embryo: Handle with care.* Seminars in Reproductive Medicine, 2008. **26**(2): 175-185.
35. Pelicano, H., D.S. Martin, R.H. Xu, and P. Huang, *Glycolysis inhibition for anticancer treatment.* Oncogene, 2006. **25**(34): 4633-4646.
36. Wang, Z.H., M.C. Kim, M. Marquez, and T. Thorsen, *High-density microfluidic arrays for cell cytotoxicity analysis.* Lab on a Chip, 2007. **7**(6): 740-745.
37. Gardner, D.K., T.B. Pool, and M. Lane, *Embryo nutrition and energy metabolism and its relationship to embryo growth, differentiation, and viability.* Seminars in Reproductive Medicine, 2000. **18**(2): 205-218.
38. Ryan, D. and K. Robards, *Metabolomics: The greatest omics of them all?* Analytical Chemistry, 2006. **78**(23): 7954-7958.
39. Christofk, H.R., M.G. Vander Heiden, M.H. Harris, A. Ramanathan, R.E. Gerszten, R. Wei, M.D. Fleming, S.L. Schreiber, and L.C. Cantley, *The M2 splice isoform of pyruvate kinase is important for cancer metabolism and tumour growth.* Nature, 2008. **452**(7184): 230-U74.
40. Borini, A., C. Lagalla, M. Cattoli, E. Sereni, R. Sciajno, C. Flamigni, and G. Coticchio, *Predictive factors for embryo implantation potential.* Reprod Biomed Online, 2005. **10**(5): 653-68.
41. Reddy, U.M., R.J. Wapner, R.W. Rebar, and R.J. Tasca, *Infertility, assisted reproductive technology, and adverse pregnancy outcomes: executive summary of a National Institute of Child Health and Human Development workshop.* Obstet Gynecol, 2007. **109**(4): 967-77.

42. Sakkas, D. and D.K. Gardner, *Noninvasive methods to assess embryo quality.* Current Opinion in Obstetrics & Gynecology, 2005. **17**(3): 283-288.

43. Leese, H.J., *Metabolism of the preimplantation mammalian embryo.* Oxford Rev. of Reprod. Biol., 1991. **13**: 35-72.

44. Wallace, D.C., *Mitochondria and cancer: Warburg addressed.* Cold Spring Harb Symp Quant Biol, 2005. **70**: 363-74.

45. Gardner, D.K., M. Lane, J. Stevens, and W.B. Schoolcraft, *Noninvasive assessment of human embryo nutrient consumption as a measure of developmental potential.* Fertil Steril, 2001. **76**(6): 1175-80.

46. Lowry, O.H. and J.V. Passonneau, *A Flexible System of Enzymatic Analysis.* 1972, New York, NY: Academic Press.

47. Gardner, D.K., *Noninvasive Metabolic Assessment of Single Cells*, in *Single Cell Diagnostics: Methods and Protocols*, A. Thornhill, Editor. 2007, Humana Press. p. 1-9.

48. Brison, D.R., K. Hollywood, R. Arnesen, and R. Goodacre, *Predicting human embryo viability: the road to non-invasive analysis of the secretome using metabolic footprinting.* Reproductive Biomedicine Online, 2007. **15**(3): 296-302.

49. Houghton, F.D. and H.J. Leese, *Metabolism and developmental competence of the preimplantation embryo.* European Journal of Obstetrics Gynecology and Reproductive Biology, 2004. **115**: S92-S96.

50. Lopes, A.S., T. Greve, and H. Callesen, *Quantification of embryo quality by respirometry.* Theriogenology, 2007. **67**(1): 21-31.

51. Seli, E., D. Sakkas, R. Scott, S.C. Kwok, S.M. Rosendahl, and D.H. Burns, *Noninvasive metabolomic profiling of embryo culture media using Raman and near-infrared spectroscopy correlates with reproductive potential of embryos in women undergoing in vitro fertilization.* Fertility and Sterility, 2007. **88**(5): 1350-1357.

52. Leegsma-Vogt, G., K. Venema, N. Brouwer, J.B. Gramsbergen, S. Copray, and J. Korf, *Quantitative on-line monitoring of cellular glucose and lactate metabolism in vitro with slow perfusion.* Analytical Chemistry, 2004. **76**(18): 5431-5435.

53. Eklund, S.E., D. Taylor, E. Kozlov, A. Prokop, and D.E. Cliffel, *A microphysiometer for simultaneous measurement of changes in extracellular glucose, lactate, oxygen, and acidification rate.* Analytical Chemistry, 2004. **76**(3): 519-527.

54. Shiku, H., T. Shiraishi, H. Ohya, T. Matsue, H. Abe, H. Hoshi, and M. Kobayashi, *Oxygen consumption of single bovine embryos probed by scanning electrochemical microscopy.* Analytical Chemistry, 2001. **73**(15): 3751-3758.

55. Ciobanu, M., D.E.T. Jr., J.P. Willburn, and D.E. Cliffel, *Glucose and Lactate Biosensors for Scanning Electrochemical Microscopy Imaging of Single Live Cells.* Analytical Chemistry, 2008. **In press**.

56. Cai, X.X., N. Klauke, A. Glidle, P. Cobbold, G.L. Smith, and J.M. Cooper, *Ultra-low-volume, real-time measurements of lactate from the single heart cell using microsystems technology.* Analytical Chemistry, 2002. **74**(4): 908-914.

57. Cheng, W., N. Klauke, H. Sedgwick, G.L. Smith, and J.M. Cooper, *Metabolic monitoring of the electrically stimulated single heart cell within a microfluidic platform.* Lab on a Chip, 2006. **6**(11): 1424-1431.

58. Schulz, C.M., L. Scampavia, and J. Ruzicka, *Real-time monitoring of lactate extrusion and glucose consumption of cultured cells using a lab-on-valve system.* Analyst, 2002. **127**(12): 1583-1588.

59. Gardner, D.K. and H.J. Leese, *Concentrations of Nutrients in Mouse Oviduct Fluid and Their Effects on Embryo Development and Metabolism Invitro.* Journal of Reproduction and Fertility, 1990. **88**(1): 361-368.

60. Studer, V., G. Hang, A. Pandolfi, M. Ortiz, W.F. Anderson, and S.R. Quake, *Scaling properties of a low-actuation pressure microfluidic valve.* Journal of Applied Physics, 2004. **95**(1): 393-398.

61. Gardner, D.K. and M. Lane, *Culture and selection of viable blastocysts: a feasible proposition for human IVF?* Human Reproduction Update, 1997. **3**(4): 367-382.

62. Urbanski, J.P., W. Thies, C. Rhodes, S. Amarasinghe, and T. Thorsen, *Digital microfluidics using soft lithography.* Lab on a Chip, 2006. **6**(1): 96-104.

63. Thies, W., J.P. Urbanski, T. Thorsen, and S. Amarasinghe, *Abstraction Layers for Scalable Microfluidic Biocomputing.* Journal of Natural Computing, 2007.

64. Chou, H.-P., M.A. Unger, and S.R. Quake, *A microfabricated rotary pump.* Biomedical Microdevices, 2001. **3**(4): 323-30.

65. Hansen, C.L., M.O.A. Sommer, and S.R. Quake, *Systematic investigation of protein phase behavior with a microfluidic formulator.* Proceedings of the National Academy of Sciences of the United States of America, 2004. **101**(40): 14431-14436.

66. Thorsen, T., S.J. Maerkl, and S.R. Quake, *Microfluidic large-scale integration.* Science, 2002. **298**(5593): 580-584.

67. Cabrera, L.M., Y.S. Heo, J. Ding, S. Takayama, and G.D. Smith. *Improved Blastocyst Development with Microfluidics and Braille Pin Actuator Enabled Dynamic Culture.* in *American Society for Reproductive Medicine (ASRM) Annual Meeting.* 2006: Fertil. Steril. **86**: S43-S43.

68. Raty, S., E.M. Walters, J. Davis, H. Zeringue, D.J. Beebe, S.L. Rodriguez-Zas, and M.B. Wheeler, *Embryonic development in the mouse is enhanced via microchannel culture.* Lab on a Chip, 2004. **4**(3): 186-190.

69. Roach, L.S., H. Song, and R.F. Ismagilov, *Controlling nonspecific protein adsorption in a plug-based microfluidic system by controlling interfacial chemistry using fluorous-phase surfactants.* Analytical Chemistry, 2005. **77**(3): 785-796.

70. Shaikh, K.A., K.S. Ryu, E.D. Goluch, J.M. Nam, J.W. Liu, S. Thaxton, T.N. Chiesl, A.E. Barron, Y. Lu, C.A. Mirkin, and C. Liu, *A modular microfluidic architecture for integrated biochemical analysis.* Proceedings of the National Academy of Sciences of the United States of America, 2005. **102**(28): 9745-9750.

71. Bormann, C.L., L.M. Cabrera, C.N. Chisolm, H.S. Yeo, S. Takayama, and G.D. Smith, *Development of a sensitive assay to measure lactate production of preimplantation embryos.* Fertil Steril, 2006. **86**: s115.

72. King, K.R., S.H. Wang, D. Irimia, A. Jayaraman, M. Toner, and M.L. Yarmush, *A high-throughput microfluidic real-time gene expression living cell array.* Lab on a Chip, 2007. **7**(1): 77-85.

73. Zeringue, H.C., M.B. Wheeler, and D.J. Beebe, *A microfluidic method for removal of the zona pellucida from mammalian embryos.* Lab on a Chip, 2005. **5**(1): 108-110.

74. Amin, N., W. Thies, and S. Amarasinghe. *Micado.* [http://cag.csail.mit.edu/micado/.]

75. Lane, M. and D.K. Gardner, *Effect of Incubation Volume and Embryo Density on the Development and Viability of Mouse Embryos Invitro.* Human Reproduction, 1992. **7**(4): 558-562.

76. Gardner, D.K., *Dissection of culture media for embryos: the most important and less important components and characteristics.* Reproduction Fertility and Development, 2008. **20**(1): 9-18.

77. Lim, J.M., B.C. Reggio, R.A. Godke, and W. Hansel, *A continuous flow, perifusion culture system for 8- to 16-cell bovine embryos derived from in vitro culture.* Theriogenology, 1996. **46**(8): 1441-1450.

78. Chan, N.G., J.T. Lyman, S.J. Choi, H.C. Zeringue, I.K. Glasgow, D.J. Beebe, and M.B. Wheeler, *Development of an embryo transport and analysis system: Material biocompatability.* Theriogenology, 1999. **51**(1): 234-234.

79. Wheeler, M.B., E.M. Walters, and D.J. Beebe, *Toward culture of single gametes: The development of microfluidic platforms for assisted reproduction.* Theriogenology, 2007. **68**: S178-S189.

80. Beebe, D., M. Wheeler, H. Zeringue, E. Walters, and S. Raty, *Microfluidic technology for assisted reproduction.* Theriogenology, 2002. **57**(1): 125-135.

81. Glasgow, I.K., H.C. Zeringue, D.J. Beebe, S.J. Choi, J.T. Lyman, N.G. Chan, and M.B. Wheeler, *Handling individual mammalian embryos using microfluidics*. Ieee Transactions on Biomedical Engineering, 2001. **48**(5): 570-578.

82. Di Carlo, D., L.Y. Wu, and L.P. Lee, *Dynamic single cell culture array*. Lab on a Chip, 2006. **6**(11): 1445-1449.

83. Futai, N., W. Gu, J.W. Song, and S. Takayama, *Handheld recirculation system and customized media for microfluidic cell culture*. Lab on a Chip, 2006. **6**(1): 149-154.

84. Harris, S.E., N. Gopichandran, H.M. Picton, H.J. Leese, and N.M. Orsi, *Nutrient concentrations in murine follicular fluid and the female reproductive tract*. Theriogenology, 2005. **64**(4): 992-1006.

85. Anderson, J.R., D.T. Chiu, R.J. Jackman, O. Cherniavskaya, J.C. McDonald, H.K. Wu, S.H. Whitesides, and G.M. Whitesides, *Fabrication of topologically complex three-dimensional microfluidic systems in PDMS by rapid prototyping*. Analytical Chemistry, 2000. **72**(14): 3158-3164.

86. Toepke, M.W. and D.J. Beebe, *PDMS absorption of small molecules and consequences in microfluidic applications*. Lab on a Chip, 2006. **6**(12): 1484-1486.

87. Lee, J.N., C. Park, and G.M. Whitesides, *Solvent compatibility of poly(dimethylsiloxane)-based microfluidic devices*. Analytical Chemistry, 2003. **75**(23): 6544-6554.

88. Heo, Y.S., L.M. Cabrera, J.W. Song, N. Futai, Y.C. Tung, G.D. Smith, and S. Takayama, *Characterization and resolution of evaporation-mediated osmolality shifts that constrain microfluidic cell culture in poly(dimethylsiloxane) devices*. Analytical Chemistry, 2007. **79**(3): 1126-1134.

89. Oh, K.W. and C.H. Ahn, *A review of microvalves*. Journal of Micromechanics and Microengineering, 2006. **16**(5): R13-R39.

90. Beebe, D.J., J.S. Moore, J.M. Bauer, Q. Yu, R.H. Liu, C. Devadoss, and B.H. Jo, *Functional hydrogel structures for autonomous flow control inside microfluidic channels*. Nature, 2000. **404**(6778): 588-+.

91. Chen, Z.Y., J. Wang, S.Z. Qian, and H.H. Bau, *Thermally-actuated, phase change flow control for microfluidic systems*. Lab on a Chip, 2005. **5**(11): 1277-1285.

92. Pal, R., M. Yang, B.N. Johnson, D.T. Burke, and M.A. Burns, *Phase change microvalve for integrated devices*. Analytical Chemistry, 2004. **76**(13): 3740-3748.

93. Maltezos, G., E. Garcia, G. Hanrahan, F.A. Gomez, S. Vyawhare, R.M. van Dam, Y. Chen, and A. Scherer, *Design and fabrication of chemically robust three-dimensional microfluidic valves*. Lab on a Chip, 2007. **7**(9): 1209-1211.

94. Futai, N., W. Gu, and S. Takayama, *Rapid prototyping of microstructures with bell-shaped cross-sections and its application to deformation-based microfluidic valves*. Advanced Materials, 2004. **16**(15): 1320-+.

95. Weibel, D.B., M. Kruithof, S. Potenta, S.K. Sia, A. Lee, and G.M. Whitesides, *Torque-actuated valves for microfluidics*. Analytical Chemistry, 2005. **77**(15): 4726-4733.

96. Yang, B.Z. and Q. Lin, *Planar micro-check valves exploiting large polymer compliance*. Sensors and Actuators a-Physical, 2007. **134**(1): 186-193.

97. Huh, Y.S., J.H. Choi, T.J. Park, Y.K. Hong, W.H. Hong, and S.Y. Lee, *Microfluidic cell disruption system employing a magnetically actuated diaphragm*. Electrophoresis, 2007. **28**(24): 4748-4757.

98. Pamme, N., *Magnetism and microfluidics*. Lab on a Chip, 2006. **6**(1): 24-38.

99. Easley, C.J., J.M. Karlinsey, J.M. Bienvenue, L.A. Legendre, M.G. Roper, S.H. Feldman, M.A. Hughes, E.L. Hewlett, T.J. Merkel, J.P. Ferrance, and J.P. Landers, *A fully integrated microfluidic genetic analysis system with sample-in-answer-out capability*. Proceedings of the National Academy of Sciences of the United States of America, 2006. **103**(51): 19272-19277.

100. Grover, W.H., R.H.C. Ivester, E.C. Jensen, and R.A. Mathies, *Development and multiplexed control of latching pneumatic valves using microfluidic logical structures.* Lab on a Chip, 2006. **6**(5): 623-631.

101. Grover, W.H., A.M. Skelley, C.N. Liu, E.T. Lagally, and R.A. Mathies, *Monolithic membrane valves and diaphragm pumps for practical large-scale integration into glass microfluidic devices.* Sensors and Actuators B-Chemical, 2003. **89**(3): 315-323.

102. Grover, W.H., M.G. von Muhlen, and S.R. Manalis, *Teflon films for chemically-inert microfluidic valves and pumps.* Lab on a Chip, 2008. **8**(6): 913-918.

103. Rohde, C.B., F. Zeng, R. Gonzalez-Rubio, M. Angel, and M.F. Yanik, *Microfluidic system for on-chip high-throughput whole-animal sorting and screening at subcellular resolution.* Proceedings of the National Academy of Sciences of the United States of America, 2007. **104**(35): 13891-13895.

104. Balagadde, F.K., H. Song, J. Ozaki, C.H. Collins, M. Barnet, F.H. Arnold, S.R. Quake, and L.C. You, *A synthetic Escherichia coli predator-prey ecosystem.* Molecular Systems Biology, 2008. **4**.

105. Hong, J.W., V. Studer, G. Hang, W.F. Anderson, and S.R. Quake, *A nanoliter-scale nucleic acid processor with parallel architecture.* Nature Biotechnology, 2004. **22**(4): 435-439.

106. Gomez-Sjoberg, R., A.A. Leyrat, D.M. Pirone, C.S. Chen, and S.R. Quake, *Versatile, fully automated, microfluidic cell culture system.* Analytical Chemistry, 2007. **79**(22): 8557-8563.

107. Urbanski, J.P., M.T. Johnson, D.D. Craig, D.L. Potter, D.K. Gardner, and T. Thorsen, *Noninvasive Metabolic Profiling using Microfluidics for Analysis of Single Preimplantation Embryos.* Analytical Chemistry, 2008. **In Press**.

108. Kim, M.C., Z.H. Wang, R.H.W. Lam, and T. Thorsen, *Building a better cell trap: Applying Lagrangian modeling to the design of microfluidic devices for cell biology.* Journal of Applied Physics, 2008. **103**(4).

109. Barton, M.E., *Effect of Ph on Growth Cycle of Hela Cells in Batch Suspension Culture without Oxygen Control.* Biotechnology and Bioengineering, 1971. **13**(4): 471-&.

110. Reitzer, L.J., B.M. Wice, and D. Kennell, *Evidence That Glutamine, Not Sugar, Is the Major Energy-Source for Cultured Hela-Cells.* Journal of Biological Chemistry, 1979. **254**(8): 2669-2676.

111. Barban, S. and H. Schulze, *The Effects of 2-Deoxyglucose on the Growth and Metabolism of Cultured Human Cells.* The Journal of Biological Chemistry, 1961. **236**(7): 1887-1890.

112. Ledoux, S., R.C. Yang, G. Friedlander, and D. Laouari, *Glucose depletion enhances P-glycoprotein expression in hepatoma cells: Role of endoplasmic reticulum stress response.* Cancer Research, 2003. **63**(21): 7284-7290.

113. Maher, J.C., A. Krishan, and T.J. Lampidis, *Greater cell cycle inhibition and cytotoxicity induced by 2-deoxy-D-glucose in tumor cells treated under hypoxic vs aerobic conditions.* Cancer Chemotherapy and Pharmacology, 2004. **53**(2): 116-122.

114. Hua, F., Y.G. Sun, A. Gaur, M.A. Meitl, L. Bilhaut, L. Rotkina, J.F. Wang, P. Geil, M. Shim, J.A. Rogers, and A. Shim, *Polymer imprint lithography with molecular-scale resolution.* Nano Letters, 2004. **4**(12): 2467-2471.

115. Ajdari, A., *Pumping liquids using asymmetric electrode arrays.* Physical Review E, 2000. **61**(1): R45-R48.

116. Bazant, M.Z. and Y. Ben, *Theoretical prediction of fast 3D AC electro-osmotic pumps.* Lab on a Chip, 2006. **6**(11): 1455 - 1461.

117. Bazant, M.Z. and T.M. Squires, *Induced-charge electrokinetic phenomena: Theory and microfluidic applications.* Physical Review Letters, 2004. **92**(6): 066101.

118. Laser, D.J. and J.G. Santiago, *A review of micropumps.* Journal of Micromechanics and Microengineering, 2004. **14**(6): R35-R64.

119. Urbanski, J.P., T. Thorsen, J.A. Levitan, and M.Z. Bazant, *Fast AC electro-osmotic micropumps with nonplanar electrodes.* Applied Physics Letters, 2006. **89**(14): 143508.

120. Brown, A.B.D., C.G. Smith, and A.R. Rennie, *Pumping of water with ac electric fields applied to asymmetric pairs of microelectrodes.* Physical Review E, 2001. **63**(2): 016305.

121. Kartalov, E.P., A. Scherer, S.R. Quake, C.R. Taylor, and W.F. Anderson, *Experimentally validated quantitative linear model for the device physics of elastomeric microfluidic valves.* Journal of Applied Physics, 2007. **101**(6).

122. Fu, J.P., R.B. Schoch, A.L. Stevens, S.R. Tannenbaum, and J.Y. Han, *A patterned anisotropic nanofluidic sieving structure for continuous-flow separation of DNA and proteins.* Nature Nanotechnology, 2007. **2**(2): 121-128.

123. Huang, L.R., E.C. Cox, R.H. Austin, and J.C. Sturm, *Continuous particle separation through deterministic lateral displacement.* Science, 2004. **304**(5673): 987-990.

124. Kartalov, E.P., C. Walker, C.R. Taylor, W.F. Anderson, and A. Scherer, *Microfluidic vias enable nested bioarrays and autoregulatory devices in Newtonian fluids.* Proceedings of the National Academy of Sciences of the United States of America, 2006. **103**(33): 12280-12284.

125. Hecht, E., *Optics.* 4 ed. 2001: Addison-Wesley.

126. Hansen, C. and S.R. Quake, *Microfluidics in structural biology: smaller, faster... better.* Current Opinion in Structural Biology, 2003. **13**(5): 538-544.

127. Hansen, C.L., S. Classen, J.M. Berger, and S.R. Quake, *A microfluidic device for kinetic optimization of protein crystallization and in situ structure determination.* Journal of the American Chemical Society, 2006. **128**(10): 3142-3143.

128. Hansen, C.L., E. Skordalakes, J.M. Berger, and S.R. Quake, *A robust and scalable microfluidic metering method that allows protein crystal growth by free interface diffusion.* Proceedings of the National Academy of Sciences of the United States of America, 2002. **99**(26): 16531-16536.

129. Shim, J.U., G. Cristobal, D.R. Link, T. Thorsen, Y.W. Jia, K. Piattelli, and S. Fraden, *Control and measurement of the phase behavior of aqueous solutions using microfluidics.* Journal of the American Chemical Society, 2007. **129**(28): 8825-8835.

130. Zheng, B., L.S. Roach, and R.F. Ismagilov, *Screening of protein crystallization conditions on a microfluidic chip using nanoliter-size droplets.* Journal of the American Chemical Society, 2003. **125**(37): 11170-11171.

131. Lau, B.T.C., C.A. Baitz, X.P. Dong, and C.L. Hansen, *A complete microfluidic screening platform for rational protein crystallization.* Journal of the American Chemical Society, 2007. **129**(3): 454-455.

132. Kelly, B.T., J.C. Baret, V. Taly, and A.D. Griffiths, *Miniaturizing chemistry and biology in microdroplets.* Chemical Communications, 2007(18): 1773-1788.

133. Miller, O.J., K. Bernath, J.J. Agresti, G. Amitai, B.T. Kelly, E. Mastrobattista, V. Taly, S. Magdassi, D.S. Tawfik, and A.D. Griffiths, *Directed evolution by in vitro compartmentalization.* Nature Methods, 2006. **3**(7): 561-570.

134. Zhang, H., E. Tumarkin, R.M.A. Sullan, G.C. Walker, and E. Kumacheva, *Exploring microfluidic routes to microgels of biological polymers.* Macromolecular Rapid Communications, 2007. **28**(5): 527-538.

135. De Geest, B.G., J.P. Urbanski, T. Thorsen, J. Demeester, and S.C. De Smedt, *Synthesis of monodisperse biodegradable microgels in microfluidic devices.* Langmuir, 2005. **21**(23): 10275-10279.

136. Jensen, K. and A. Lee, *The science & applications of droplets in microfluidic devices - Foreword.* Lab on a Chip, 2004. **4**(4): 31N-32N.

137. Li, W., E.W.K. Young, M. Seo, Z. Nie, P. Garstecki, C.A. Simmons, and E. Kumacheva, *Simultaneous generation of droplets with different dimensions in parallel integrated microfluidic droplet generators.* Soft Matter, 2008. **4**(2): 258-262.

138. Huang, S.H., W.H. Tan, F.G. Tseng, and S. Takeuchi, *A monolithically three-dimensional flow-focusing device for formation of single/double emulsions in closed/open microfluidic systems.* Journal of Micromechanics and Microengineering, 2006. **16**(11): 2336-2344.

139. Nisisako, T. and T. Torii, *Microfluidic large-scale integration on a chip for mass production of monodisperse droplets and particles.* Lab on a Chip, 2008. **8**(2): 287-293.
140. Haubert, K., T. Drier, and D. Beebe, *PDMS bonding by means of a portable, low-cost corona system.* Lab on a Chip, 2006. **6**(12): 1548-1549.
141. Lee, S.W. and S.S. Lee, *Shrinkage ratio of PDMS and its alignment method for the wafer level process.* Microsystem Technologies-Micro-and Nanosystems-Information Storage and Processing Systems, 2008. **14**(2): 205-208.

Appendices

Appendix A - Reagents for metabolic assays

Enzyme Cocktails. Metabolite specific enzyme cocktails were prepared following Gardner and Leese[13, 14]. All reagents in this research were purchased through Sigma-Aldrich unless noted otherwise.

Standards for glucose, lactate and pyruvate were prepared by adding known amounts of the particular metabolite to either water or media formulations.

Single use glucose and pyruvate aliquots were stored at -20°C, and lactate cocktails were prepared fresh immediately prior to experiments.

Stock solutions:

- 5 mM DTT (DL-dithiothreitol) (Sigma, D-5545, 1g, 4°C); 7.72 mg in 10 ml H_2O
- 37 mM $MgSO_4 7H_2O$ (Sigma, 230391-25G); 91.2 mg in 10 ml H_2O
- 10 mM ATP (Roche, 10519979001, 1g, 4°C); 30.3 mg in 5 ml H_2O
- 10 mM NADP (Roche, 10128031001, 100mg, 4°C); 39.4 mg in 5 ml H_2O
- 5 mM NADH (Roche, 10128015001, 500mg, 4°C); 17.73 mg in 5 ml H_2O
- 4.76 mM NAD+ (Roche, 10127981001, 1g, 4°C); 31.58 mg in 10 ml H_2O

EPPS buffer:

- 2.25 g EPPS (Sigma, E-1894, 25g, RT)
- 10 mg penicillin (Sigma, P-8721, 10MU, 4°C)
- 10 mg streptomycin (Sigma, S-9137, 25g, 4°C)
- 200 ml H_2O
- balance to pH 8.0 with 1M NaOH

Glycine-hydrazine buffer:

- 7.5 g glycine (Sigma, G7126-100G)
- 5.2mg hydrazine (Sigma, 215155-50G)
- 0.2 mg EDTA (ethylenediaminetetraacetic acid) (Sigma, ED-100G)
- 50 ml H_2O
- balance to pH 9.0 with 1M NaOH

Glucose Cocktail: Individual 1.2 ml [or 24 ml] aliquots of cocktail contained:

- 0.75 ml [15 ml] EPPS buffer
- 0.1 ml [2 ml] 5 mM DTT
- 0.1 ml [2 ml] 37 mM $MgSO_47H_2O$
- 50 µl [1 ml] 10 mM ATP
- 150 µl [3 ml] 10 mM NADP
- 50 µl [1 ml] hexokinase/G-6-PDH (Roche, 10127825001, 15mg/5ml, 4°C)

Aliquots were frozen at -80°C in Eppendorf tubes, and thawed prior to use.

Pyruvate Cocktail:

Individual 0.735 ml [or 14.7 ml] aliquots of cocktail contained:

- 0.7 ml [14 ml] EPPS buffer
- 15 µl [0.3 ml] 5 mM NADH (Roche, 10128015001, 500mg, 4°C)
- 20 µl [0.4 ml] LDH (Roche, 127 876, 25mg/5ml, 4°C)

Aliquots were frozen at -80°C in Eppendorf tubes, and thawed prior to use.

Lactate Cocktail:

Individual aliquots of cocktail contained

- 75 µl 4.76 mM NAD+
- 400 µl H_2O
- 450 µl Glycine-Hydrazine buffer
- 25 µl LDH

Aliquots of NAD+ were frozen at -80°C in Eppendorf tubes, and the remaining reagents were mixed prior to use.

Using NAD(P)H linked reactions, a variety of substrates can be studied fluorometrically with the appropriate choice of enzyme cocktails. Lowry has described recipes for measuring hundreds of unique substrates46. The following reactions are of particular relevance for metabolic profiling.

Pyruvate Assay:

$$\text{Lactate Dehydrogenase}$$
$$\text{Pyruvate} + \text{NADH} + \text{H}^+ \quad \rightarrow \quad \text{Lactate} + \text{NAD}^+$$

Lactate Assay:

$$\text{Lactate Dehydrogenase}$$
$$\text{Lactate} + \text{NAD}^+ \quad \rightarrow \quad \text{Pyruvate} + \text{NADH}^+ + \text{H}^+$$

Glucose Assay:

Step 1:

$$\text{Hexokinase}$$
$$\text{Glucose} + \text{ATP} \quad \rightarrow \quad \text{glucose-6-phosphate} + \text{ADP}$$

Step 2:

$$\text{Glucose-6-phosphate Dehydrogenase}$$
$$\text{Glucose-6-phosphate} \quad \rightarrow \quad \text{6-phosphogluconate} + \text{NADPH} + \text{H}^+$$
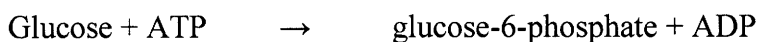
Glutamine Assay

Step 1:

$$\text{Glutaminase}$$
$$\text{Glutamine} + \text{H}_2\text{O} \quad \rightarrow \quad \text{Glutamate} + \text{NH}_3$$
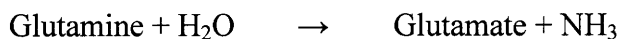
Step 2:

$$\text{Glutamate Dehydrogenase}$$
$$\text{Glutamate} + \text{H}_2\text{O} + \text{NAD}^+ \quad \rightarrow \quad \alpha\text{-ketoglutarate} + \text{NADH} + \text{NH}_4^+$$

Appendix B - Microfluidic Embryo Culture Supporting Data

Summaries of these murine embryo culture trials appear in Figures 3.3 - 3.5. All cell counts were performed by David Potter at the Fertility Labs of Colorado.

Trial One (August 10, 2007):

Type	Name	Ethanol	# Embryos	Culture Volume	PDMS	G1v3-HSA	G2v3 Plus	Total cell number	Cell Number Average	Cell Number Average (w/o Degenerates)	Degenerate	Hatched	TE	TE avg	ICM	ICM avg
device	7A2	yes	3	1 uL	10:10	yes	no	21; 86; 66	58	76	1 of 3	0 of 3	-; 60; 47	54	-; 26; 19	23
device	7A4	yes	2	1 uL	10:10	yes	no	64; 57	61	61	0 of 2	0 of 2	43; 38	41	21; 19	20
device	11A1	yes	3	1 uL	10:10	yes	no	53; 56; 54	54	54	0 of 3	2 of 3	33; 36; 33	34	20; 20; 21	20
device	11A2	yes	3	1 uL	10:10	yes	yes	48; 70; 67	62	62	0 of 3	2 of 3	32; 47; 41	40	16; 23; 26	22
device	12A1	yes	3	1 uL	5:20	yes	no	31; 62; -	47	62	1 of 3	0 of 3	40; ?	40	22; ?	22
device	12A2	yes	3	1 uL	5:20	yes	yes	41; 81; 57	60	69	1 of 3	1 of 3	-; 54; 36	45	-; 27; 21	24
droplet	C1-1	n/a	1	1 uL		yes	no	38	38	n/a	1 of 1	0 of 1	21	21	17	17
droplet	C1-2	n/a	5	10 uL		yes	no	66; 69; 51; 25; 33	49	62	2 of 5	0 of 5	40; 39; 31; -; -	37	26; 30; 20; -; -	25
droplet	C1-3	n/a	4	10 uL		yes	no	53; 66; -; -	60	60	1 of 4	1 of 4	33; 44; ?; ?	39	20; 22; ?; ?	21
droplet	C1-4	n/a	3	1 uL		yes	no	48; -; -	48	48			35; ?; ?	35	13; ?; ?	13
droplet	C1-5	n/a	3	1 uL		yes	yes	76; 84; -	80	80	1 of 3	1 of 3	51; 60; ?	56	25; 24; ?	25

Trial Two (August 17, 2007):

Type	Name	Ethanol	# Embryos	Culture Volume	PDMS	G1v3-HSA	G2v3 Plus	Total cell number	Cell Number Average	Cell Number Average (w/o Degenerates)	Degenerate	Hatched
device	11A3	no	3	1 uL	5:20	yes	no	68 81 74	74	n/a	n/a	n/a
device	11A4	yes	3	1 uL	5:20	yes	no	83 69 101	84	n/a	n/a	n/a
device	12A3	no	3	1 uL	10:10	yes	no	52 71 87	70	n/a	n/a	n/a
device	12A4	yes	3	1 uL	10:10	yes	no	84 91 88	88	n/a	n/a	n/a
droplet	C2-1	n/a	10	20 uL		yes	no	72 82 71 52 59 66 71 n/a n/a n/a	68	n/a	n/a	n/a
droplet	C2-2	n/a	10	20 uL		yes	no	68 47 78 n/a n/a	64	n/a	n/a	n/a
droplet	C2-3	n/a	3	1 uL		yes	no	62 64 n/a	63	n/a	n/a	n/a
droplet	C2-4	n/a	3	1 uL		yes	no	76 n/a	76	n/a	n/a	n/a

Trial Three (August 24, 2007):

Type	Name	Ethanol	# Embryos	Culture Volume	PDMS	G1v3-HSA	G2v3 Plus	Total cell number	Cell Number Average	Cell Number Average (w/o Degenerates)	Degenerate	Hatched
device	13-1	yes	3	1 uL	10:10	yes	yes	n/a / n/a / n/a	n/a	n/a	0 of 3	3 of 3
device	13-2	yes	3	1 uL	10:10	yes	no	89 / 92 / n/a	91	91	0 of 3	3 of 3
device	13-3	yes	3	1 uL	10:10	yes	no	66 / 63 / 42	57	65	1 of 3	0 of 3
device	13-4	yes	3	1 uL	10:10	yes	yes	111 / 104 / 110	108	108	0 of 3	3 of 3
droplet	C3-1	n/a	3	1 uL		yes	no	70 / 90 / 57	72	80	0 of 3	1 of 3
droplet	C3-2	n/a	3	1 uL		yes	no	89 / 61 / 79	76	76	0 of 3	0 of 3
droplet	C3-3	n/a	4	6 uL		yes	no	75 / 67 / 58 / 51	63	67	1 of 4	1 of 4
droplet	C3-4	n/a	3	1 uL		yes	yes	95 / 91 / 80	89	89	0 of 3	2 of 3
droplet	C3-5	n/a	3	1 uL		yes	yes	74 / 87 / n/a	81	81	1 of 3	1 of 3
droplet	C3-6	n/a	3	6 uL		yes	yes	77 / 98 / 100	92	92	0 of 3	2 of 3

Appendix C - Culture Device Volume Characterization

It was believed that volume variance between nominally similar microfluidic devices was due in part to the PDMS curing time. To address this concern, a study was completed where dimensions of culture channels were measured periodically over an extended curing process. Volume discrepancies based on prior measurements indicated that actual channel volumes were often 10-20% smaller than nominal, and at times, even devices cast off the same mold exhibited several percent variation.

Thick layers cast using 5:1 PDMS in conventional soft-lithography are known to contract after removal from molds. A nominal shrinkage ratio of 100/101.7 is therefore accounted for when preparing multilayer soft-lithography devices, to ensure detailed features from the thick layer will register with those on the thin layer during alignment. However, this empirical shrinkage factor ratio is based on 5:1 PDMS for very short cure periods. To ensure successful embryo culture, it was found necessary to cure chips using a 10:1 PDMS ratio for a minimum of 48 hours prior use. No prior studies were identified which have presented data regarding the effects of extended cure times on PDMS shrinkage.

Flow and a control layer of the embryo culture devices in this research were fully cured separately before using a plasma treatment for assembly (Under normal MSL assembly it be possible to assemble the layers using thermal bonding, but since the same ratio of PDMS was used for both flow and control channels, sealing was found to be superior with plasma bonding). Due to scheduling difficulties when devices were prepared, the actual curing time used for device fabrication often ranged anywhere from 50, to more than 60 hours, since longer bakes were also considered adequate for embryo culture. For this reason, it was necessary to characterize culture device shrinkage as a function of time and determine whether this process parameter was to blame for volume variations in channels.

Key questions to address were: 1) What is the typical linear and volumetric shrinkage expected for such culture chambers during extended curing protocols, 2) What is the expected variation, if any, from devices cast off the same molds under identical conditions, and finally, 3) Whether the curing time is the cause of significant discrepancies between measured and nominal volumes.

Twelve devices were cast from two different culture device molds containing the same channel pattern. The same batch of 10:1 PDMS was used for all devices to avoid variations in polymer mixtures. Initially 20 minute bakes were completed at 90°C until the devices were sufficiently cured that they could be removed from the molds and cross sectioned. Initial images of two culture channels were captured using an inverted microscope at 10X before returning samples to the curing oven. The device design used and a typical cross section are presented in Figure C1. During the bake periods, PDMS chips were placed channel side up on a tissue to allow unrestricted device contraction if shrinkage were to occur. Once a day, cross section images were acquired for every sample and channel measurements were performed using ImageJ software. For reference, nominal values of channel height and width were 150 μm and 667 μm, respectively.
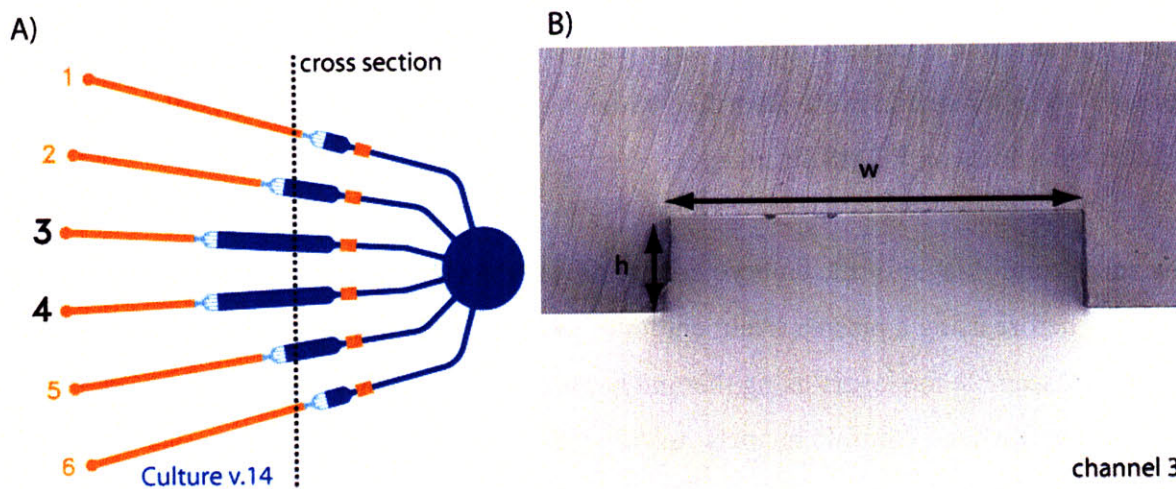

Figure C1: Cross sections used for shrinkage characterization. A) Channels 3 and 4 were cross sectioned on six identically prepared culture chips. B) The height and width of channels were measured for every sample over a one week cure period.

It is difficult to ensure that manually cut sections were precisely perpendicular to channels. As such, the width may differ slightly from expected values. Nonetheless, we are interested in examining the effect of bake times on dimensions relative to initial size of the channel. Additional parameters such as photomask resolution and lithography exposure may result in channel mold widths which differ from nominal values.

Over an extended cure time of more than 100 hours, minimal shrinkage was observed for PDMS samples. Results of width and thickness measurements are summarized in Figure C2. Large error bars are the result of difficulties in identifying clean channel edges for dimensioning (these difficulties were alleviated slightly when using sharpened images). Within the limits of measurement resolution, however, it is evident that channel heights contracted by almost 2%, while the channel widths actually widened by less than 0.5% when the results are averaged over all twelve channels. No significant variation chip-to-chip was observed in six separate chips used in this study.
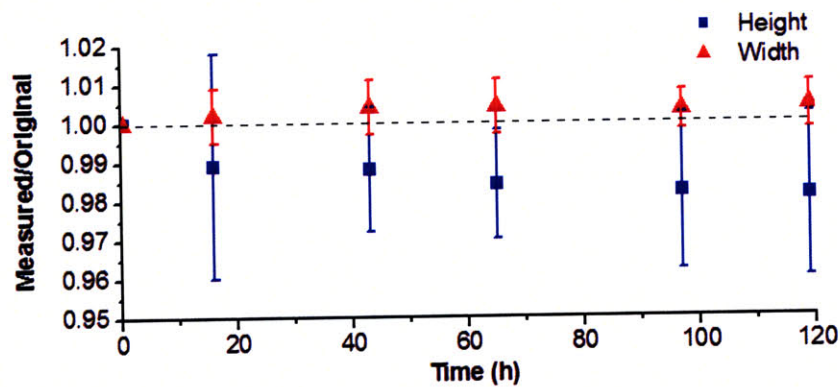

Figure C2: Channel height and width measurements averaged over twelve channels. Error bars represent one standard deviation of error.

This indicates that during contraction of the elastomer device (in this case a block of approximately 4 mm x 20 mm x 20 mm) dimensions of the original chip play a role in distortion of features. It is likely that the entire PDMS block was contracting at a uniform strain ratio. Distortion through the 20 mm lengths may have been minimal as a percentage, but absolute values may have been significant working to pulls the channel walls apart from only another. By conservation of mass, this larger absolute strain in the lateral direction ($\varepsilon w/\varepsilon w_0$) would have increased the thickness of the device, counteracted slightly by the strain through the thickness of the device. This hypothesis is supported by the fact that the average ratio of strains in this experiment, $\varepsilon w/\varepsilon h$, is ~0.22, similar to the aspect ratio width to height of the elastomer chip (4/20 mm). In any case, further characterization of PDMS distortion as a function of cure time is beyond the scope this concise study.

These measurements eliminated the possibility that that observed culture volume variations on the order of 10% or greater were not primarily the result of baking time. Through examination of numerous cross sections, however, many obvious variations in height were observed which identified the mold manufacturing as the main cause. Uncertainties in the lithography process, namely photoresist solvent content and proper leveling of hotplates during pre-bakes, are most likely the culprit of variations. These factors have been a previous concern in fabricating thick (> 50 μm) features from SU-8. Width variations on mid-resolution (3386 dpi) lithography masks used to prepare these samples were also observed on the channel cross sections. As a result of this questions raised in this study, higher resolution masks were obtained for future devices, only newer bottles of SU-8 was used for fabrication of such tall molds, and the dimensions of all features were verified using an interferometer prior to casting.

Appendix D - Example BioStream routine for metabolic profiling

BioStream is an open source programming environment for microfluidics first developed by Bill Thies of MIT CSAIL, which has been used for controlling all the microfluidics in this thesis. Beyond management of microsolenoids used to actuate on chip MSL valves, the BioStream environment has since been extended for control of additional external hardware including motorized stages, microscopes and cameras. Due to the powerful and intuitive nature of this software, is highly recommended to others working in this field.

The following routines written in JAVA were used to complete the integrated assays in Chapter 4. These routines are extensions of the subroutines used to complete sample analysis with the microfluidic detector in Chapter 2. Example lines of code, for calibration of fluorometric standards and measurement for glucose concentration in spent media, is provided to demonstrate the flexibility of our approach.

```
public static void runRoutine() {
        for (int i=0; i<6; i++){            //routine reps - about (1.5 + 1.5) hours each

// GLU ASSAY
        // refresh bypass and cell chamber with fresh media, then allow to culture
        Oocyte9Driver.doInputToCultureBypassPumpTimed(Oocyte9Mapping.MEDIA1,60000);
        Oocyte9Driver.doInputToCultureSievePumpTimed(Oocyte9Mapping.MEDIA1,10000);
        Oocyte9Driver.doTimedMix(2, 30000);

        // culture routine with periodic circulation - about 6 x (5 min) = 30 mins
        for (int j=0; j<6; j++) {
                Oocyte9Driver.wait(240000);         // allow culture
                Oocyte9Driver.doTimedMix(2, 30000); // circulate culture
        }

        for (int p=0; p<4; p++) {                   //calibrate - stds 1 through 4
                runStandardTest(p, Oocyte9Mapping.GLUCOSE);
        }

        Oocyte9Driver.doTimedMix(2, 30000);         // circulate media prior to assays
        for (int a=0; a<3; a++) {                    // assay from sieve and bypass - 3x each
                assayCocktail(Oocyte9Mapping.MEDIA1, Oocyte9Mapping.GLUCOSE);
                }

        for (int p=0; p<4; p++) {                   //calibrate - stds 1 through 4
                runStandardTest(p, Oocyte9Mapping.GLUCOSE);
        }


}
```

Details and downloads of BioStream are available at http://www.cag.csail.mit.edu/biostream/. Also refer to Urbanski[62] and Thies[63].